PROBABILITY AND CURRENT PROPAGATORS IN NON-RELATIVISTIC QUANTUM MECHANICS, WITH APPLICATIONS TO RECENT INTERFEROMETER EXPERIMENTS

by

Langhorne Putney Withers, Jr.
A Dissertation
Submitted to the
Graduate Faculty
of
George Mason University
In Partial Fulfillment of
The Requirements for the Degree
of
Doctor of Philosophy
Physics

Committee:

____________________ Dr. Francesco Narducci, Dissertation Director

____________________ Prof. Maria Dworzecka, Committee Chair

____________________ Prof. Erhai Zhao, Committee Member

____________________ Prof. Paul So, Committee Member

____________________ Prof. Maria Dworzecka, Acting Director, School of Physics, Astronomy, and Computational Sciences

____________________ Prof. Peggy Agouris, Dean, College of Science

____________________ Prof. Donna M. Fox, Associate Dean, Office of Student Affairs & Special Programs, College of Science

Date: ____________________ Spring Semester 2015
George Mason University
Fairfax, VA

Probability and Current Propagators in Non-Relativistic Quantum Mechanics, With Applications to Recent Interferometer Experiments

A dissertation submitted in partial fulfillment of the requirements for the degree of Doctor of Philosophy at George Mason University

By

Langhorne Putney Withers, Jr.
Master of Arts
University of Colorado, 1975
Bachelor of Science
California Institute of Technology, 1973

Director: Dr. Francesco Narducci
School of Physics, Astronomy, and Computational Science

Spring Semester 2015
George Mason University
Fairfax, VA

Dedication

To my wife
Tina
and to my parents
Lang and Betty

Acknowledgments

I have many people to thank, whom I can't thank enough. First of all, I want to thank my advisor, Dr. Francesco Narducci, for taking me aboard, and for his many thoughtful comments and discussions in the shaping of this dissertation. He has very wisely guided my work in useful and profitable directions, been remarkably openminded but honest, exercised sober judgement, and has cheerfully answered all my questions, in our almost weekly meetings via Skype.

I am also thankful for and grateful to my other Committee members, Prof. Maria Dworzecka (who taught me quantum mechanics) Prof. Erhai Zhao, and Prof. Paul So (who taught me classical mechanics), for their kindness, fairness, and integrity, and for their willingness to oversee and believe in an older student doing work that would normally be done in one's younger years.

Prof. So, as the SPACS Physics PhD Graduate Coordinator, has been an invaluable counselor, steering me across what were sometimes like colliding tectonic plates as the Physics PhD program formed at GMU over the past several years. Thank you, Prof. So, for not letting this student fall through the cracks.

My thanks go to all of the outstanding teachers I had at GMU. Taking your courses was a privilege. In chronological order of my courses: Professors David Walnut, Peter Becker, Maria Dworzecka, Joseph Weingartner, Neil Goldman, Robert Ellsworth, Jeffrey Tollaksen, Yakir Aharonov, Indubala Satija, Ernest Barreto, Paul So. You are an awesome army; thank you for your wise instruction and for sharing your valuable knowledge.

I thank my company, MITRE, for reimbursing almost all of my tuition while I attended GMU part time. I want to thank the anonymous reviewers of the IOP for their constructive comments, references to the work of Yukawa and others, and for bringing [61] and [42] to my attention. I thank Dr. Gregg Gallatin for the references to the Keldysh rotation, and for recommending Kleinert's book [29] to me. My thanks also go to my neighbor, Mr. John Gibbons, for voluntarily mowing my lawn and others' nearby with his mighty Toro for more than three entire summers.

I thank my loving, lovely, honest, and too-smart wife, Tina, for letting me go off and do this. She and my daughters Carolyn, Rebecca, and Hannah, cheered me on to the finish line and refused to let me consider giving up on this effort. I thank my Dad, who conveyed his enthusiasm and keen appreciation for life, and for the physical world and its properties, to us children. He gave me my first geometry lesson. As an infantryman in WWII and the Korean Conflict, my father defended freedom and democracy. Of course, I have had many other excellent teachers whom I remember with thankfulness, beginning with my Mom.

Ultimately, I want to thank God, "a very present help in trouble," whose awesome creation inspires all of our calculations. To write down Maxwell's equations is one thing, but to make real electrons and photons (and all the rest) is an accomplishment that is clearly completely beyond us human beings. To paraphrase William Blake's poem "The Tyger" (with some loss of poetry):

Figure 1: George Mason (1725-1792), father of the U.S. Bill of Rights.

Photon, photon, bouncing bright,
in the spaces of the night
What immortal hand or eye
Could frame thy fearful symmetry?

Because of God's amazing grace in my life, this dissertation came about. May his be the glory!

Table of Contents

List of Tables

List of Figures

Abstract

PROBABILITY AND CURRENT PROPAGATORS IN NON-RELATIVISTIC QUANTUM MECHANICS, WITH APPLICATIONS TO RECENT INTERFEROMETER EXPERIMENTS

Langhorne Putney Withers, Jr., PhD

George Mason University, 2015

Dissertation Director: Dr. Francesco Narducci

In this dissertation, a theory of **probability propagation** is developed for standard quantum mechanics. This theory is applied to study three contemporary **interferometer experiments**: three-slit tests of Born's probability law, a modified version of the Steinberg two-slit mean-path experiment using a twin detector, and light-pulse atom interferometry.

The theory is based on path integrals to propagate both the probability and current densities for a quantum-mechanical system. We find that, in order to propagate the probability and current densities, we must extend them to displaced or bilocal probability and current densities. We interpret these bilocal quantities to represent wavelike interference of a particle with itself at any two locations in space. Then we find there are two types of bilocal current, which include the usual current and the so-called osmotic current as special cases. A probabilistic Schrödinger equation for the bilocal probability density results, which is equivalent to the usual Schrödinger equation. By asking quantum mechanics how to propagate probability, we discover that quantum mechanics is inherently bilocal.

Chapter 1: Introduction

Quantum mechanics and its extension to relativistic field theories gives the best account of the physical world that we experience and measure, but we are still testing it and trying to understand its meaning about 100 years after its birth as a theory. At its core, it assigns complex-valued amplitudes to particle events, whose probability densities are then given by the norm-squares of the amplitudes. This is Born's rule, which might be said to make tangible sense (probability) out of abstract nonsense (the amplitudes). Einstein's reaction to this part of the theory that he and Planck launched was to say, "I can't believe that God plays dice with the world." This is, of course, only the first of many paradoxical features of quantum mechanics, such as entangled particles and intrinsic spin. That quantum mechanics somehow represents the real world makes it very interesting. We all want to know how it works, how God does it.

The amplitudes are typically represented as wavefunctions. They evolve or propagate over time, as governed by the Schrödinger equation. Propagators solve the Schrödinger equation. For a given Hamiltonian energy expression, the propagator moves the initial wavefunction forward in time. These amplitude propagators are often hard to compute, and path integrals for the associated Lagrangian action are often the easiest and most intuitive way. A natural question comes up. Can we express quantum mechanics in terms of probabilities alone, without using amplitudes? How would we propagate the probabilities?

This dissertation presents a theory of probability propagation for standard quantum mechanics. The theory is based on path integrals to propagate both the probability and current densities for a quantum-mechanical system. We find that, in order to propagate the probability and current densities, we must extend them to displaced or bilocal probability and current densities. We interpret these bilocal quantities to represent wavelike interference of a particle with itself at any two locations in space. Then we find there are two types of bilocal current, which include the usual current and the so-called osmotic current as special cases. The probabilistic Schrödinger equation results, which is equivalent to the usual Schrödinger equation. By asking quantum mechanics how to propagate probability, we discover that quantum mechanics is inherently bilocal.

This theory is applied to study three contemporary interferometer experiments:

- Three-slit tests of Born's probability rule
- A modified version of the Steinberg two-slit mean path experiment, using a twin detector
- Light-pulse atom interferometry.

This dissertation contains two chapters of theory and two chapters of applications. Each chapter has its own introduction, main body, and conclusion. Chapter 2 develops the Blue functions that propagate the probability and current densities in time. They are analogous to the Green functions that propagate the wavefunction amplitudes in time. From the Blue function path integral, we derive a bicontinuity equation for the probability and current densities. Four examples are given. The Wigner distribution is interpreted in terms of Blue propagators.

Chapter 3 goes on to develop a bilocal picture of quantum mechanics. We present a probability theory that shows that at most two events can interfere in standard quantum mechanics, and immediately apply this to recent experiments to test Born's rule. The concept of a twin detector, necessary for actual bilocal detection of an arriving quantum particle, is introduced. Simple expressions for both kinds of bilocal current are given. By understanding the currents, we see that the probabilistic Schrödinger equation follows from the bicontinuity equation. We solve this equation for energy-difference eigenstates, and directly obtain the von Neumann equation for the density-of-states.

Chapter 4 applies the theory of chapters 2 and 3 to modify the recent weak-value interferometer experiment of Steinberg *et al.*. By using a twin detector to permit wavelike interference, we predict the counter-intuitive result that the de Broglie average path for a photon should change when the detection mechanism changes. Closed-form formulas for the predicted probability and current densities are given. Examples of the measured photon's tranverse momenta and consequent mean path are plotted.

Chapter 5 addresses light-path atom interferometers, currently being developed as sensitive gravity and magnetic field gradiometers, as well as sensitive rotation sensors and atomic clocks. We apply the von Neumann equation for the density-of-states, as derived in chapter 3, to stimulated Raman transitions in a three-level atom. Counter- or co-propagating laser pulses are coherently applied to a cloud of trapped alkali atoms to stimulate a two-photon absorption and emission that compose the Raman transition. We show how to reduce the six density-of-states equations for three levels down to three such equations for an effective two-level system, using an adiabatic approximation. An interesting feature of this theory as developed by Aspect, Chu, and others, is the concept of closed momentum families associated with the three atomic levels. Various sequences of laser pulses are possible. For a Hahn sequence of $\pi/2$, π, $\pi/2$ pulses, we describe the well-known analogy with the Mach-Zehnder interferometer, in which a $\pi/2$ laser pulse acts as a beamsplitter, and a π laser pulse acts as a pair of mirrors.

My conclusions are summarized in chapter 6. Supporting calculations are given in the appendices.

My hope is that the reader will enjoy the ideas and methods presented here, that they will lead him or her to new insights, and that some of them will prove useful in making new applications.

Chapter 2: Probability and Current Density Propagation

Like a Green function to propagate a particle's wavefunction in time, a Blue function is introduced to propagate the particle's probability and current density. Accordingly, the complete Blue function has four components. They are constructed from path integrals involving a quantity like the action that we call the motion. The Blue function acts on the *displaced* probability density as the kernel of an integral operator. As a result, we find that the Wigner density occurs as an expression for physical propagation. We also show that, in quantum mechanics, the displaced current density is conserved bilocally (in two places at one time), as expressed by a generalized continuity equation.

2.1 Introduction

How particles and waves move, and change states in general, is a central concern of physics. In quantum theory, moving objects are modeled by propagating their complex-valued probability amplitudes over time. But in experiments, we typically observe the associated probabilities, the absolute squared norms of the total amplitudes [1]. The probability current density is known to be locally conserved. Theories of mixed states and interaction with external systems often require working with probabilities. These considerations motivate us to study the probabilities in their own right. Specifically, we ask how the probabilities evolve in time, as the wavefunction evolves in time. It is plausible that a direct approach to the moving probabilities should give us new insight and simpler calculations.

The Wigner-Weyl approach to non-relativistic quantum mechanics replaces amplitudes by quasi-probability densities [2][3]. Let us review just enough of this theory to glean one important hint from it: a simple change of variables. Consider a wavefunction $\psi(x', t') =$

$\langle x'|\psi\rangle$ for a particle or system of particles in the state $|\psi\rangle$ at some time t'. (In a moment, we will also be using a later time t''.) It is the probability amplitude to find the particles at position coordinates $x' = (x_1, x_2, \ldots, x_d)$. The Weyl transform converts an operator A into a function over phase space:

$$A(x', p') = \frac{1}{(2\pi\hbar)^d} \int_{-\infty}^{\infty} e^{ip'\cdot\tau'/\hbar} \langle x' + \tfrac{\tau'}{2}|\ A\ |x' - \tfrac{\tau'}{2}\rangle\ d\tau', \tag{2.1}$$

for the system at position and momentum (x', p') at time t'. In particular, for the density operator $\rho = |\psi\rangle\langle\psi|$ of a pure state $|\psi\rangle$, we define the *displaced* (two-location) or *split* probability as

$$\begin{aligned} \mathsf{P}(x't', \tau') &:= \langle x' + \tfrac{\tau'}{2}|\ \rho\ |x' - \tfrac{\tau'}{2}\rangle \\ &= \psi^*(x' - \tfrac{\tau'}{2})\psi(x' + \tfrac{\tau'}{2}). \end{aligned} \tag{2.2}$$

It is complex-valued, but for $\tau' = 0$ it reduces to the real-valued probability $|\psi(x')|^2$. It has an associated displaced current which is conserved, as we will show later. (It is easy to extend this expression (2.2) to a mixed state with density operator $\sum_k p_k \rho_k$, where each state k has probability p_k.) Thus for the density operator, the Weyl transform (2.1) is the Wigner density[1]

$$w(x', p') = \frac{1}{(2\pi\hbar)^d} \int_{-\infty}^{\infty} \psi^*(x' - \tfrac{\tau'}{2}) e^{ip'\cdot\tau'/\hbar} \psi(x' + \tfrac{\tau'}{2}) d\tau'. \tag{2.3}$$

An extra variable τ', the spatial separation, has been introduced above. This variable makes the integral in (2.3) non-local, since it simultaneously probes the wavefunction in opposite directions about x' by variations $\frac{\tau'}{2}$ of every size. The integral is the same when

[1] Wigner and Szilard constructed this density about the same time as Weyl. Wigner applied it to quantum corrections in thermodynamics [4][5]. It was anticipated by Dirac and Heisenberg as well.

we substitute $-\tau'$ for τ', and therefore equals its own complex conjugate. So w is always real-valued. But it is negative in places, except for Gaussian wavefunctions, so it is not a true probability density over phase space [6]. However, its marginal integrals along lines parallel to the p' and x' axes give the squared probability densities of the wavefunction over position and momentum, respectively:

$$\int w(x', p')dx' = |\psi(p')|^2 \tag{2.4}$$

$$\int w(x', p')dp' = |\psi(x')|^2. \tag{2.5}$$

The first integral separates as soon as we change the spatial variables to $r' = x' - \frac{\tau'}{2}$, $s' = x' + \frac{\tau'}{2}$, with unit Jacobian. The second integral results because $\left(\frac{1}{2\pi\hbar}\right)^d \int_{-\infty}^{\infty} e^{ip'\cdot\tau'/\hbar}dp' = \delta(\tau' - 0)$. The total integral over all of phase space is 1. We may recover ψ itself, up to a constant (global) phase factor, from the inverse Fourier transform of w [2]. Also, the expectation value of an operator A given the state $|\psi\rangle$ is

$$\begin{aligned}\langle A \rangle &\equiv \langle \psi^* | A | \psi \rangle = \int \psi^*(x')A\psi(x')dx' \\ &= \mathrm{tr}(\rho A) = \iint A(x', p')w(x', p')\, dx'dp'.\end{aligned} \tag{2.6}$$

A proof of the last equality is given in [3]. Here w plays the role of a signed density or measure over phase space. For further information about the Wigner-Weyl approach see, e.g., [7–12].

Besides the marginal integral properties above, Wigner found other axioms which the quasi-density w satisfies, such as how it transforms under Galilean translations, and invariance under time and spatial inversion [13][14]. But the physical meaning or motivation of the Weyl and Wigner integrals defined by (2.1) and (2.3) is not immediately apparent. For example, there is no obvious reason that leads us a priori to construct the Fourier transform of the displaced probabilities (2.2), based on introducing the auxilliary spacing variable τ'. But these abstract integrals produce meaningful results, so they should possess inherent meaning that we can find out. Ahead, we will come to a bridge in quantum theory from path integrals to the Wigner density.

The outline of the rest of this chapter is as follows. The path-integral approach to quantum mechanics is reviewed in section 2.2. In this theory, a Green function propagates the wavefunction forward in space and time. The Green function itself is a transition probability amplitude, given by a "sum over histories." This is a sum of phasors of form $\exp\{iS/\hbar\}$. Each phase angle is given by the Lagrangian action integral $S = \int_0^t \mathcal{L}$ for one possible path.

In section 2.3, we fuse two of these Green functions to form a Blue function to propagate the probability density, by means of the simple change of variables above. In section 2.4, the Blue function is constructed as a path integral involving a quantity like the action that we call the motion. The classical equations of motion are studied in section 2.5. In section 2.6, we see that the Blue kernel path integral implies a bilocal, generalized continuity equation, much as the Green kernel path integral implies the Schrödinger equation. We consider the four-fold symmetry of the Blue path integral in section 2.7. In section 2.8, we find that the Wigner density results as a natural expression for zero-time propagation of probability. We also consider how to propagate the probability density forward in time using line integrals of the Wigner density in phase space. In section 2.9, we find that the complete Blue function is a (non-Lorentzian) four-vector kernel, acting upon the displaced probability density. One component propagates the probability density. The associated 3-vector, given by a related path integral, produces the propagated probability current density.

2.2 Green propagator

Let any path of the particle from x' at time t' to x'' at time t'' be given at N time increments $\epsilon = T/N$, as $x_0 = x', x_1, x_2, \ldots, x_N = x''$. Here $x_n = x(n\epsilon), n = 1, 2, 3, \ldots,$ and $T = t'' - t'$. The path integral expression developed by Feynman for the Green function propagator is given by [1] [15] [16] [17]:

$$
\begin{aligned}
G(x''t''; x't') &= \int \mathcal{D}x(t)\ e^{iS[x(t)]/\hbar} \\
&= \tfrac{1}{C(\epsilon)} \int \tfrac{dx_1}{C(\epsilon)} \int \tfrac{dx_2}{C(\epsilon)} \ \cdots \ \int \tfrac{dx_{N-1}}{C(\epsilon)} \\
& \quad \exp\left\{ \tfrac{i\epsilon}{\hbar} \sum_{n=1}^{N} \tfrac{m}{2} \left[\left(\tfrac{x_n - x_{n-1}}{\epsilon} \right)^2 - V\left(\tfrac{x_n + x_{n-1}}{2} \right) \right] \right\}
\end{aligned} \tag{2.7}
$$

where $S[x(t)] = \int_{t'}^{t''} \left(\frac{m}{2} \dot{x}^2 - V(x, \dot{x}) \right) dt$ is the Lagrangian action for any path $x(t)$, and $C(\epsilon)$ is a normalizing constant. As described in section 6 of [18], this formula extends directly to the case of multiple particles with different masses in Cartesian space, and can be transformed into other coordinates. Here we introduce a special integral symbol, based on an Euler-Cornu spiral, to suggest graphically the vector sum of unit phasors over paths. The phasors typically rotate slowly for paths near the classical stationary path, as depicted in the middle of the symbol, and rapidly otherwise, as on the extremes of the symbol.

2.3 Blue from Green propagator

To propagate the wavefunction to a later time t'', we use the Green function or matrix element $G(x''t''; x't') = \langle x''t'' | x't' \rangle$. It is the complex amplitude to go from $x't'$ to $x''t''$. Then we operate on the wavefunction by an integral with kernel G: $\psi(x'', t'') = \int G(x''t''; x't') \psi(x', t') dx'$. In this way, the Green function G propagates ψ forward in space and time.

To propagate the probability density $|\psi(x',t')|^2$ directly, we define the *Blue function* B as

$$B(x''t'';x't'\tau') = G^*(x''t'';x'+\tfrac{\tau'}{2},t')\cdot G(x''t'';x'-\tfrac{\tau'}{2},t'). \tag{2.8}$$

The Blue function[2] is the kernel in a two-sided, two-variable integral operator. It propagates the probability density of the wavefunction. We see this because the integral splits easily into a product of two integral operators with the Green propagator as kernel:

$$\begin{aligned}
& \iint dx'd\tau'\psi^*(x'-\tfrac{\tau'}{2})B(x''t'';x't';\tau')\psi(x'+\tfrac{\tau'}{2}) && (2.9)\\
= & \iint dx'd\tau'\psi^*(x'-\tfrac{\tau'}{2})G^*(x''t'';x'-\tfrac{\tau'}{2},t') \\
& \qquad\qquad \cdot G(x''t'';x'+\tfrac{\tau'}{2},t')\psi(x'+\tfrac{\tau'}{2}) \\
= & \iint dr'ds'\psi^*(r')G^*(x''t'';r')G(x''t'';s')\psi(s') \\
= & \int dr'\psi^*(r')G^*(x''t'';r')\cdot\int ds'G(x''t'';s')\psi(s') \\
= & \ \psi^*(x'',t'')\cdot\psi(x'',t'') = |\psi(x'',t''))|^2, && (2.10)
\end{aligned}$$

where we change variables to $r' = x' - \frac{\tau'}{2}$, $s' = x' + \frac{\tau'}{2}$.[3] As $t'' \to t'$, the Green function $G \to \delta(x''-x')$, while the Blue function $B \to \delta(x''-x'+\frac{\tau'}{2})\cdot\delta(x''-x'-\frac{\tau'}{2})$. Note that, as defined, the Blue function operates, not on the probability density, $\mathsf{P}(x't') = |\psi(x',t'))|^2$, but on the more general displaced probability density (2.2). To fuse the Green functions into one Blue kernel, we must split or displace the probabilities in this way. As the operand of the Blue kernel, this complex displaced density (2.2) is the key to this dissertation.

[2]This is not named after anyone. The colour merely suggests its close relation and role to the functions named for George Green.

[3]It is encouraging that Richard Feynman considered propagation of probability in section 12-7 of [1]. This was done to include a stochastic external force $[f(t)]$. To compute state transition probabilities, he began with the product of Green function kernels $G^*(x''t'';x't')\cdot G(y''t'';y't')$, and expressed this as a double path integral. But there was no change of variables to form a Blue function.

We can propagate the displaced probability density itself from time t' to t'', in the usual sense, if we generalize the Blue function slightly by including a final displacement τ'', as follows:

$$
\begin{aligned}
& \iint dx' d\tau' B(x''t''\tau''; x't'\tau') \cdot \mathsf{P}(x't', \tau') \\
= & \iint dx' d\tau' \psi^*(x' - \tfrac{\tau'}{2}) B(x''t''\tau''; x't'\tau') \psi(x' + \tfrac{\tau'}{2}) \\
= & \iint dx' d\tau' \psi^*(x' - \tfrac{\tau'}{2}) G^*(x'' - \tfrac{\tau''}{2}, t''; x' - \tfrac{\tau'}{2}, t') \\
& \qquad \cdot G(x'' + \tfrac{\tau''}{2}, t''; x' + \tfrac{\tau'}{2}, t') \psi(x' + \tfrac{\tau'}{2}) \\
= & \int dr' \psi^*(r') G^*(x'' - \tfrac{\tau''}{2}, t''; r') \cdot \int ds' G(x'' + \tfrac{\tau''}{2}, t''; s') \psi(s') \\
= & \psi^*(x'' - \tfrac{\tau''}{2}, t'') \cdot \psi(x'' + \tfrac{\tau''}{2}, t'') \equiv \mathsf{P}(x''t'', \tau''). \qquad (2.11)
\end{aligned}
$$

Often our interest is in $\tau'' = 0$, and then we will omit it from the Blue function's arguments, and write $B(x''t''0; x't'\tau') = B(x''t''; x't'\tau')$.

A few examples of the Blue functions for a particle in one dimension will be illuminating. They are based on familiar Green functions. The Blue functions are simpler. Here we find that, when used to propagate probability, they naturally produce the Wigner density.

Example 0. The Green propagator (matrix element) for a free particle [1] is

$$
\begin{aligned}
G_0(x''t''; x't') &= \langle x''t'' \,|x't' \rangle \\
&= \left(\frac{m}{2\pi i \hbar T} \right)^{\frac{1}{2}} \exp \left\{ \frac{i}{\hbar} \left[\frac{m}{2T} (x'' - x')^2 \right] \right\}. \qquad (2.12)
\end{aligned}
$$

where $T = t'' - t'$ is the elapsed time. Then the Blue propagator is

$$\begin{aligned}
B_0(x''t''; x't'\tau') &= G_0^*\left(x''t''; x' - \tfrac{\tau'}{2}, t'\right) G_0\left(x''t''; x' + \tfrac{\tau'}{2}, t'\right) \\
&= \left(\frac{m}{2\pi\hbar T}\right) \exp\left\{-\frac{i}{\hbar}\left[\frac{m}{2T}(x'' - x' + \tfrac{\tau'}{2})^2\right]\right\} \\
&\qquad \times \exp\left\{\frac{i}{\hbar}\left[\frac{m}{2T}(x'' - x' - \tfrac{\tau'}{2})^2\right]\right\} \\
&= \left(\frac{m}{2\pi\hbar T}\right) \exp\left\{-\frac{i}{\hbar}\left[m\frac{x'' - x'}{T}\right] \cdot \tau'\right\}. \qquad (2.13)
\end{aligned}$$

The expression in square brackets is the constant momentum

$$p(x', x'', T) = m\frac{x'' - x'}{T}, \qquad (2.14)$$

which takes the classical free particle from x' to x'' in the time T. For any given final point $x''t''$, this is the equation of a straight line ℓ in phase space (x', p') at the initial time t'. Therefore, when we integrate with the Blue function as kernel to propagate the wavefunction probability, we can interpret the integral (2.9) as a line integral in phase space:

$$\begin{aligned}
|\psi(x'', t''))|^2 &= \iint dx' d\tau' \psi^*(x' - \tfrac{\tau'}{2}) B_0(x''t'', x't'\tau') \psi(x' + \tfrac{\tau'}{2}) \\
&= \left(\frac{m}{2\pi\hbar T}\right) \iint dx' d\tau' \psi^*(x' - \tfrac{\tau'}{2}) \psi(x' + \tfrac{\tau'}{2}) \exp\left\{-\frac{i}{\hbar}\left[m\frac{x'' - x'}{T}\right] \cdot \tau'\right\} \\
&= \left(\frac{m}{2\pi\hbar T}\right) \int_\ell dx' \int d\tau' \psi^*(x' - \tfrac{\tau'}{2}) \psi(x' + \tfrac{\tau'}{2}) \exp\left\{-\frac{i}{\hbar} p(x', x'', T) \cdot \tau'\right\} \\
&= \left(\frac{1}{2\pi\hbar}\right) \int_\ell dp' \int d\tau' \psi^*(x' - \tfrac{\tau'}{2}) \psi(x' + \tfrac{\tau'}{2}) \exp\left\{\frac{i}{\hbar} p' \cdot \tau'\right\}. \qquad (2.15)
\end{aligned}$$

We see the line integral with parameter dx' in the (x', p') plane in the next to last equality above. For the last equality, we reparametrize the line integral in terms of momentum using the slope $\partial p'/\partial x' = -m/T$. We recognize this as the line integral of the Wigner density $w(x', p')$ (2.3), valid for any propagation time T. For the special case of zero propagation time, $x' = x''$ is constant, the lines become vertical, and the integral is the same as (2.5).

Example 1. The Green propagator for a linear potential $V(x) = -fx$ is [1]

$$\begin{aligned} G_1(x''t''; x't') &= \langle x''t'' \,|x't' \rangle \\ &= \left(\frac{m}{2\pi i\hbar T}\right)^{\frac{1}{2}} \exp\left\{-\frac{i}{\hbar}\left[\frac{m}{2T}(x''-x')^2 + \frac{fT}{2}(x''+x') - \frac{1}{24m}f^2T^3\right]\right\} \end{aligned} \tag{2.16}$$

Then the Blue propagator is

$$B_1(x''t''; x't'\tau') = \tfrac{m}{2\pi\hbar T}\cdot \exp\left\{-\frac{i}{\hbar}\left[m\frac{x''-x'}{T} - \frac{fT}{2}\right]\cdot \tau'\right\}. \tag{2.17}$$

With no accelerating force f, the classical particle would only have reached $x'' - \frac{1}{2}(f/m)T^2$ by the time t''. So the expression above in square brackets is the initial momentum

$$p'(x', x'', T) = m\frac{x''-x'}{T} - \frac{fT}{2}. \tag{2.18}$$

The impulse fT (momentum change) delivered by the constant force f over the time T will push the particle from x' to x''. (It will have momentum $p'' = p' + fT$ at time t''.) For any given end point $x''t''$, this is again the equation of a straight line ℓ in phase space (x', p') at the initial time t'. Operating with the Blue function as kernel to propagate the wavefunction probability, much as for a free particle we interpret the integral (2.9) as a line

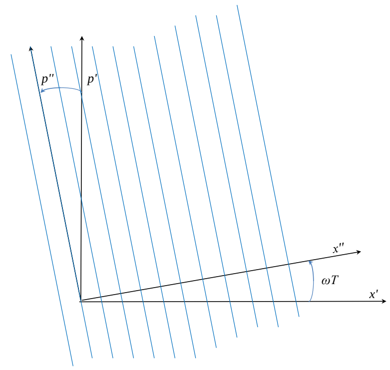

Figure 2.1: Slanted lines in the phase plane for integrating the quantum harmonic oscillator's Wigner density. For each fixed destination x'', the line has the form $x'\cos\omega T + (p'/m\omega)\sin\omega T = x'' + x[f(s)]$, where x is a functional of the forcing function $f(s)$ as in equation (2.21). Integrating it along these lines gives the wavefunction's probability density propagated to time $T = t'' - t'$. The lines are rotated about the origin by the angle ωT. The integrals have the form of a Radon projection of the Wigner density $w(x', p')$ in this example.

integral in phase space:

$$\begin{aligned}
|\psi(x'', t''))|^2 = & \iint dx' d\tau' \psi^*(x' - \tfrac{\tau'}{2}) B_1(x''t'', x't'\tau')\psi(x' + \tfrac{\tau'}{2}) \\
= & \frac{m}{2\pi\hbar T} \iint dx' d\tau' \psi^*(x' - \tfrac{\tau'}{2})\psi(x' + \tfrac{\tau'}{2}) \exp\left\{-\frac{i}{\hbar}\left[m\frac{x'' - x'}{T} - \frac{fT}{2}\right] \cdot \tau'\right\} \\
= & \frac{m}{2\pi\hbar T} \int_\ell dx' \int d\tau' \psi^*(x' - \tfrac{\tau'}{2})\psi(x' + \tfrac{\tau'}{2}) \exp\left\{-\frac{i}{\hbar} p'(x', x'', T) \cdot \tau'\right\} \\
= & \frac{1}{2\pi\hbar} \int_\ell dp' \int d\tau' \psi^*(x' - \tfrac{\tau'}{2})\psi(x' + \tfrac{\tau'}{2}) \exp\left\{\frac{i}{\hbar} p' \cdot \tau'\right\}.
\end{aligned} \tag{2.19}$$

For the last step, we reparametrized the line integral in terms of momentum using $\partial p'/\partial x' = -m/T$ again. We see the line integral of the Wigner density $w(x', p')$ (2.3). Again for zero propagation time, $x' = x''$ is constant, the lines are vertical, and the integral reproduces (2.5).

Example 2. The quantum harmonic oscillator is an important example in both elementary and advanced quantum mechanics. It begins with a quadratic potential $V(x) = \frac{1}{2}m\omega^2 x^2 - f(t)x$, for any external driving force $f(t)$. The Green propagator is [1]

$$\begin{aligned} G_2(x''t''; x't') = & \ \langle x''t'' \left| x't' \right\rangle \\ = & \ e^{-i\theta} \left(\frac{m\omega}{2\pi\hbar |\sin\omega T|} \right)^{\frac{1}{2}} \exp\left\{ \frac{im\omega}{2\hbar \sin\omega T} \left[\left((x''^2 + x'^2) \cos\omega T - 2x''x' \right. \right. \right. \\ & + \frac{2x''}{m\omega} \int_{t'}^{t''} f(t) \sin\omega(t - t')\, dt + \frac{2x'}{m\omega} \int_{t'}^{t''} f(t) \sin\omega(t'' - t)\, dt \\ & \left. \left. \left. - \frac{2}{m^2\omega^2} \int_{t'}^{t''} \int_{t'}^{t} f(t) f(s) \sin\omega(t'' - t) \sin\omega(s - t')\, ds\, dt \right] \right\}, \end{aligned}$$

where $\theta = \frac{\pi}{4}\left(1 + 2\lfloor \frac{\omega T}{\pi} \rfloor\right)$, and $\lfloor x \rfloor$ denotes the greatest integer $n \leq x$. The Blue propagator is

$$\begin{aligned} B_2(x''t''; x't'\tau') = & \ \frac{m\omega}{2\pi\hbar \left|\sin\omega T\right|} \\ & \times \exp\left\{ \frac{im\omega}{\hbar \sin\omega T} \left[x' \cos\omega T - x'' + \frac{1}{m\omega} \int_{t'}^{t''} f(t) \sin\omega(t'' - t)\, dt \right] \cdot \tau' \right\} \\ = & \ \frac{m\omega}{2\pi\hbar \left|\sin\omega T\right|} \cdot \exp\left\{ -\frac{i}{\hbar} p' \cdot \tau' \right\}. \end{aligned} \tag{2.20}$$

Again we see the classical *initial* momentum p' as the coefficient of $i\tau'/\hbar$ in the exponent above:

$$p'(x't',\ x''t'') \ = \ \frac{m\omega}{\sin\omega T} \left[x'' - x' \cos\omega T - \frac{1}{m\omega} \int_{t'}^{t''} f(t) \sin\omega(t'' - t)\, dt \right] \tag{2.21}$$

This interpretation follows, first, by integrating the classical equation of motion for the unforced harmonic oscillator, which gives us its path $x(t'') = x' \cos\omega(t'' - t') + (p'/m\omega) \sin\omega(t'' - t')$.

Second, the integral part is from the inhomogeneous solution using the Green function for the classical harmonic oscillator to include the driving force $f(t)$ [19]. For any given end point $x''t''$, (2.21) is again the equation of a straight line ℓ in phase space (x', p') at the initial time t'. Propagating the wavefunction probability by means of the Blue function, again we may interpret the integral (2.9) as a line integral in phase space:

$$\begin{aligned}
|\psi(x'', t''))|^2 = & \iint dx' d\tau' \psi^*(x' - \tfrac{\tau'}{2}) B_2(x''t'', x't'\tau') \psi(x' + \tfrac{\tau'}{2}) \\
= & \frac{m\omega}{2\pi\hbar\,|\sin\omega T|} \int_\ell dx' \int d\tau' \psi^*(x' - \tfrac{\tau'}{2}) \psi(x' + \tfrac{\tau'}{2}) \exp\left\{ -\frac{i}{\hbar} p'(x', x'', T) \cdot \tau' \right\} \\
= & \frac{1}{2\pi\hbar\,|\cos\omega T|} \int_\ell dp' \int d\tau' \psi^*(x' - \tfrac{\tau'}{2}) \psi(x' + \tfrac{\tau'}{2}) \exp\left\{ \frac{i}{\hbar} p' \cdot \tau' \right\}.
\end{aligned} \tag{2.22}$$

For the last step, we reparametrized the line integral in terms of momentum using $\partial p'/\partial x' = -\frac{m\omega\cos\omega T}{\sin\omega T}$, based on equation (2.21). The line integrals in this case naturally constitute a Radon projection [20][21] of the Wigner density $w(x', p')$ (2.3) for offset distance x'' and tilt angle $\theta = \omega T$, as shown in figure 2.1. For zero propagation time, $x' = x''$ is constant, $\theta = 0$, the lines are vertical, and the integral reproduces (2.5).

For the quantum harmonic oscillator, the probability propagation equation (2.22) shows us directly that the Wigner density of the propagated wavefunction is just the original wavefunction's Wigner density rotated about the origin by ωT. This fact is well-known (see, e.g., [14] [3] [22]), but here we have a direct physical explanation for the fact. We will confirm in section 2.8 that, in general, probability propagation can be expressed naturally as integration of a generalized Wigner density along curves in phase space.

2.4 General form of Blue functions as path integrals

To construct B as a path integral, we begin with the paths for possible motion in configuration (x) space. From the Green function path integral (2.7), the Blue function can also be developed as a path integral. Since $B(x''t''\tau'';x't'\tau') = G^*(x'' - \frac{\tau''}{2}, t''; x' - \frac{\tau'}{2}, t')G(x'' + \frac{\tau''}{2}, t''; x' + \frac{\tau'}{2}, t')$, we begin with two copies of the path integral for G. Let the two sampled paths be labeled as

$$\begin{aligned}
\tilde{x}_0 &= \left(x' - \tfrac{\tau'}{2}\right), \tilde{x}_1, \ldots, \tilde{x}_{N-1}, \tilde{x}_N = \left(x'' - \tfrac{\tau''}{2}\right) \\
x_0 &= \left(x' + \tfrac{\tau'}{2}\right), x_1, \ldots, x_{N-1}, x_N = \left(x'' + \tfrac{\tau''}{2}\right),
\end{aligned}$$

for G^* and G, respectively. Both paths take place over the same time slices $n = 0, \ldots, N$. Their end points are displaced. We write the Blue function as

$$\begin{aligned}
B(x''t''\tau''; x't'\tau') &= \tfrac{1}{C(\epsilon)} \prod_{n=1}^{N-1} \int \tfrac{d\tilde{x}_n}{C(\epsilon)} \exp\left\{ \tfrac{-i\epsilon}{\hbar} \sum_{n=1}^{N} \left[\tfrac{m}{2} \left(\tfrac{\tilde{x}_n - \tilde{x}_{n-1}}{\epsilon} \right)^2 - V\left(\tfrac{\tilde{x}_n + \tilde{x}_{n-1}}{2} \right) \right] \right\} \\
&\quad \cdot \tfrac{1}{C(\epsilon)} \prod_{n=1}^{N-1} \int \tfrac{dx_n}{C(\epsilon)} \exp\left\{ \tfrac{i\epsilon}{\hbar} \sum_{n=1}^{N} \left[\tfrac{m}{2} \left(\tfrac{x_n - x_{n-1}}{\epsilon} \right)^2 - V\left(\tfrac{x_n + x_{n-1}}{2} \right) \right] \right\} \\
&= \tfrac{1}{|C(\epsilon)|^2} \iint \tfrac{d\tilde{x}_1 dx_1}{|C(\epsilon)|^2} \iint \tfrac{d\tilde{x}_2 dx_2}{|C(\epsilon)|^2} \cdots \iint \tfrac{d\tilde{x}_{N-1} dx_{N-1}}{|C(\epsilon)|^2} \\
&\quad \exp\left\{ \tfrac{i\epsilon}{\hbar} \sum_{n=1}^{N} \left(\tfrac{m}{2} \left[\left(\tfrac{x_n - x_{n-1}}{\epsilon} \right)^2 - \left(\tfrac{\tilde{x}_n - \tilde{x}_{n-1}}{\epsilon} \right)^2 \right] \right. \right. \\
&\quad \left. \left. - \left[V\left(\tfrac{x_n + x_{n-1}}{2} \right) - V\left(\tfrac{\tilde{x}_n + \tilde{x}_{n-1}}{2} \right) \right] \right) \right\}. \qquad (2.23)
\end{aligned}$$

The variables are now paired in time order. Next, introduce the change of variables $\tilde{x}_n = q_n - \tau_n/2$, $x_n = q_n + \tau_n/2$. At the path endpoints we have $q_0 = x'$, $\tau_0 = \tau'$, and $q_N = x''$, $\tau_N = \tau''$. (The change of variables removes the τ displacements at endpoints, while introducing the variation by $\tau(t)$ at the points in between.) This intertwines the double integrand for each time n:

$$\begin{aligned} B(x''t''\tau'';x't'\tau') &= \tfrac{1}{|C(\epsilon)|^2} \iint \tfrac{dq_1 d\tau_1}{|C(\epsilon)|^2} \iint \tfrac{dq_2 d\tau_2}{|C(\epsilon)|^2} \cdots \iint \tfrac{dq_{N-1} d\tau_{N-1}}{|C(\epsilon)|^2} \\ & \exp\left\{ \tfrac{i\epsilon}{\hbar} \textstyle\sum_{n=1}^{N} \left(\tfrac{m}{2} \left[\left(\tfrac{q_n - q_{n-1} + (\tau_n - \tau_{n-1})/2}{\epsilon} \right)^2 - \left(\tfrac{q_n - q_{n-1} - (\tau_n - \tau_{n-1})/2}{\epsilon} \right)^2 \right] \right.\right. \\ & \left.\left. - \left[V\left(\tfrac{q_n + q_{n-1} + (\tau_n + \tau_{n-1})/2}{2} \right) - V\left(\tfrac{q_n + q_{n-1} - (\tau_n + \tau_{n-1})/2}{2} \right) \right] \right) \right\}. \end{aligned}$$

This reduces to

$$\begin{aligned} B(x''t''\tau'';x't'\tau') &= \tfrac{1}{|C(\epsilon)|^2} \iint \tfrac{dq_1 d\tau_1}{|C(\epsilon)|^2} \iint \tfrac{dq_2 d\tau_2}{|C(\epsilon)|^2} \cdots \iint \tfrac{dq_{N-1} d\tau_{N-1}}{|C(\epsilon)|^2} \\ & \exp\left\{ \tfrac{i\epsilon}{\hbar} \textstyle\sum_{n=1}^{N} \left(\tfrac{m(q_n - q_{n-1})}{\epsilon} \cdot \tfrac{(\tau_n - \tau_{n-1})}{\epsilon} \right.\right. \\ & \left.\left. - \left[V\left(\bar{q}_n + \tfrac{\bar{\tau}_n}{2} \right) - V\left(\bar{q}_n - \tfrac{\bar{\tau}_n}{2} \right) \right] \right) \right\}. \end{aligned} \tag{2.24}$$

For brevity, in the last step we defined the average values $\bar{q}_n = \frac{1}{2}(q_n + q_{n-1})$, etc. As $N \to \infty$ and $\epsilon \to 0$, keeping $N\epsilon = T$, the Blue function (2.24) can be represented as the continuous path integral

$$B(x''t''\tau'';x't'\tau') = \iint \mathcal{D}q(t)\mathcal{D}\tau(t)\, e^{i\Delta S[q(t),\tau(t)]/\hbar}, \tag{2.25}$$

where the *displaced action* or *motion* is the line integral

$$\begin{aligned} \Delta S[q(t),\tau(t)] &= \int_{t'}^{t''} \left(m\dot{q}\dot{\tau} - \left[V(q + \tfrac{\tau}{2}) - V(q - \tfrac{\tau}{2}) \right] \right) dt \\ &= \int_{t'}^{t''} \left[p \cdot \dot{\tau} - \Delta V \right] \, dt. \end{aligned} \tag{2.26}$$

Given any function f, we define its displaced difference by $\Delta f = \Delta f(q,\tau) = f(q+\frac{\tau}{2}) - f(q-\frac{\tau}{2})$. The motion[4] is formally the line integral of a difference of displaced Lagrangians,

$$\begin{aligned}\Delta L(q,\dot{q},\tau,\dot{\tau}) &= L(q+\tfrac{\tau}{2},\dot{q}+\tfrac{\dot{\tau}}{2}) - L(q-\tfrac{\tau}{2},\dot{q}-\tfrac{\dot{\tau}}{2}) \\ &= m\dot{q}\cdot\dot{\tau} - \Delta V. \end{aligned} \tag{2.27}$$

To generalize this Lagrangian, two Legendre transformations [23] (replacing independent variables $\dot{\tau}$ by $p \equiv \frac{\partial \Delta L[q(t)]}{\partial \dot{\tau}} = m\dot{q}$, and $\dot{q}$ by $\sigma \equiv \frac{\partial \Delta L[q(t)]}{\partial \dot{q}} = m\dot{\tau}$), produce a Hamiltonian as a function of the new variables,

$$-\Delta H(q,p,\tau,\sigma) \equiv \Delta L - p\cdot\dot{\tau} - \sigma\cdot\dot{q}. \tag{2.28}$$

So in phase space the motion is given formally by

$$\Delta S = \int_{t'}^{t''} \left[p\cdot\dot{\tau} + \sigma\cdot\dot{q} - \Delta H(q,\tau,p,\sigma)\right]\, dt. \tag{2.29}$$

This form is confirmed in appendix A, where we derive the Blue propagator path integral in phase space.

Integrating the first term of the motion (2.26) by parts, we find

$$\begin{aligned}\Delta S[q(t),\tau(t)] &= \textstyle\int_{t'}^{t''} \left[m\dot{q}\dot{\tau} - \Delta V\right]\, dt = \int_{t'}^{t''} \left[p\cdot\dot{\tau} - \Delta V\right]\, dt \\ &= p\cdot\tau|_{t'}^{t''} - \textstyle\int_{t'}^{t''}\left[m\ddot{q}\cdot\tau + \Delta V\right]\, dt \\ &= p''\cdot\tau'' - p'\cdot\tau' - \textstyle\int_{t'}^{t''}\left[m\ddot{q}\cdot\tau + \Delta V\right]\, dt \end{aligned} \tag{2.30}$$

[4] Coincidentally, the motion has the form of a phase space action [16][17]; see equation (A.1) in appendix A. It is similar to another action in a phase space, the low-energy action $\int\left[\frac{qB}{m}x\dot{y} - V(x,y)\right]dt$ for the lowest Landau level of a charge q moving in a plane with a normal uniform magnetic field B [16, Ch. 21]. A potential acts as the Hamiltonian in both this action and the motion.

where we used endpoint values $\tau(t'') = \tau''$ and $\tau(t') = \tau'$. The discrete form of $m\ddot{q}$ is a second difference. To be precise, the motion has this discrete form:

$$\begin{aligned}
\Delta S[q_n, \tau_n] &= m\tfrac{(x''-q_{N-1})}{\epsilon} \cdot \tau'' - m\tfrac{(q_1-x')}{\epsilon} \cdot \tau' \\
&\quad -\epsilon \textstyle\sum_{n=1}^{N-1} m \tfrac{(q_{n+1}-2q_n+q_{n-1})}{\epsilon^2} \cdot \tau_n \\
&\quad -\epsilon \textstyle\sum_{n=1}^{N} \left[V\left(\bar{q}_n + \tfrac{\bar{\tau}_n}{2}\right) - V\left(\bar{q}_n - \tfrac{\bar{\tau}_n}{2}\right)\right]. \qquad (2.31)
\end{aligned}$$

It is easy to verify that this equals the discrete motion in the exponent of (2.24) above.

Because the Blue function (2.24) operates as a unified kernel inside a double integral propagator, as in (2.11), we can develop a perturbation theory for relatively weak $\Delta V(x\tau t)$, similar to that for Green propagators [1][23]. This is based on the series expansion

$$e^{-\frac{i}{\hbar}\int_{t'}^{t''}\Delta V\, dt} = 1 - \tfrac{i}{\hbar}\left(\textstyle\int_{t'}^{t''}\Delta V\, dt\right) - \tfrac{1}{2!\hbar^2}\left(\textstyle\int_{t'}^{t''}\Delta V\, dt\right)^2 + \cdots.$$

We express the Blue function as $B(x''t''\tau''; x't'\tau') = B_0 + B_{(1)} + B_{(2)} + \cdots$, beginning with the free particle Blue propagator B_0 and the first order correction B_1. These are evaluated in appendices B and C, respectively:

$$\begin{aligned}
B_0 &= \iint \mathcal{D}x(t)\mathcal{D}\tau(t)\exp\left\{\tfrac{i}{\hbar}\textstyle\int_{t'}^{t''} m\dot{x}\dot{\tau}\right\} = \left[\tfrac{m}{2\pi\hbar(t''-t')}\right]^d \exp\left\{\tfrac{i}{\hbar}p_0(x''t''x't')\cdot[\tau''-\tau']\right\} \\
B_{(1)} &= -\tfrac{i}{\hbar}\textstyle\iiint B_0(x''t''\tau''; xt\tau)\Delta V(xt\tau)B_0(xt\tau; x't'\tau')\, dx d\tau dt \\
&= -\tfrac{i}{\hbar T^3}\left[\tfrac{m}{2\pi\hbar}\right]^4 \left[\textstyle\int V(r)\left[\tfrac{1}{|r-r'|} + \tfrac{1}{|r-r''|}\right]\exp\left\{\tfrac{im}{2\hbar T}\left[|r-r'| + |r-r''|\right]^2\right\}\, dr\right. \\
&\qquad \left. - \textstyle\int V(s)\left[\tfrac{1}{|s-s'|} + \tfrac{1}{|s-s''|}\right]\exp\left\{-\tfrac{im}{2\hbar T}\left[|s-s'| + |s-s''|\right]^2\right\}\, ds\right] \qquad (2.32) \\
B_{(2)} &= -\tfrac{1}{\hbar^2}\textstyle\iiint\iiint B_0(x''t''\tau''; x_2t_2\tau_2)\Delta V(x_2t_2\tau_2) \\
&\qquad B_0(x_2t_2\tau_2; x_1t_1\tau_1)\Delta V(x_1t_1\tau_1)B_0(x_1t_1\tau_1; x't'\tau')\, dx_1 d\tau_1 dt_1\, dx_2 d\tau_2 dt_2
\end{aligned}$$

where $r', s' = x' \pm \frac{\tau'}{2}$, and $r'', s'' = x'' \pm \frac{\tau''}{2}$. The first-order term $B_{(1)}$ of the Blue probability kernel takes the simple form of a difference of two displaced copies of the first-order term of the Green amplitude kernel (the second copy conjugated; see equation (6.29) in [1]). It can be shown that $B_{(1)}$ is $-\frac{i}{\hbar}B_0 \times \xi$, for ξ real; this may be true similarly for $B_{(2)}$ etc. One may evaluate $B_{(2)}$ and higher-order terms as ordinary integrals as well. Then substitution of this perturbation expansion for the Blue kernel B in the propagation integral (2.11) gives the Born expansion for the wavefunction's future probability density. But we will not develop this any further here.

2.5 Classical motion

The classical path $q(t)$ and its path displacement $\tau(t)$, together, are stationary paths of the displaced action ΔS. This form of Hamilton's principle produces coupled equations of motion for the pair of paths.

Consider a small path variation $\eta(t)$ about the stationary path $q(t)$, and a small path variation $\zeta(t)$ about the stationary path displacement $\tau(t)$. Both variations are 0 at their endpoints for $t = t', t''$. Then the two paths are extremal, when the first variation of the motion integral (2.26) is zero for any small path variations:

$$0 = \delta\Delta S \quad = \quad \int_{t'}^{t''} \eta\frac{\partial L}{\partial \eta} + \dot{\eta}\frac{\partial L}{\partial \dot{\eta}} + \zeta\frac{\partial L}{\partial \zeta} + \dot{\zeta}\frac{\partial L}{\partial \dot{\zeta}}\, dt$$

Integrating the second and fourth terms by parts and applying the 0 endpoints gives us

$$0 = \delta\Delta S \quad = \quad \int_{t'}^{t''} \eta\left(\frac{\partial L}{\partial q} - \frac{d}{dt}\frac{\partial L}{\partial \dot{q}}\right) + \zeta\left(\frac{\partial L}{\partial \tau} - \frac{d}{dt}\frac{\partial L}{\partial \dot{\tau}}\right) dt.$$

Since this must hold for arbitrary small path variations, the two expressions in parentheses are both 0. Therefore, we have a pair of Euler-Lagrange equations of motion

$$0 \quad = \quad \frac{\partial L}{\partial q} - \frac{d}{dt}\frac{\partial L}{\partial \dot{q}} \qquad 0 = \frac{\partial L}{\partial \tau} - \frac{d}{dt}\frac{\partial L}{\partial \dot{\tau}}. \tag{2.33}$$

For the Blue Lagrangian $L(q, \dot{q}, \tau, \dot{\tau})$ defined in (2.26), these immediately yield the classical equations of motion

$$m\ddot{q} \quad = \quad -\frac{\partial}{\partial \tau}\left[V(q + \tfrac{\tau}{2}) - V(q - \tfrac{\tau}{2})\right] \tag{2.34}$$

$$m\ddot{\tau} \quad = \quad -\frac{\partial}{\partial q}\left[V(q + \tfrac{\tau}{2}) - V(q - \tfrac{\tau}{2})\right]. \tag{2.35}$$

Since $\frac{\partial(V^+ - V^-)}{\partial \tau} = \frac{1}{2}\frac{\partial(V^+ + V^-)}{\partial q}$, and $\frac{\partial(V^+ - V^-)}{\partial q} = \frac{1}{2}\frac{\partial(V^+ + V^-)}{\partial \tau}$, the two equations almost separate:

$$m\ddot{q} \quad = \quad -\frac{\partial}{\partial q}\frac{1}{2}\left[V(q + \tfrac{\tau}{2}) + V(q - \tfrac{\tau}{2})\right] \tag{2.36}$$

$$m\ddot{\tau} \quad = \quad -\frac{\partial}{\partial \tau}\frac{1}{2}\left[V(q + \tfrac{\tau}{2}) + V(q - \tfrac{\tau}{2})\right]. \tag{2.37}$$

These are apparently Newtonian equations of motion for a particle moving in the average potential

$$\bar{V}(q, \tau) = \tfrac{1}{2}\left[V(q + \tfrac{\tau}{2}) + V(q - \tfrac{\tau}{2})\right], \tag{2.38}$$

when we fix τ or q, respectively. This potential $\bar{V}$ is an even function of τ. (Also note that equations (2.34) and (2.35) revert to two separate copies of Newton's equation of motion, if we change variables back to $x_n = q_n + \tau_n/2$, $\tilde{x}_n = q_n - \tau_n/2$.)

Let us evaluate the classical motion ΔS_{cl}. Using the classical equation of motion (2.34) in the expression (2.30), for the case $\tau'' = 0$ the motion integral (2.26) for the stationary (classical) path becomes

$$
\begin{aligned}
\Delta S_{\rm cl} &= -p'\tau' - \textstyle\int_{t'}^{t''} \Big[V(q+\frac{\tau}{2}) - V(q-\frac{\tau}{2}) \\
&\qquad\qquad -\tau\frac{\partial}{\partial\tau}\left(V(q+\frac{\tau}{2}) - V(q-\frac{\tau}{2})\right)\Big]\, dt. \\
&= -p'\tau' + \textstyle\int_{t'}^{t''} \left[\frac{1}{12}V^{(3)}(q)\tau^3 + \frac{1}{920}V^{(5)}(q)\tau^5 \cdots\right] dt,
\end{aligned}
$$

where the last expression is one-dimensional and $V^{(k)}$ denotes the kth derivative of V. Note that the Legendre transform to replace the variable τ by $\chi = \frac{\partial \Delta V}{\partial \tau}$ in $\Delta V(x,\tau)$ is $U(x,\chi) = \Delta V - \tau \cdot \frac{\partial \Delta V}{\partial \tau} = \Delta V - \tau \cdot \chi$. In these terms, the classical action becomes $\Delta S_{\rm cl} = -p' \cdot \tau' - \int_{t'}^{t''} U\, dt$.

If V is quadratic, the motion $\Delta S_{\rm cl} = -\frac{i}{\hbar} p' \cdot \tau'$. Then by substituting expressions for the respective initial momenta $p' = p'(x''t'', x't')$ into Examples 0,1,2, we easily recover their Blue functions. If V is smooth, with small odd derivatives of order 3 and higher (as for semi-classical WKB approximation), the initial momentum term $-p'\tau'$ dominates the motion integral. This is significant, since we know the paths that contribute most to the path integral $B = \iint \mathcal{D}q\mathcal{D}\tau \exp\{-\frac{i}{\hbar}\Delta S[q(t),\tau(t)]\}$ as in (2.24) are those near the stationary path. So when V is smooth, $B \sim e^{-\frac{i}{\hbar}p'\tau'}$.

Our final classical application is to modify the discrete version of the motion integral (2.30), by using classical path segments between the discrete steps of the Blue path integral [1, p.34]. This is to account for the potential's acting on the particle as it goes from $q_{n-1} \to q_n$ as it follows any path (now not just the classical path). The discrete motion (2.31) corresponds to straight-line (free) motion between steps.

What are the force and initial momentum for the classical short path segment? For fixed τ, the Newtonian equation (2.36) tells us to replace our second difference for $m\ddot{q}$ in

(2.30) by $-\nabla_q \bar{V}$ given in (2.38), where we write $\nabla_q \equiv \partial/\partial q$. For small τ, we note that

$$\begin{aligned} \bar{V} &\approx V(q) \\ -\tau\nabla_q \bar{V} &\approx -\tau\nabla_q V(q) \\ \Delta V(q,\tau) &\approx \quad \tau\nabla_q V(q). \end{aligned} \tag{2.39}$$

Integrating (2.36) twice over a short time $\epsilon = t_n - t_{n-1}$ for time step n, we also get

$$mq_n \quad = \quad mq_{n-1} + p_{n-1}\epsilon - \tfrac{1}{2}\left(\nabla_q \bar{V}\right)\epsilon^2.$$

We solve this for the initial classical momentum p_{n-1} within each interval:

$$p_{n-1} \quad = \quad \tfrac{m(q_n - q_{n-1})}{\epsilon} + \tfrac{\epsilon}{2}\nabla_q \bar{V}. \tag{2.40}$$

For small displacements τ_n, using (2.36) and (2.40) for classical motion between steps, with approximations (2.39), the discrete path sum (2.31) for the motion integral becomes:

$$\begin{aligned} \Delta S(x''\tau''t''; x'\tau't') &= m\tfrac{(q_N - q_{N-1})}{\epsilon} \cdot \tau'' - \tfrac{\epsilon}{2}\Delta V(q_N, \tau'') \\ &\quad - \left[m\tfrac{(q_1 - q_0)}{\epsilon} \cdot \tau' + \tfrac{\epsilon}{2}\Delta V(q_0, \tau')\right] \\ &\quad + \epsilon \cdot \textstyle\sum_{n=1}^{N-1}\left[\nabla_{q_n}\bar{V} - \Delta V(q_n, \tau_n)\right] \\ &\approx p''_{\text{cl}} \cdot \tau'' - p'_{\text{cl}} \cdot \tau' + \epsilon \cdot 0, \end{aligned} \tag{2.41}$$

where the path endpoints are $q_N = x''$ and $q_0 = x'$. The classically interpolated discrete functional for the motion along any path $q(t)$ with a small variation $\tau(t)$ reduces approximately to a function of the endpoints.

2.6 Four-fold path-pair symmetry

Consider the definition of displaced probability (2.2). For any given pair of points $x' \pm \frac{\tau'}{2}$, there are four ways to occupy one or both locations at once. The associated probability $\overline{\mathsf{P}}(x' \pm \frac{\tau'}{2}, t')$ is given by

$$\begin{aligned} \overline{\mathsf{P}}(x' \pm \tfrac{\tau'}{2}, t') &= \tfrac{1}{4}\Big[\mathsf{P}(x't', \tau') + \mathsf{P}(x't', -\tau') + \mathsf{P}(x' + \tfrac{\tau'}{2}, t', 0) + \mathsf{P}(x' - \tfrac{\tau'}{2}, t', 0)\Big] \\ &= \Big|\tfrac{1}{2}\Big[\psi(x' + \tfrac{\tau'}{2}) + \psi(x' - \tfrac{\tau'}{2})\Big]\Big|^2 \geq 0. \end{aligned} \tag{2.42}$$

The first two probabilities in the sum represent wavelike, bilocal presence of the object. As a conjugate pair, their sum may be negative; but in absolute value this never exceeds the sum of the last two probabilities for the usual particle-like, unilocal presence of the object at one of the two locations (and no other). Note that for $\tau' = 0$, the complete probability reduces to the usual probability of location at a single position x'. This is why we normalize it by a factor of 1/4.

Similarly, the path pairs $x(t) \pm \frac{\tau}{2}(t)$ being integrated in the path integral (2.24) for the Blue function also contain a fourfold symmetry. First, clearly there is a spatial mirror symmetry for the displacement $\tau(t)$: the path pair remains the same under the substitution at each point in time

$$\tau(t) \mapsto -\tau(t). \tag{2.43}$$

The two paths are exchanged, keeping the same path pair, but conjugating the motion in the path integral (2.24) for the Blue kernel. The path endpoints are fixed and do not get reflected, so $\tau'' = 0$ at the final endpoint. When we integrate the Blue function over the initial endpoint's spatial values τ' at time t' to propagate as in (2.11), both values $\pm\tau'$ are included, and the entire displaced path and its reflection under (2.43) are present inside the two instances of the Blue kernel. The conjugate displaced probabilities are likewise present with them: $\mathsf{P}(x',\tau',t') = \psi^*(x'-\frac{\tau'}{2})\psi(x'+\frac{\tau'}{2})$, $\mathsf{P}^*(x',-\tau',t') = \psi^*(x'+\frac{\tau'}{2})\psi(x'-\frac{\tau'}{2})$. (If at the final endpoint $\tau'' \neq 0$, to have full symmetry we must include all four final endpoints that comprise the complete probability $\overline{\mathsf{P}}(x'' \pm \frac{\tau''}{2}, t'')$.) Let us label these two path orientations or parametrizations as cases (i) and (ii), respectively. The paths are exchanged under the displacement parity operation (2.43).

Second, each path alone can be obtained as a doubled path or doubly-covered path-pair by the substitution

$$\begin{aligned} \tau'(t) &\mapsto \tilde{\tau}(t) = 0 \\ x'(t) &\mapsto \tilde{x}(t) = x'(t) \pm \tfrac{\tau'}{2}(t) \end{aligned} \tag{2.44}$$

for the + path, or for the - path, respectively. (Again the endpoints are fixed for all paths in one instance of the Blue kernel, but are found mapped this way outside the kernel.) For integration over the initial endpoint, these two path coverings have the associated probabilities $\mathsf{P}(x'-\frac{\tau'}{2},0,t') = |\psi^*(x'-\frac{\tau'}{2})|^2$, and $\mathsf{P}(x'+\frac{\tau'}{2},0,t') = |\psi^*(x'+\frac{\tau'}{2})|^2$. For any path with $\tilde{\tau}(t) = 0$, the motion (2.26) is 0 in the path integral (2.24). Let us call these two path orientations cases (iii) and (iv), respectively. Thus for every physical path pair, four different orientations of the path pair are integrated in the path integral.

Therefore, we may write the propagation formula (2.11) for the four parts of the complete or total probability as a path integral

$$\begin{aligned} \overline{\mathsf{P}}(x'' \pm \tfrac{\tau''}{2}, t'') &= \tfrac{1}{4} \iint dx'd\tau' \int\!\!\int \mathcal{D}q(t)\mathcal{D}\tau(t) \\ &\quad \left| \psi(x'+\tfrac{\tau'}{2}) e^{\frac{i}{2\hbar}\Delta S[q(t),\tau(t)]} + \psi(x'-\tfrac{\tau'}{2}) e^{-\frac{i}{2\hbar}\Delta S[q(t),\tau(t)]} \right|^2. \end{aligned} \tag{2.45}$$

The four-way symmetry is apparent in a familiar and fundamental example:

Example 3. The double slit interference experiment is depicted in figure 2.2. The vertical

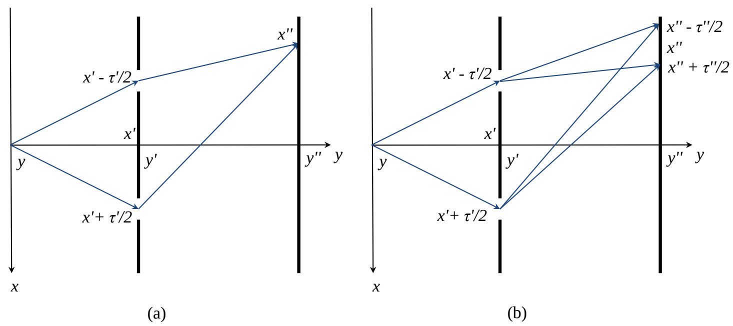

Figure 2.2: Double slit experiment. (a) Single-endpoint probability of arrival ($\tau'' = 0$): There are two wave-like, and two particle-like events. In events (i) and (ii), the particle passes through both slits. In either event, the displaced path-pair probability is complex, showing interference. The two are complex conjugates. In events (iii) and (iv), the particle path passes through one slit or the other, and either path probability is non-negative. (b) Two-endpoint (displaced) probability of arrival ($\tau'' \neq 0$): for the two endpoints, we also have four distinct events or outcomes: two single arrivals, two simultaneous arrivals.

screen in the middle has ∞ potential except at two slits. As drawn, the particle moves free of interactions in the two regions on either side of the screen, propagated by the free Blue kernel (2.13). It departs from a point source at (x', y) at time 0 on the left-hand side, passes through the two small openings in the screen at $(x' \pm \frac{\tau'}{2}, y')$ at time t', and then arrives at point $(x''y'')$ at time t''. We want to calculate the probability of arrival as a function of vertical position x'', using the Blue propagator. From using other methods, we know that the resulting probability or intensity is an interference pattern [1][24]. Moreover, it is natural here to calculate total probabilities of co-arrival at displaced positions $x'' \pm \frac{\tau''}{2}$. Perhaps twin detectors could detect second or fourth-order correlations based on these co-arrival probabilities.

As we just noted, the x, τ parameters for the Blue integral actually specify four alternative pairs of paths the particle can take through the two slits, modeled here simply as point apertures. For our two-leg paths, the permitted path pairs are represented in terms of delta functions for the screen in the middle:

$$\begin{aligned}\alpha(\hat{x},\hat{\tau}) &= \delta(\hat{x}-x')\left[\delta(\hat{\tau}-\tau')+\delta(\hat{\tau}+\tau')\right] \\ &\quad +\delta(\hat{\tau}-0)\left[\delta(\hat{x}-[x'-\tfrac{\tau'}{2}])+\delta(\hat{x}-[x'+\tfrac{\tau'}{2}])\right]. \qquad (2.46)\end{aligned}$$

Let us call $\alpha(\hat{x},\hat{\tau})$ the aperture function. The first two terms correspond to the double-slit paths for $\hat{\tau}=\pm\tau'$. The second two terms are for single-slit paths for $\hat{\tau}=\pm 0$, for which both paths in a pair are the same. (Now the $\frac{\tau'}{2}$ value appears directly, added or subtracted, with x'.) The first leg enroute to the screen begins at the source. Because of the symmetric source-slit configuration we chose, the exponent of the Blue kernel (2.13) is zero, and the four (displaced) probabilities for passage through the slits are all equal to $\left(\frac{m}{2\pi\hbar t'}\right)^3$. For the second leg, the paths can be sifted out of the Blue propagation integral:

$$\mathsf{P}(x''t'',\tau'') = \iint d\hat{x}\,d\hat{\tau}\;\alpha(\hat{x},\hat{\tau})B_0(x''t''\tau'';\hat{x}t'\hat{\tau})\mathsf{P}(\hat{x}t',\hat{\tau}). \qquad (2.47)$$

The free Blue propagator (2.13) is, for three dimensions (see appendix B),

$$B_0(x''t''\tau'';x't'\tau') = \left(\frac{m}{2\pi\hbar T}\right)^3 \exp\left\{\frac{i}{\hbar}\left[m\frac{x''-x'}{T}\right]\cdot\left[\tau''-\tau'\right]\right\}.$$

Here only the x-component of τ' is non-zero. To simplify, we treat the single-endpoint case $\tau''=0$ (figure 2.2a). Then the four parts of the aperture function α result in four displaced probabilities to reach $(x'',y'',0)$, conditional on each path-pair orientation $(\hat{x},\hat{\tau})=$

$(x', \tau'), (x', -\tau'), (x' + \frac{\tau'}{2}, 0), (x' - \frac{\tau'}{2}, 0)$ for cases (i), (ii), (iii), (iv), respectively:

$$\begin{aligned} \mathsf{P}(x''t''0; \hat{x}t'\hat{\tau}) &= B_0(x''t''0; \hat{x}t'\hat{\tau}) \cdot 1 \\ &= \left(\frac{m}{2\pi\hbar T}\right)^3 \cdot \begin{cases} \exp\left\{-\frac{im(x''-x')\tau'}{\hbar T}\right\} & \text{(i)} \\ \exp\left\{+\frac{im(x''-x')\tau'}{\hbar T}\right\} & \text{(ii)} \\ 1 & \text{(iii)} \\ 1 & \text{(iv).} \end{cases} \end{aligned} \tag{2.48}$$

The total probability of arrival at point $(x'', y'', 0)$ in any of the four ways is their sum

$$\mathsf{P}(x''t''0) = 2 + 2\cos\left[\frac{m(x''-x')\tau'}{\hbar T}\right] = 2 + 2\cos\left[\frac{\bar{p}'_x\tau'_x}{\hbar}\right] \tag{2.49}$$

$$= 4\cos^2\left[\frac{m(x''-x')\tau'}{2\hbar T}\right]. \tag{2.50}$$

An easy calculation has led us to the nonnormalizable toy interference pattern, omitting the factor $\left(\frac{m}{2\pi\hbar t'}\right)^3\left(\frac{m}{2\pi\hbar T}\right)^3$ [24]. Based on the Blue function, the phase angles for cases (i) and (ii) of (2.48) have physical meaning as $\pm\frac{m(x''-x')\tau'}{\hbar T} = \pm\frac{p'_x\tau'_x}{\hbar} = \pm k_x\tau'_x$, for vertical wavenumber k_x.

Suppose that at time t' we turn on a linear potential $-fx$ in the region to the right of the slits. This could be done for a charged particle, by placing oppositely charged parallel capacitor plates horizontally (parallel to the yz-plane), one plate above and one plate below the slits. Then we propagate through the region between the plates using the Blue function

B_1 (2.17) from example 1. This modifies the results (2.48) for a free particle as:

$$\begin{aligned}
\mathsf{P}(x''t''\tau''; \hat{x}t'\hat{\tau}) &= B_1(x''t''0; \hat{x}t'\hat{\tau}) \cdot 1 \\
&= \left(\frac{m}{2\pi\hbar T}\right)^3 \cdot \begin{cases} \exp\left\{-\frac{i}{\hbar}\left[\frac{m(x''-x')}{T} - fT\right]\tau'\right\} & \text{(i)} \\ \exp\left\{+\frac{i}{\hbar}\left[\frac{m(x''-x')\tau'}{T} - fT\right]\tau'\right\} & \text{(ii)} \\ 1 & \text{(iii)} \\ 1 & \text{(iv).} \end{cases}
\end{aligned} \tag{2.51}$$

The total probability of arrival at point $(x'', y'', 0)$ now has a phase shift, still consistent with the average initial momentum component $\bar{p}'_x$ departing from the two slits:

$$\mathsf{P}(x''t''0) = 2 + 2\cos\left[\frac{1}{\hbar}\left(\frac{m(x''-x')}{T} - fT\right)\tau'\right] = 2 + 2\cos\left[\frac{\bar{p}'_x \tau'_x}{\hbar}\right]. \tag{2.52}$$

For simplicity, from now on we let x and related quantities be vectors for one particle in Cartesian space of dimension $d = 3$. In only a few cases, for emphasis and clarity, will we use bold type for Cartesian 3-vectors. The generalizations to more degrees of freedom will be evident.

2.7 Equivalence to the continuity equation for the displaced quantum probability current

Just as the Schrödinger equation derives from the path integral for the Green propagator G [1], so also the path integral form of the Blue propagator B implies the corresponding continuity equation for the quantum probability density $\mathsf{P}(x,t) = |\psi(x,t)|^2$ and its probability current density $\mathbf{j} = \frac{\hbar}{2mi}\left(\psi^* \nabla \psi - \psi \nabla \psi^*\right)$:

$$\frac{\partial \mathsf{P}}{\partial t} = -\nabla \cdot \mathbf{j}. \tag{2.53}$$

This familiar equation expresses the local conservation of probability flow as time goes on. In fact, the Blue path integral propagator implies a more general equation, expressing bilocal conservation of the displaced probability flow.

To show this, let us apply the Blue function (2.24) to propagate the displaced probability over a short time step $\epsilon = t'' - t'$:

$$\begin{aligned}
\psi^*(x'' - \tfrac{\tau''}{2}, t'')\psi(x'' + \tfrac{\tau''}{2}, t'') &= \iint \psi^*(x' - \tfrac{\tau'}{2}, t')B(x''t''\tau''; x't'\tau')\psi(x' + \tfrac{\tau'}{2}, t')d\tau' dx' \\
&= \frac{1}{|C(\epsilon)|^2}\int_{-\infty}^{\infty}\int_{-\infty}^{\infty} \psi^*(x' - \tfrac{\tau'}{2}, t')\psi(x' + \tfrac{\tau'}{2}, t') \\
&\qquad \times \exp\left\{\frac{im}{\hbar}\frac{(x'' - x')}{\epsilon} \cdot (\tau'' - \tau')\right\} \\
&\qquad \times \exp\left\{\frac{i\epsilon}{\hbar}\left[V\left(\frac{x'' + x' - \frac{\tau'}{2} - \frac{\tau''}{2}}{2}\right)\right.\right. \\
&\qquad\qquad \left.\left. - V\left(\frac{x'' + x' + \frac{\tau'}{2} + \frac{\tau''}{2}}{2}\right)\right]\right\} d\tau' dx'. \qquad (2.54)
\end{aligned}$$

Denote the corresponding space steps by $\eta = x'' - x'$ and $\beta = \tau'' - \tau'$. The phase of the first exponential above oscillates rapidly, tending to cancel itself unless $m\eta \cdot \beta/\hbar\epsilon < \pi$, or $\eta \cdot \beta < \pi\hbar\epsilon/m$. To first order in the time step ϵ, and therefore to second order in products of η and β, we have for $\nabla = \nabla_{x''}$,

$$\begin{aligned}\psi(x' \pm \tfrac{\tau'}{2}, t') &= \psi(x'' - \eta \pm (\tfrac{\tau''}{2} - \tfrac{\beta}{2}), t') \\ &= \psi(x'' \pm \tfrac{\tau''}{2}, t') - \left(\eta \pm \tfrac{\beta}{2}\right) \nabla\psi(x'' \pm \tfrac{\tau''}{2}, t') \\ &\qquad + \tfrac{1}{2!}\left(\eta \pm \tfrac{\beta}{2}\right)^2 \nabla^2\psi(x'' \pm \tfrac{\tau''}{2}, t').\end{aligned}$$

So to first order in ϵ, the displaced probability inside the integral in equation (2.54) is

$$\begin{aligned}\psi^*(x' - \tfrac{\tau'}{2}, t')\psi(x' + \tfrac{\tau'}{2}, t') &= \psi^*(x'' - \tfrac{\tau''}{2}, t')\psi(x'' + \tfrac{\tau''}{2}, t') \\ &- \left(\eta + \tfrac{\beta}{2}\right)\psi^*(x'' - \tfrac{\tau''}{2}, t')\nabla\psi(x'' + \tfrac{\tau''}{2}, t') \\ &- \left(\eta - \tfrac{\beta}{2}\right)\psi(x'' + \tfrac{\tau''}{2}, t')\nabla\psi^*(x'' - \tfrac{\tau''}{2}, t') \\ &+ \left(\eta^2 - (\tfrac{\beta}{2})^2\right)\left(\nabla\psi^*(x'' - \tfrac{\tau''}{2}, t') \cdot \nabla\psi(x'' + \tfrac{\tau''}{2}, t')\right) \\ &+ \tfrac{1}{2}\left(\eta + \tfrac{\beta}{2}\right)^2 \psi^*(x'' - \tfrac{\tau''}{2}, t')\nabla^2\psi(x'' + \tfrac{\tau''}{2}, t') \\ &+ \tfrac{1}{2}\left(\eta - \tfrac{\beta}{2}\right)^2 \psi(x'' + \tfrac{\tau''}{2}, t')\nabla^2\psi^*(x'' - \tfrac{\tau''}{2}, t'). \qquad (2.55)\end{aligned}$$

To first order in ϵ, the exponential of the potential difference is

$$\begin{aligned}&\exp\left\{\tfrac{i\epsilon}{\hbar}\left[V\left(x'' - \tfrac{\tau''}{2} - \tfrac{1}{2}\left(\eta - \tfrac{\beta}{2}\right)\right) - V\left(x'' + \tfrac{\tau''}{2} - \tfrac{1}{2}\left(\eta + \tfrac{\beta}{2}\right)\right)\right]\right\} \\ &\qquad = 1 + \tfrac{i\epsilon}{\hbar}\left[V\left(x'' - \tfrac{\tau''}{2}\right) - V\left(x'' + \tfrac{\tau''}{2}\right)\right] \\ &\qquad \equiv 1 - \frac{i\epsilon}{\hbar}\Delta V(x'', \tau''), \qquad (2.56)\end{aligned}$$

since we neglect terms of order $\epsilon\eta$ and $\epsilon\beta$. Note that $\epsilon\Delta V = 0$ to first order if $\tau'' = 0$. The left hand side of equation (2.54) can be expressed in terms of the time step ϵ as

$$\begin{aligned}\psi^*(x''-\tfrac{\tau''}{2},t'')\psi(x''+\tfrac{\tau''}{2},t'') &= \psi^*(x''-\tfrac{\tau''}{2},t')\psi(x''+\tfrac{\tau''}{2},t') \\ &\quad +\epsilon\frac{\partial}{\partial t'}\left(\psi^*(x''-\tfrac{\tau''}{2},t')\psi(x''+\tfrac{\tau''}{2},t')\right).\end{aligned}$$

With these approximations, equation (2.54) becomes

$$\begin{aligned}&\psi^*(x''-\tfrac{\tau''}{2},t')\psi(x''+\tfrac{\tau''}{2},t')+\epsilon\frac{\partial}{\partial t'}\left[\psi^*(x''-\tfrac{\tau''}{2},t')\psi(x''+\tfrac{\tau''}{2},t')\right] \\ &= \frac{1}{|C(\epsilon)|^2}\int_{-\infty}^{\infty}\int_{-\infty}^{\infty}\exp\left(\frac{i}{\hbar}\frac{m\eta\cdot\beta}{\epsilon}\right) \\ &\times\left[1-\frac{i\epsilon}{\hbar}\Delta V(x'',\tau'')\right]\left[\psi^*(x''-\tfrac{\tau''}{2},t')\psi(x''+\tfrac{\tau''}{2},t')\right. \\ &+\tfrac{1}{2}\eta\beta\left(\psi^*(x''-\tfrac{\tau''}{2},t')\nabla^2\psi(x''+\tfrac{\tau''}{2},t')\right. \\ &\left.\left.-\ \psi(x''+\tfrac{\tau''}{2},t')\nabla^2\psi^*(x''-\tfrac{\tau''}{2},t')\right)\right]d\beta d\eta \\ &= \left[1-\frac{i\epsilon}{\hbar}\Delta V(x'',\tau'')\right]\psi^*(x''-\tfrac{\tau''}{2},t')\psi(x''+\tfrac{\tau''}{2},t') \\ &-\frac{i\hbar\epsilon}{2m}\nabla\cdot\left[\psi^*(x''-\tfrac{\tau''}{2},t')\nabla\psi(x''+\tfrac{\tau''}{2},t')\right. \\ &\left.-\ \psi(x''+\tfrac{\tau''}{2},t')\nabla\psi^*(x''-\tfrac{\tau''}{2},t')\right].\end{aligned} \tag{2.57}$$

The leading term $\psi^*(x''-\tfrac{\tau''}{2},t')\psi(x''+\tfrac{\tau''}{2},t')$ on the right hand side must have coefficient 1 to agree with the left side . Therefore, the integral of the exponential must equal $|C|^2$, so $|C|^2=\left(\frac{2\pi\hbar\epsilon}{m}\right)^d$ for d Cartesian dimensions. We have used these double integrals for one dimension:

$$\frac{1}{2\pi}\iint e^{-i\eta\beta}d\eta d\beta = \int \delta(\beta-0)d\beta = 1 \tag{2.58}$$

$$\frac{1}{2\pi}\iint \beta^k e^{-i\eta\beta}d\eta d\beta = \int \beta^k\delta(\beta-0)d\beta = 0, \text{ for k} = 1,2 \tag{2.59}$$

$$\frac{1}{2\pi}\iint \eta\beta e^{-i\eta\beta}d\eta d\beta = -i. \tag{2.60}$$

(The last integral can be expressed in terms of imaginary gaussian integrals, since $i\eta\beta = \frac{i}{2}\left[(\eta+\beta/2)^2-(\eta-\beta/2)^2\right]$.) Keeping terms of order ϵ, we use the definition (2.2) of the displaced probability to rewrite (2.57) as the *bicontinuity equation* that generalizes (2.53): for any displacement τ'' about the location x'', at any given time $t' \to t''$,

$$\boxed{\left[\frac{\partial}{\partial t''}-\frac{1}{i\hbar}\Delta V(x''\tau'')\right]\mathsf{P}(x''\tau''t'') = -\nabla_{x''}\cdot\mathbf{j}(x''\tau''t''),} \tag{2.61}$$

where the *displaced current density* is defined as

$$\begin{aligned}\mathbf{j}(x''\tau''t'') &= \frac{\hbar}{2mi}\Big(\psi^*(x''-\tfrac{\tau''}{2},t'')\nabla\psi(x''+\tfrac{\tau''}{2},t'') \\ &\qquad -\psi(x''+\tfrac{\tau''}{2},t'')\nabla\psi^*(x''-\tfrac{\tau''}{2},t'')\Big).\end{aligned} \tag{2.62}$$

For the special case $\tau''=0$, $\Delta V=0$ and $\mathbf{j}$ is the usual, real-valued probability current. We note that P and $\mathbf{j}$, as well as $\frac{1}{i\hbar}\Delta V(x''\tau'')$, are conjugate even functions of τ''; that is, $\mathsf{P}(x'',-\tau'',t'') = +\mathsf{P}^*(x'',\tau'',t'')$ and $\mathbf{j}(x'',-\tau'',t'') = \mathbf{j}^*(x'',\tau'',t'')$. The bicontinuity equation (2.61) can also be derived easily from the Schrödinger equation and its conjugate. However, note that from the displaced probability $\mathsf{P}(x'',\tau'',t'')$ we can recover the wavefunction ψ up to a phase factor. (For $x''=\frac{\tau''}{2}$, we have $\mathsf{P}(x'',\tau'',t'') = \psi^*(0)\psi(\tau'')$.

Also $\mathsf{P}(0,0,t'') = |\psi(0)|^2$.) Therefore the bicontinuity equation is fully equivalent to the Schrödinger equation.

2.8 Wigner density from Blue propagator

There is another thing for us to learn from the short-time path integral (2.54). For simplicity we take the case $\tau'' = 0$, so that $\Delta V = 0$ to first order, as in (2.56). We may interpret $p' = \frac{m\eta}{\epsilon} = \frac{m(x''-x')}{\epsilon}$ as the unique momentum at time t' for the particle at position x'. Again this defines a line through phase space, $\frac{\epsilon}{m}p' + x' = x''$. To first order, the Blue function to propagate over the short time step $\epsilon = t'' - t'$ is just

$$B \;=\; \left(\frac{m}{2\pi\hbar\epsilon}\right)^d \exp\left(-\tfrac{i}{\hbar}p'\cdot\tau'\right). \tag{2.63}$$

Then we may rewrite (2.54) as

$$\begin{aligned}
|\psi(x'',t'')|^2 &= \left(\frac{m}{2\pi\hbar\epsilon}\right)^d \iint \psi^*(x'-\tfrac{\tau'}{2},t')\psi(x'+\tfrac{\tau'}{2},t')\exp\left(-\tfrac{i}{\hbar}p'\cdot\tau'\right)d\tau' d\eta \\
&= \left(\frac{1}{2\pi\hbar}\right)^d \iint \psi^*(x'-\tfrac{\tau'}{2},t')\psi(x'+\tfrac{\tau'}{2},t')\exp\left(\tfrac{i}{\hbar}p'\cdot\tau'\right)d\tau' dp' \\
&= \int_\ell w(x',p')dp'.
\end{aligned} \tag{2.64}$$

Here the Wigner function results naturally as an expression for short-time propagation. As explained in example 0 in section 2.2, we change variables from x' to p', using the line slope $\partial p'_a/\partial x'_a = -m/\epsilon$. Taking the limit as $\epsilon \to 0$, this becomes a vertical line ℓ in phase space that passes through the constant $x' = x''$ on the position axis.

From the Blue function path integral (2.24), we can generalize the Wigner density to a "sum over histories" in phase space, which will propagate the wavefunction probability over a finite time. The basic idea is to consider the initial momentum $p'(x' = x_0, x_1, \epsilon)$ for each path $x(t)$, inside the path integral for the Blue kernel when we propagate the displaced probability. Beginning with (2.11) and (3.85), we have

$$
\begin{aligned}
\mathsf{P}(x''t''\tau'') &= \iint dx' d\tau' \mathsf{P}(x't'\tau') B(x''t''\tau''; x't'\tau') \\
&= \iint dx' d\tau' \mathsf{P}(x't'\tau') \int\!\!\int \mathcal{D}x(t)\mathcal{D}\tau(t) \exp\{-\tfrac{i}{\hbar}\Delta S[x(t), \tau(t)]\} \\
&= \int \mathcal{D}x(t) \int dx' \left[\int \int \mathcal{D}\tau(t) d\tau' \mathsf{P}(x't'\tau') \exp\left\{-\tfrac{i}{\hbar}\Delta S\right\} \right]. \qquad (2.65)
\end{aligned}
$$

In the last path integral above, it may be helpful to consider each initial point as appended to its path given in discrete form. That is, $x' = x_0$ is appended to the path $x(t)$ given as $x_1, \ldots, x_N = x''$. Similarly $\tau' = \tau_0$ is appended to $\tau(t)$.

Each path departs from x' and shortly passes through its specified choice of x_1. Then (2.40) uniquely determines the value p' of the initial momentum, for the classical path segment. The local gradient tensor of the curve ℓ in phase space is

$$
\begin{aligned}
\partial p'/\partial x' &= -m/\epsilon - \frac{\epsilon}{2}\nabla_{x'} \left[\Delta V(x', \tau')\right] \\
&\approx -m/\epsilon - \frac{\epsilon}{2}\nabla^2_{x'} V(x'), \qquad (2.66)
\end{aligned}
$$

for small τ' by (2.39). Let its associated Jacobian be $J'(x', t') = \det|\partial p'/\partial x'|$. Changing the integration variables in (2.65) from x' to p', we have the expression

$$
\begin{aligned}
\mathsf{P}(x''t''\tau'') &= \int \mathcal{D}x(t) \int_{\ell} dp' \\
&\qquad \left[J' \int \int \mathcal{D}\tau(t) d\tau' \mathsf{P}(x't'\tau') \exp\left\{ -\tfrac{i}{\hbar} \Delta S \right\} \right] \\
&= \int \mathcal{D}x(t) \int_{\ell} dp' \mathsf{w}(x'p', [x(t)]).
\end{aligned} \tag{2.67}
$$

To recover the wavefunction probability, above we take the line integral of the Wigner density w along the contour line ℓ through a snapshot of phase space at time t'. The Wigner density is now a functional integral, defined for each path $x(t)$ as

$$
\mathsf{w}(x'p', [x(t)]) = \left[J' \int \int \mathcal{D}\tau(t) d\tau' \mathsf{P}(x't'\tau') e^{-\frac{i}{\hbar}\Delta S} \right]. \tag{2.68}
$$

The displacement paths $\tau(t)$ are being integrated away. Since the integral is again unchanged by reversing the sign of $\tau(t)$, and then equals its own complex conjugate, $\mathsf{w}(x'p', [x(t)])$ is real-valued at each point x', p' in (initial) phase space.

To get a much simpler but approximate expression for (2.68), consider small displacements $\tau(t)$. We expect most of the coherent integration to result from small τ. Using (2.41) in (2.68), we find

$$
\mathsf{w}(x'p', [x(t)]) \approx \left[AJ' \int d\tau' \mathsf{P}(x't'\tau') \exp\left\{ -\tfrac{i}{\hbar} p''_{\text{cl}} \tau'' + p'_{\text{cl}} \tau' \right\} \right]. \tag{2.69}
$$

Refer to (2.41) for details of the classical initial and final momenta p' and p'' along the path $x(t)$. A fine point to note is that again we have reversed the signs of the momenta. This is done after changing variables from x' to p'. Then when we integrate $\int_{\ell} dp'$, p' can go in its usual sense from $p' = -\infty$ to ∞. We have also assumed that normalization makes $\oint \mathcal{D}\tau(t) = A$, a scalar constant. The total integral of (2.67) with (2.69) must be nearly 1.

2.9 What is a Blue function?

The propagator G is the Green function for the Schrödinger equation. It has the property that

$$\left(i\hbar\frac{\partial}{\partial t''} - H\right) G(x''t''; x't') = -i\hbar\delta(t''-t')\delta(x''-x'). \tag{2.70}$$

What property characterizes the Blue function B, and what equation is it associated with?

Let us write out the property (2.70) for both G and its complex conjugate G^*, including the initial and final translations by $\pm\frac{\tau'}{2}$ and $\pm\frac{\tau''}{2}$, respectively. As a shorthand, put $G_\pm = G(x'' \pm \frac{\tau''}{2}, t''; x' \pm \frac{\tau'}{2}, t')$. Then

$$\begin{aligned}
\frac{\partial G_+}{\partial t''} + \frac{\hbar}{2im}\nabla^2_{x''}G_+ - \frac{1}{i\hbar}V(x''+\tfrac{\tau''}{2})G_+ &= -\delta(t''-t')\delta(x''-x'+\tfrac{\tau''}{2}-\tfrac{\tau'}{2}) \\
\frac{\partial G_-^*}{\partial t''} - \frac{\hbar}{2im}\nabla^2_{x''}G_-^* + \frac{1}{i\hbar}V(x''-\tfrac{\tau''}{2})G_-^* &= -\delta(t''-t')\delta(x''-x'-\tfrac{\tau''}{2}+\tfrac{\tau'}{2})
\end{aligned}$$

Multiply the two equations by G_-^* and G_+, respectively,

$$\begin{aligned}
G_-^*\frac{\partial G_+}{\partial t''} + \frac{\hbar}{2im}G_-^*\nabla^2_{x''}G_+ - \frac{1}{i\hbar}V(x''+\tfrac{\tau''}{2})G_-^*G_+ &= -\delta(x''-x'-\tfrac{\tau''}{2}+\tfrac{\tau'}{2})\delta(t''-t') \\
&\quad \times\delta(x''-x'+\tfrac{\tau''}{2}-\tfrac{\tau'}{2}) \\
G_+\frac{\partial G_-^*}{\partial t''} - \frac{\hbar}{2im}G_+\nabla^2_{x''}G_-^* + \frac{1}{i\hbar}V(x''-\tfrac{\tau''}{2})G_-^*G_+ &= -\delta(x''-x'+\tfrac{\tau''}{2}-\tfrac{\tau'}{2})\delta(t''-t') \\
&\quad \times\delta(x''-x'-\tfrac{\tau''}{2}+\tfrac{\tau'}{2}),
\end{aligned}$$

using the fact that as $t'' \to t'$, $G(x''t'', x't') \to \delta(x'' - x')$. Then add the two equations:

$$\begin{aligned}\left(\frac{\partial}{\partial t''} - \frac{1}{i\hbar}\Delta V\right) G_-^* G_+ + \frac{\hbar}{2im}\left(G_-^* \nabla_{x''}^2 G_+ - G_+ \nabla_{x''}^2 G_-^*\right) &= -2\delta(x'' - x' + \tfrac{\tau''}{2} - \tfrac{\tau'}{2})\delta(t'' - t') \\ &\quad \times \delta(x'' - x' - \tfrac{\tau''}{2} + \tfrac{\tau'}{2}),\end{aligned}$$

where ΔV is as defined in equation (2.56). We may write this as

$$\begin{aligned}\left(\frac{\partial}{\partial t''} - \frac{1}{i\hbar}\Delta V\right) B(\tau') + \nabla_{x''} \cdot \mathbf{B}(\tau') &= -2\delta(t'' - t')\delta(x'' - x' + \tfrac{\tau''}{2} - \tfrac{\tau'}{2}) \\ &\quad \times \delta(x'' - x' - \tfrac{\tau''}{2} + \tfrac{\tau'}{2}), \qquad (2.71)\end{aligned}$$

where we define the Blue current density propagator

$$\mathbf{B}(\tau') = \frac{\hbar}{2im}\left[G_-^* \nabla_{x''} G_+ - G_+ \nabla_{x''} G_-^*\right]. \qquad (2.72)$$

Equation (2.71) characterizes the Blue matter probability density kernel and its associated Blue current density kernel for each value of τ'.

We can integrate (2.71) over τ', putting $b(x''t''\tau''; x't') = \int B(x''t''\tau''; x't'\tau')d\tau'$ and $\mathbf{b}(x''t''\tau''; x't') = \int \mathbf{B}(x''t''\tau''; x't'\tau')d\tau'$. Both integrals are real-valued, because they do not change under the spatial-displacement reversal path substitution $\tau(t) \mapsto -\tau(t)$, thus equal their own complex conjugates. Since $\int \delta(a - y)\delta(y - b)dy = \delta(a - b)$, the right hand side of (2.71) integrates to $\int \delta(x'' - x' + \left[\frac{\tau''}{2} - \frac{\tau'}{2}\right]) \cdot \delta(x'' - x' - \left[\frac{\tau''}{2} - \frac{\tau'}{2}\right])d[\tau' - \tau'']/2 \cdot 2 = 2\delta(2(x'' - x')) = \delta(x'' - x')$. The result is that

$$\left(\frac{\partial}{\partial t''} - \frac{1}{i\hbar}\Delta V\right) b + \nabla_{x''} \cdot \mathbf{b} = -\delta(t'' - t')\delta(x'' - x'). \qquad (2.73)$$

The *integrated* probability and current density kernels are real-valued *Green* functions for the operator of the generalized continuity equation (2.61).

The kernel $\mathbf{B}$, in effect, propagates the current density to $(x''t'')$:

$$\iint dx'd\tau'\psi^*(x'-\tfrac{\tau'}{2})\mathbf{B}(x''t''\tau'';x't'\tau')\psi(x'+\tfrac{\tau'}{2})$$

$$=\frac{\hbar}{2im}\iint dx'd\tau'\ \psi^*(x'-\tfrac{\tau'}{2})\left[G_-^*\nabla_{x''}G_+ - G_+\nabla_{x''}G_-^*\right]\psi(x'+\tfrac{\tau'}{2})$$

$$=\frac{\hbar}{2im}\iint dr'ds'\psi^*(r')\Big[G^*(x''-\tfrac{\tau''}{2},r')\nabla_{x''}G(x''+\tfrac{\tau''}{2},s')$$

$$-G(x''+\tfrac{\tau''}{2},s')\nabla_{x''}G^*(x''-\tfrac{\tau''}{2},r')\Big]\psi(s')$$

$$=\frac{\hbar}{2im}\Big[\psi^*(x''-\tfrac{\tau''}{2},t'')\nabla_{x''}\psi(x''+\tfrac{\tau''}{2},t'')-\psi(x''+\tfrac{\tau''}{2},t'')\nabla_{x''}\psi^*(x''-\tfrac{\tau''}{2},t'')\Big]$$

$$\equiv \mathbf{j}(x''t''\tau''), \quad (2.74)$$

where we change variables as we did in (2.11), to $r'=x'-\frac{\tau'}{2}$, $s'=x'+\frac{\tau'}{2}$.

Like B, the kernel function $\mathbf{B}$ actually operates on the displaced probability density $\mathsf{P}(x't',\tau')=\psi^*(x'-\frac{\tau'}{2})\psi(x'+\frac{\tau'}{2})$ to produce the current at the spacetime point $x''t''$; it does not operate on the current itself. Therefore we can express both the Blue function and probability density as non-Lorentzian 4-vectors $B^\mu=(B,\mathbf{B})$ and $j^\mu=(\mathsf{P},\mathbf{j})$, and in compact notation the complete probability propagation update is

$$j^\mu(x''t''\tau'')=\iint B^\mu(x''t''\tau'';x't'\tau')\cdot\mathsf{P}(x't',\tau')\ d\tau'\ dx'. \quad (2.75)$$

We can also develop the path integral for the Blue current density propagator, much as we did for the Blue probability density propagator. We return to its definition (2.72) above. Consider the product (2.23) of two path integrals for B, before changing variables. Now we must apply $\nabla_{x''}$ to G_+ and then to $-G_-^*$. This merely multiplies the path integrand for

$G_-^* G_+$ in (2.23) by the sum

$$\frac{im}{\hbar\epsilon}\left(\tilde{x}_N - \tilde{x}_{N-1}\right) - \frac{im\epsilon}{\hbar}\nabla_{x''}V(\tfrac{1}{2}[\tilde{x}_N + \tilde{x}_{N-1}])$$

$$+\frac{im}{\hbar\epsilon}\left(x_N - x_{N-1}\right) - \frac{im\epsilon}{\hbar}\nabla_{x''}V(\tfrac{1}{2}[x_N + x_{N-1}]). \tag{2.76}$$

After changing variables as in (2.24), and multiplying by the current coefficient $\frac{\hbar}{2im}$, this sum becomes

$$\frac{\left(q_N - q_{N-1}\right)}{\epsilon} - \epsilon\nabla_{x''}\bar{V}(\bar{q}_N, \bar{\tau}_N), \tag{2.77}$$

using the average potential $\bar{V}$ defined in (2.38). But in the limit as the time increment $\epsilon \to 0$, the term with the potential gradient on the right hand side of (2.77) will vanish. Then the current kernel is just the B path integrand times $\left(q_N - q_{N-1}\right)/\epsilon$, or formally $\dot{\mathbf{q}}'' = \mathbf{p}''/m$. So the formal expression for the current kernel path integral is

$$\mathbf{B}(\tau') \quad = \quad \frac{1}{m}\iint \mathbf{p}'' e^{i\Delta S/\hbar}\mathcal{D}\mathbf{q}(t)\mathcal{D}\boldsymbol{\tau}(t). \tag{2.78}$$

This result, for any discrete path, agrees with the fact that, for the continuous action along the classical (stationary) path, $\partial S_{\text{cl}}/\partial x'' = p''$, the final momentum [1][16]. This path integral (3.53) for $\mathbf{B}$, with the probability density kernel B (3.85) and the displaced action (2.26), gives us all four components of the complete Blue propagator kernel.

Having a way to propagate current, suggests that there may be a Wigner current density, which we could find along the lines of section 2.8.

2.10 Conclusion

In this chapter, we have adopted a displacement concept of Weyl and Wigner to take a fresh look at probability propagation in its own right. We found that, in this context, Blue propagators replace Green propagators. They are given by path integrals where the action is replaced by a simpler line integral we called the motion, or displaced action. The complete set of four Blue functions acts on the displaced probability density, to propagate not only the probability density, but also the current density vector.

We found that the displaced current density is bi-locally conserved via a generalized continuity equation. A four-way symmetry was noted for the path pairs over which the the Blue kernel is integrated. This symmetry was illustrated by the double slit experiment. We showed that the Wigner density occurs naturally as an expression for physical probability propagation. Looking ahead, we hope to use a space-time four-vector displacement τ to extend Blue propagators to relativistic, many-particle field theories.

Chapter 3: A Bilocal Picture of Quantum Mechanics

A new, bilocal picture of quantum mechanics is developed. We show that Born's rule supports a virtual probability for a particle to arrive, as a wave, at any two locations (but no more). We discuss two ways to implement twin detectors suitable for detecting bilocal arrivals. The bilocal picture sheds light on currents in quantum mechanics. We find there are two types of bilocal current density, whose polar form and related mean velocities are given. In the bilocal context, the definitions of both current types simplify. In the unilocal case, the two types become the usual current and a fluctuation current. Their respective mean velocity fields are the usual de Broglie-Madelung-Bohm velocity and the imaginary (osmotic) velocity. We obtain a new, probabilistic Schrödinger equation for the bilocal probability by itself, solve the example of a free particle, develop the dyadic stationary states, and find that the von Neumann equation for time-varying density of states follows directly from the new equation. We also show how to include the electromagnetic potentials in this probabilistic Schrödinger equation.

3.1 Introduction

The right transformation of variables or operators can interact with an equation of physics in a striking way, bringing insights that we would not have expected from the simplicity of the transformation itself. Examining an equation or theory, we may see that it contains a symmetry or an implicit invariant form which enables us to simplify the equation and perhaps solve it in some circumstances.

The transformation we take up in this chapter concerns how events at two locations q_1, q_2 and at one time are related. In [25] and chapter 2, we saw that this simple change of the two variables is important for propagating probability:

$$\begin{aligned} q_1 &= x - \tfrac{\tau}{2} \\ q_2 &= x + \tfrac{\tau}{2}. \end{aligned} \tag{3.1}$$

The goal of this chapter is to extend the theory of probability and current density propagators in chapter 2 [25], to develop a bilocal picture of quantum mechanics.

This change of variables (3.1) was introduced in the quantum density matrix transform of Weyl and Wigner [4][5][25]. Since $x = \frac{1}{2}(q_1 + q_2)$, and $\tau = (q_2 - q_1)$, x is the centroid and τ is the separating distance. This change of variables (for space-time coordinates) is also used in quantum nonequilibrium dynamics, where it is known as the Keldysh rotation [26, below eq.(61)][27] [28, Ch.5] [29].

The bilocal transformation (3.1) is very close to the familiar change of variables used in classical mechanics to find the motion of two attracting or repelling bodies, whose interaction potential depends only on their separating distance. We transform their position vectors into their center of mass and a separation vector. This transformation reduces the problem of two bodies to that of one body with reduced mass in a central force field [30]. Bilocal field theories of Yukawa and others, prior to string theory, proposed similar two-location systems to model a particle as a body that occupies a finite spacetime region [31][32]. The subject of this chapter, however, is unrelated to these relativistic theories.

Changing a Lagrangian into a Hamiltonian, by means of Legendre transformations, is a very general transformation that is also familiar to us. This doubles the number of independent variables, changing from configuration space to phase space, and reduces each second-order equation of motion into two first-order equations. We found in [25] that including the change of variables (3.1), to form the probability propagator, produced the difference of displaced Lagrangians.

In this chapter, our aim is to develop a picture of quantum mechanics that emphasizes its inherently bilocal aspects. We show that, given several possible events, Born's rule (if it is exactly true) implies that they can interfere at most in pairs. For example, the amplitudes for a particle to arrive at two locations at once can interfere. But for three or more locations, the amplitudes can only interfere in pairs. We also study bilocal currents, leading us to two types of current. We find an analog of the Schrödinger equation, for the bilocal probabilities instead of amplitudes. At this early stage, it appears that the value of this bilocal picture may rest in the theoretical insights that a new perspective on standard quantum mechanics offers. Occasionally, it may provide simpler formulas to work with.

3.1.1 Chapter overview

An outline of the bilocal picture of quantum mechanics initiated in [25] is presented in section 3.2. The rest of the chapter unfolds basic principles of the bilocal picture. Section 3.3 gives a careful analysis of bilocal probability, based on Born's rule. In section 3.4, the usual polar form of de Broglie-Bohm velocity and associated current is generalized to the bilocal case. Section 3.5 introduces a new, bilocal fluctuation-current density. In particular, this leads to the well-known osmotic velocity field, and a simple new expression for the usual current density in quantum mechanics. Section 3.6 presents a bilocal probabilistic Schrödinger equation for the bilocal probability density, and also develops that equation for an external electromagnetic field. We conclude in section 3.7.

3.2 A bilocal picture of quantum mechanics

To propagate the probability and current densities of a quantum particle, we can use a bilocal equivalent of the Schrödinger picture, introduced in [25] and in chapter 2. We briefly review its basic elements, as follows.

Consider a quantum-mechanical particle whose state is spatially represented by a wavefunction $\psi(x)$. We begin with the *displaced* (bilocal) probability density for the simultaneous arrival of the particle at time t at two places $q_1, q_2 = x \pm \frac{\tau}{2}$,

$$\mathsf{P}(xt,\tau) \quad = \quad \psi^*(x - \tfrac{\tau}{2}, t)\psi(x + \tfrac{\tau}{2}, t). \tag{3.2}$$

It is complex-valued and thus is only a quasi-probability density; but for spacing $\tau = 0$ it reduces to the real-valued probability of arrival $|\psi(x,t)|^2$. It has an associated displaced (bilocal) current density

$$\begin{aligned} \mathsf{j}(xt,\tau) \quad = \quad & \frac{\hbar}{2im}\left[\psi^*(x-\tfrac{\tau}{2},t)\nabla_x\psi(x+\tfrac{\tau}{2},t)\right. \\ & \left. -\psi(x+\tfrac{\tau}{2},t)\nabla_x\psi^*(x-\tfrac{\tau}{2},t)\right]. \end{aligned} \tag{3.3}$$

The bilocal probability and current densities in equations (3.2) and (3.3) together satisfy a continuity equation,

$$\left[i\hbar\frac{\partial}{\partial t} - \Delta V(xt,\tau)\right]\mathsf{P}(xt,\tau) \quad = \quad -i\hbar\nabla_x \cdot \mathsf{j}(xt,\tau), \tag{3.4}$$

where we define

$$\Delta V(xt,\tau) \quad = \quad V\left(x + \tfrac{\tau}{2}, t\right) - V\left(x - \tfrac{\tau}{2}, t\right) \tag{3.5}$$

and V is the possibly time-dependent potential. For a particle of charge e in an electromagnetic field with scalar electric potential ϕ and vector magnetic potential A, we replace the momentum gradients $-i\hbar\nabla_x$ in the first and second terms of the current (3.3) by $-i\hbar\nabla_x - \frac{e}{c}A\left(x \pm \frac{\tau}{2}, t\right)$, respectively, and we replace V by ϕ in (3.5) [1].

This equation (3.4) was shown in [25] and in chapter 2 to be equivalent to the Schrödinger equation.[1] Both equations employ the energy and momentum operators, but equation (3.4)

[1] Errata in [25]: (i) formula (55): ΔV should match its definition in (26) and here; (ii) equations (67), (69): add the term $-\frac{1}{i\hbar}\Delta V \cdot B(\tau)$ (respectively $-\frac{1}{i\hbar}\Delta V \cdot b$) to the left hand side.

is a first order equation instead of second order. Equation (3.4) is bilocal, but simpler than the two Madelung equations for quantum mechanics. For $\tau = 0$, (3.4) reduces to the usual single-location continuity equation, which is the first Madelung equation. But as is characteristic of hydrodynamical equations, the second Madelung equation has several terms [33][58, problem 4.2].

3.2.1 Probability and current density propagators

The solution of the Schrödinger equation at time $t' \geq t$ is

$$\psi(x't') = \int dx \;\; G(x't';xt)\psi(xt), \tag{3.6}$$

for a Green kernel function G, given as a path integral in [1]. The solution of the bilocal continuity equation (3.4) at time $t' \geq t$ is

$$\mathsf{P}(x't',\tau') = \iint dx\, d\tau \; B(x't'\tau';xt\tau)\mathsf{P}(xt,\tau) \tag{3.7}$$

$$\mathsf{j}(x't',\tau') = \iint dx\, d\tau \; \mathbf{B}(x't'\tau';xt\tau)\mathsf{P}(xt,\tau), \tag{3.8}$$

for Blue kernel functions $B, \mathbf{B}$, given as path integrals in [25] and chapter 2. The Green kernel propagates the wavefunction. The Blue kernels propagate the displaced probability density, as well as the current density.

If there is no potential field ($V = 0$), the free Green propagator is [1]

$$\begin{aligned} G_0(x't';xt) &= \langle x't' \,| xt \rangle \\ &= \left(\tfrac{m}{2\pi i\hbar T}\right)^{\frac{3}{2}} \exp\left\{\tfrac{im}{2\hbar T}|x'-x|^2\right\}. \end{aligned} \tag{3.9}$$

where $T = t' - t$ is the elapsed time. The free Blue probability propagator is [25]

$$B_0(x't'\tau'; xt\tau) \quad = \quad \left(\tfrac{m}{2\pi\hbar T}\right)^3 \exp\left\{\tfrac{im}{\hbar T}(x'-x)\cdot(\tau'-\tau)\right\}, \tag{3.10}$$

and the free current propagator is $\mathbf{B}_0 = \mathbf{v}B_0^0$, where $\mathbf{v}^k = \frac{(x'-x)^k}{T}$ for $k = 1,2,3$ (see appendix B). Green and Blue propagators for quadratic and other potentials are given in [1], and in [25] and chapter 2, respectively.

3.2.2 Completeness properties for the propagators

We can propagate the bilocal probability and current density in two path legs or stages in succession. For example, this is useful for a particle that propagates through a slit. We split the time interval $[t, t'']$ at the time t' (such that $t \leq t' \leq t''$) when the particle arrives at the slits, and likewise split the path integral kernel into two parts, using the property that

$$B(x''t''\tau''; xt\tau) \quad = \quad \iint dx'\, d\tau'\; B(x''t''\tau''; x't'\tau')B(x't'\tau'; xt\tau). \tag{3.11}$$

This property follows from the path integral for the Blue function, given by equation (24) in [25]. This property allows us, for example, to insert an aperture or window function to represent two slits at the time t', to restrict the possible paths from source to detector to those passing through the twin slits.

The current blue function $\mathbf{B}$ satisfies a similar, but mixed, completeness property that follows from its path integral, as expressed by equation (74) in [25] and (3.53) in chapter 2:

$$\mathbf{B}(x''t''\tau''; xt\tau) \quad = \quad \iint dx'\, d\tau'\; \mathbf{B}(x''t''\tau''; x't'\tau')B(x't'\tau'; xt\tau). \tag{3.12}$$

For the potential-free case, with $\mathbf{B}_0 = \mathbf{v}''B_0$, the key difference in splitting this current propagator (versus splitting the probability propagator (3.11)) is that the final endpoint velocity factor $\mathbf{v}''$ only occurs in the later path segment.

3.3 Elementary probability theory for the wavefunction of a particle

We have just seen that, to propagate the wavefunction's real-valued probability density into the future, it is necessary and sufficient to operate upon the complex-valued probability density (3.2) given at the present time t [25]. The integral operator with its four-component Blue kernel acts on (3.2), to give the future probability and current density. In this sense, the displaced probability density (3.2) provides operational closure. Its central role in probability propagation suggests that it should have physical meaning. We will see that its real part (times two) may be interpreted as a signed, *virtual probability* of self-interference, which occurs during the wavefunction's collapse to produce the observed probability of detection.

For any two locations 1 and 2, given by coordinates $q_1, q_2 = x \pm \frac{\tau}{2}$, there are four ways for the particle to arrive in one or both locations at once, as shown in figure 3.1. It may behave like a particle, arriving at either place (left side and center of figure 3.1), with probability elements $\mathsf{P}_1 \equiv \mathsf{P}(x + \frac{\tau}{2}, t)\mathrm{d}^3x$ and $\mathsf{P}_2 \equiv \mathsf{P}(x - \frac{\tau}{2}, t)\mathrm{d}^3x$ to arrive (and be detected) at one of the two locations. The quantum-mechanical particle may also behave like a wave, arriving at both places simultaneously (right side of figure 3.1). This arrival may be considered to occur in two ways, oriented in an up (1,2) or down (2,1) sense, with respective probability elements denoted by $\mathsf{P}_{12} \equiv \mathsf{P}(xt, \tau)\mathrm{d}^3x$ and $\mathsf{P}_{21} \equiv \mathsf{P}(xt, -\tau)\mathrm{d}^3x$. From (3.2), these two quasi-probabilities or interference terms are complex conjugates: $\mathsf{P}_{21} = \mathsf{P}_{12}^*$.

Suppose that we place a detector at each of the two locations. For two single (independent) detectors, as shown in figure 3.2, the associated total probability element $\mathsf{P}(x \pm \frac{\tau}{2}, t)\mathrm{d}^3x$ for the particle to arrive (and be detected) at one of the two locations (not both), each with

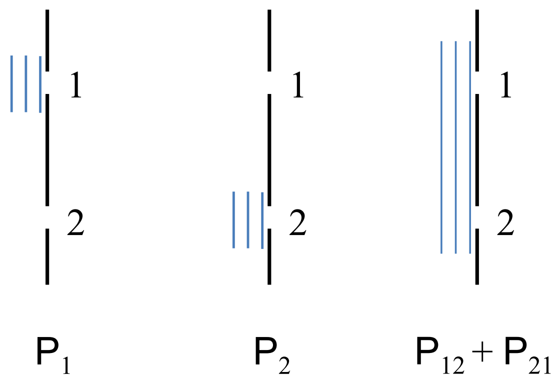

Figure 3.1: Bilocal events, for locations 1 and 2 at time t, and a particle depicted as a wavefront: (left) particle arrives at 1 with probability P_1; (center) particle arrives at 2 with probability P_2; (right) particle arrives at both 1 and 2 (wavelike arrival) with virtual probability $\mathsf{P}_{12}+\mathsf{P}_{21}$. The combined event of arrival at 1 or 2 or both has probability given by the sum $\bar{\mathsf{P}}_{1,2}=\mathsf{P}_1+\mathsf{P}_2+(\mathsf{P}_{12}+\mathsf{P}_{21})$, equation (3.15). The event of wavelike arrival at both locations (right) is considered to be a virtual event, which occurs only with the single-location events. If, by some means, we can determine which location the particle passed through, the virtual probability vanishes (i.e., $(\mathsf{P}_{12}+\mathsf{P}_{21})=0$, resulting in equation (3.13)). In this chapter, we consider these probability densities, as well as the current densities j and mean velocities v associated with these events.

volume element d^3x, is given by

$$\begin{aligned}\mathsf{P}(x\pm\tfrac{\tau}{2},t)\,\mathrm{d}^3x &= \mathsf{P}(x+\tfrac{\tau}{2},t,0)\mathrm{d}^3x+\mathsf{P}(x-\tfrac{\tau}{2},t,0)\mathrm{d}^3x &(3.13)\\ &= \left|\psi(x+\tfrac{\tau}{2})\right|^2\mathrm{d}^3x+\left|\psi(x-\tfrac{\tau}{2})\right|^2\mathrm{d}^3x. &(3.14)\end{aligned}$$

We can also conjoin the two detectors to make a double detector, as shown in figure 3.2 on the right, so that the particles arriving at either location are counted together.The associated total probability $\overline{\mathsf{P}}(x\pm\frac{\tau}{2},t)\mathrm{d}^3x$ to arrive and be detected at one or both locations is given by

$$\begin{aligned}\overline{\mathsf{P}}(x\pm\tfrac{\tau}{2},t)\mathrm{d}^3x &= \mathsf{P}(x+\tfrac{\tau}{2},t,0)\mathrm{d}^3x+\mathsf{P}(x-\tfrac{\tau}{2},t,0)\mathrm{d}^3x\\ &\quad+\mathsf{P}(xt,\tau)\mathrm{d}^3x+\mathsf{P}(xt,-\tau)\mathrm{d}^3x &(3.15)\\ &= \left|\psi(x+\tfrac{\tau}{2})+\psi(x-\tfrac{\tau}{2})\right|^2\mathrm{d}^3x\geq 0. &(3.16)\end{aligned}$$

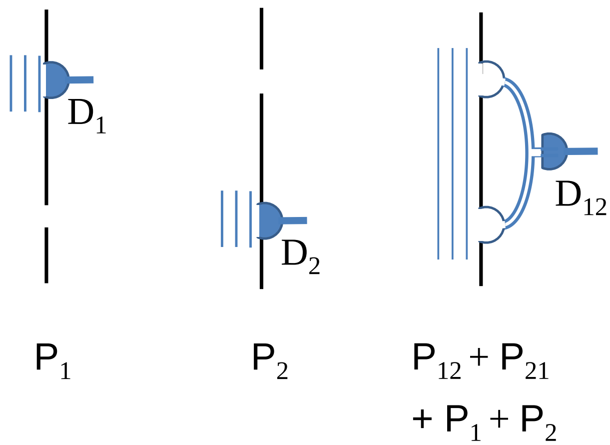

Figure 3.2: Single and double detector configurations: (*left and center*) A separate single detector counts particle-like arrivals at either port, 1 or 2, but not both. Thus we can distinguish by which of the two ports the particle arrived. But the single detectors are, by default, unresponsive to the particle's arrival via both ports at once, a third though virtual event. (*right*) A pair of conjoined detectors, i.e., a two-port or twin detector, is compliant with wave-like arrivals of the particle. It counts an arrival through either or both ports. Thus the twin detector supports the particle's virtual arrival via both ports at once. But the twin detector can only sense the occurrence of one of the three mutually exclusive events (the detection probability is a sum, as annotated above). It cannot distinguish which port or ports the particle passes through, 1 or 2 or both.

Of the four probabilities summed above, we of course recognize the first two from equation (3.13), as those of arriving at a single location. The last two probabilities in the sum (3.15) represent wavelike, bilocal presence of the object. As a conjugate pair, their sum may be negative; but in absolute value this never exceeds the sum of the first two probabilities for the usual particle-like, unilocal presence of the object at one of the two locations.

The total bicurrent $\bar{\mathsf{j}}(x \pm \frac{\tau}{2}, t)$ passing into the twin detectors is a new quantity, defined by

$$\begin{aligned} \bar{\mathsf{j}}(x \pm \tfrac{\tau}{2}, t) &= \tfrac{\hbar}{2mi} \left\{ \left[\psi(x+\tfrac{\tau}{2}) + \psi(x-\tfrac{\tau}{2})\right]^* \nabla_x \left[\psi(x+\tfrac{\tau}{2}) + \psi(x-\tfrac{\tau}{2})\right] \right. \\ & \qquad \left. - \left[\psi(x+\tfrac{\tau}{2}) + \psi(x-\tfrac{\tau}{2})\right] \nabla_x \left[\psi(x+\tfrac{\tau}{2}) + \psi(x-\tfrac{\tau}{2})\right]^* \right\} \quad (3.17) \\ &= \mathsf{j}(x+\tfrac{\tau}{2}, t, 0) + \mathsf{j}(x-\tfrac{\tau}{2}, t, 0) + \mathsf{j}(xt, \tau) + \mathsf{j}(xt, -\tau). \quad (3.18) \end{aligned}$$

The expression for total bicurrent splits into a sum of two usual currents (one at each location) and two conjugate displaced currents of form (3.3) for simultaneous, wavelike arrival at both locations. This sum (3.18) of four currents is analogous to the sum (3.16) for total probability for arrival at one or both detectors.[2]

3.3.1 Implementing the twin detector

There are doubtlessly various ways to implement the twin detector. For example, for photons, the two small ports could be coupled by means of two optic fiber couplers which feed into the input ports of an in-fiber beamsplitter. Its combined output from one port is then fed into a single detector. (Half of the photons are lost through the unused beamsplitter out-port.) This scheme is depicted in figure 3.2 on the right, without the beamsplitter.

A second way to implement the twin detector is essentially to combine the two paths by a lens, instead of a beamsplitter. This configuration is the same as that of a Michelson stellar interferometer (which, by rough analogy, inspired Ramsey to design his twin-pulse molecular beam apparatus [35][24]).

A third way to implement the twin detector is to modify a cooled two-dimensional CCD focal plane array of small square pixels of side Δs. The $N \times N$ CCD array would be replaced by a one-dimensional $1 \times N$ array of long rectangular pixels, occupying the same area as the two-dimensional array. Every column of distinct pixels in the two-dimensional array is fused in effect, to respond as though it were one pixel with the same width Δs as the original, but with length equal to the length $N\Delta s$ of the entire CCD array. A mask or reticle is placed over the new CCD photosensor array, having two square slits, both of the size Δs of the original square pixels. Both slits expose the same column pixel, and are separated by a distance τ in the vertical dimension. To collect a spatial probability density, this mask could be moved by steps of size Δs down a given column. Thus the one-dimensional columnar

[2] The total bicurrent easily extends to a total multicurrent, impinging on an array of many detector pairs located about their center x. We replace the wavefunction sum $\left[\psi(x+\frac{\tau}{2})+\psi(x-\frac{\tau}{2})\right]$ by the sum $\sum_{k=1}^{K}\left[\psi(x+\tau_k/2)+\psi(x-\tau_k/2)\right]$ everywhere inside the total current expression defined above.

CCD array with double slit mask implements a twin detector in the selected column pixel that receives the photon.

3.3.2 Virtual probability of interference

Next we present an argument to justify calling the real part of (3.2) (times two) a virtual probability. Let A be the event that the particle arrives at location 1, given by $q_1 = x + \frac{\tau}{2}$, and let B be the event that the particle arrives at location 2, given by $q_2 = x - \frac{\tau}{2}$, at the same time t. We regard these events or outcomes as sets, that belong to a suitable algebra of measurable events. In Born's interpretation of quantum mechanics, an event may be observed if and only if it has a state with a complex probability amplitude, unique up to a global phase shift of all base states. The associated probability of observing the event is the squared magnitude of the amplitude. Moreover, there is a well-known "which-way" rule. If we cannot physically distinguish the several sources or precursors of an event, we add their amplitudes before squaring the sum. Otherwise, if we can determine the sources, we square their amplitudes first, and then add the probabilities [36, vol. III].

In general, events A and B have a non-empty intersection, $A \cap B$. But we can express their union as a union of disjoint events:

$$A \cup B = (A \cap B) \cup (A \cap B^c) \cup (A^c \cap B), \tag{3.19}$$

where A^c is the complement of A. One may think of A^c as the non-event that event A does not occur, $A \cup B$ as the event that A or B or both occur, and $A \cap B$ as the event that events A and B both occur. Often $A \cap B^c$, the event that A occurs but B does not, is written as $A - B$. We assume that the probability P is an additive measure: for any two disjoint sets C and D, we have $\mathsf{P}(C \cup D) = \mathsf{P}(C) + \mathsf{P}(D)$.[3] But here we do not assume that the probability P is nonnegative, only that it is real-valued. Thus the measure P is not monotone or subadditive; *e.g.,* if $B \subseteq A$, we may not have $\mathsf{P}(B) \leq \mathsf{P}(A)$, as we will see.

[3] Since $(A \cap B^c) \cup (A \cap B) = A$, identity (3.19) immediately implies the familiar inclusion-exclusion

Table 3.1: Particle arrival events in equation (3.19). Event A is arrival at location 1, given by its point coordinates $q_1 = x + \frac{\tau}{2}$. Event B is arrival at location 2, given by $q_2 = x - \frac{\tau}{2}$. The events in the first three rows of this table are real or actual events, i.e. those that have unique amplitudes and can be observed. The event $A \cap B$ is considered virtual because it is not observed directly, but is expressible as a residue of real events. Its virtual probability density (3.20) represents self-interference of the particle. The detector, single or double (conjoined), is the one appropriate to the arrival event type.

Arrival Event	*Event set*	*Observed*	*Ampl.*	*Prob.*	*Type*	*Detector*
at 1 or 2 or both	$A \cup B$	yes	$\psi_1 + \psi_2$	$\overline{\mathsf{P}}_{1,2}$	real	double
at 1 and not at 2	$A \cap B^c$	yes	ψ_1	P_1	real	single
at 2 and not at 1	$B \cap A^c$	yes	ψ_2	P_2	real	single
at both 1 and 2	$A \cap B$	no	-	$2\Re\mathsf{P}_{12}$	virtual	none

The attributes of these events are summarized in table 3.1. Since the total event on the left-hand side of equation (3.19) and the first two events of single-location arrival on the right hand side are observable, the remaining term represents a virtual event. This virtual event $A \cap B$ of arrival at both locations is observed only indirectly, when it interferes with the other events. For two separate, single detectors, there is no arrival interference; that is, formula (3.13) follows when we substitute $\mathsf{P}(A \cap B) = 0$ in equation (3.19).

For the conjoined detector pair, formula (3.15) follows from equation (3.19), when we substitute for $\mathsf{P}(A \cap B)$ the quantum mechanical virtual probability, a signed number that represents a kind of self-interference of the particle, as its wavefront breaks over the two detectors:

$$\begin{aligned} \mathsf{P}(A \cap B)_{\mathrm{qm}} &= \mathsf{P}(xt, \tau) + \mathsf{P}(xt, -\tau) \\ &= \psi^*(x + \tfrac{\tau}{2}) \cdot \psi(x - \tfrac{\tau}{2}) + \text{c.c.} \end{aligned} \tag{3.20}$$

This expression, twice the real part of (3.2), has a form analogous to the standard definition for independent events, $\mathsf{P}(A \cap B) = \mathsf{P}(A) \cdot \mathsf{P}(B)$. Since a virtual probability is always just a cross-product that comes from squaring a sum of indistinguishable amplitudes, probabilities

formula for two events, $\mathsf{P}(A \text{ or } B) = \mathsf{P}(A) + \mathsf{P}(B) - \mathsf{P}(A \text{ and } B)$ [37].

of joint events necessarily take this form of independence. This can be viewed as a quantum-mechanical constraint on probabilities of joint events, which is not found in standard, non-negative probability theory without underlying complex amplitudes. Negative (virtual) probabilities have also been noted in, for example, [38][39][40].

3.3.3 Experimental three-slit test of Born's rule

Born's rule has passed all experimental tests up to now, including a recent three-slit experiment using single photons [41]. This experiment opens and closes the slits, to test this identity for any three complex numbers (probability amplitudes):

$$|a+b+c|^2 \;=\; |a+b|^2+|a+c|^2+|b+c|^2-(|a|^2+|b|^2+|c|^2). \tag{3.21}$$

This identity (3.21) contains no residual third-order term $\mathsf{P}(a \cap b \cap c)$ for the interference of all three slit sources, as we can verify. Interpreted with Born's rule, for corresponding events also labeled a, b, c, the identity (3.21) reads:

$$\begin{aligned}\mathsf{P}(a \cup b \cup c) \;=\;& \mathsf{P}((a \cup b) \cap c^c) + \mathsf{P}((c \cup a) \cap b^c) + \mathsf{P}((b \cup c) \cap a^c) \\ & - \left(\mathsf{P}(a \cap (b \cup c)^c) + \mathsf{P}(c \cap (a \cup b)^c) + \mathsf{P}(b \cap (c \cup a)^c)\right).\end{aligned} \tag{3.22}$$

This identity is missing a term, $\mathsf{P}(a \cap b \cap c)$. For we can partition $a \cup b \cup c$ as

$$a \cup b \cup c \;=\; (a \cap b \cap c) \cup (a \cap b^c) \cup (b \cap c^c) \cup (c \cap a^c), \tag{3.23}$$

so that, using the set identities $b \cap c^c = [(a \cup b) \cap c^c] - [a \cap (b \cup c)^c]$, *etc.*, in general we have

$$\begin{aligned}\mathsf{P}(a \cup b \cup c) \;=\;& \mathsf{P}(a \cap b \cap c) \\ & + \mathsf{P}((a \cup b) \cap c^c) + \mathsf{P}((c \cup a) \cap b^c) + \mathsf{P}((b \cup c) \cap a^c) \\ & - \left(\mathsf{P}(a \cap (b \cup c)^c) + \mathsf{P}(c \cap (a \cup b)^c) + \mathsf{P}(b \cap (c \cup a)^c)\right).\end{aligned} \tag{3.24}$$

Therefore, the third-order term in (3.22) must be

$$\mathsf{P}(a \cap b \cap c) \quad = \quad 0. \tag{3.25}$$

For example, the simultaneous wavelike arrival of a particle at three locations is an event that has zero probability. (This property is not what we would naively consider to be wavelike.) Only a bilocal arrival has a non-zero virtual probability (3.20).

3.3.4 Born's rule implies that only pairs of events interfere

We can extend these results to events involving more than three states. More generally, consider a particle with n base states, $A_1, A_2, \ldots, A_n$, having the corresponding amplitudes $a_1, a_2, \ldots, a_n$. The only events that concern us in our probability calculus are of two kinds, *actual* and *virtual* events. The *actual* or observable events belong to one of these families, defined for each $m = 1, 2, ..., n$:

$$\mathcal{A}_m^n \quad = \quad \left\{ \bigcup_{k=1}^{m} A_{\pi(k)} \cap \left(\bigcup_{k=1}^{m'} A_{\pi'(k)} \right)^c \; : \; \text{all } \pi, \pi' \right\} \tag{3.26}$$

with m' such that $m + m' = n$. The basic idea here is that in an actual, observable event, every state must be specified as either belonging or not to that event. (For a continuous example, the event of arrival at location q_1 has state $A_1 = |q_1\rangle$ with amplitude given by the Dirac delta distribution: $\psi(q) = \langle q \,|q_1\rangle = \delta(q - q_1)$, nonzero at at q_1, but zero everywhere else.) We partition the states into two subsets, states to include in the actual event, and states to exclude. Thus π indexes a combination of any m of the n states, and π' indexes the complement of the m' states that remain. (For a countably infinite set of states, $n = \infty$ and we would let $m' = \infty$.) Actual events (3.26) each have nonnegative probability, and their total probability is 1.

Similarly, the *virtual* or interference events belong to one of these families, defined for each $m = 2, 3, ..., n$:

$$\mathcal{V}_m^n \quad = \quad \left\{ \bigcap_{k=1}^{m} A_{\pi(k)} \cap \left(\bigcup_{k=1}^{m'} A_{\pi'(k)} \right)^c \;:\; \text{all } \pi, \pi' \right\} \tag{3.27}$$

By DeMorgan's formulae, we have $\left(\bigcup_{k=1}^{m'} A_{\pi'(k)}\right)^c = \bigcap_{k=1}^{m'} A^c_{\pi'(k)}$. We will show next that virtual events for $m = 2$ interfering states have a signed probability, but zero probability for $m > 2$ interfering states.

The parallel alternating identities (3.21) and (3.22) with its missing term, one for complex numbers and one for probabilities, are both true in general, for any number $n \geq 2$ of states. Quantum mechanics again connects the two identities by means of Born's rule, as follows.

First, the squared amplitudes must satisfy this identity, valid for any $n \geq 3$ complex numbers $a_1, a_2, a_3, ...$:

$$\left|\sum_{k=1}^{n} a_k\right|^2 \quad = \quad \sum_j \left|\sum_{k \neq j} a_k\right|^2 - \sum_{j_1 < j_2} \left|\sum_{k \neq j_1, j_2} a_k\right|^2 + \cdots + (-1)^n \sum_{j'} \left|a_{j'}\right|^2. \tag{3.28}$$

The right-hand side has $n - 1$ terms with alternating signs. The indices run from 1 to n, except as prevented.

Second, the event probabilities must satisfy this (new) identity for $n \geq 2$ sets:

$$\begin{aligned}\mathsf{P}\left(\bigcup_{k=1}^{n} A_k\right) &= \mathsf{P}\left(\bigcap_{k=1}^{n} A_k\right) \\ &\quad + \sum_j \mathsf{P}\left(\bigcup_{k\neq j} A_k \cap A_j^c\right) - \sum_{j_1<j_2} \mathsf{P}\left(\bigcup_{k\neq j_1,j_2} A_k \cap A_{j_1}^c \cap A_{j_2}^c\right) \\ &\quad + \cdots + (-1)^n \sum_{j'} \mathsf{P}\left(A_{j'} \cap \bigcap_{j\neq j'} A_j^c\right). \end{aligned} \tag{3.29}$$

All events above are actual, except for one virtual event. When we interpret the squared amplitudes in (3.28) as probabilities by Born's rule, we get this identity (3.29), but missing its initial term on the righthand side. Therefore, the virtual probability $\mathsf{P}\left(\bigcap_{k=1}^{n} A_k\right) = 0$ for $n > 2$.

We can immediately apply this result for any m such that $3 \leq m \leq n$, to get $\mathsf{P}\left(\bigcap_{k=1}^{m} A_{\pi(k)} \cap \left(\bigcup_{k=1}^{m'} A_{\pi'(k)}\right)^c\right) = 0$, for any two-subset partition π, π' of the set of indices $\{1, ...n\}$. This follows from the identities (3.28) and (3.29) of order m, by merely appending the fixed set intersection $\cap \left(\bigcup_{k=1}^{m'} A_{\pi'(k)}\right)^c$ to restrict every set on the left and right hand sides.

We conclude that in quantum mechanics with Born's rule, for any number n of base states, the probability of the virtual event of $m \geq 2$ base events occurring at one time (the rest not occurring) obeys this rule (for an arbitrary ordering of the states):

$$\mathsf{P}\left(\bigcap_{k=1}^{m} A_k \cap \bigcap_{k=m+1}^{n} A_k^c\right) = \begin{cases} \psi_{A_1-A_2}^* \psi_{A_2-A_1} + \text{ c.c.}, & m = 2 \\ 0, & m = 3, 4, \ldots. \end{cases} \tag{3.30}$$

Born's rule and probability theory thus imply that states only interfere in pairs. We also note that when two states interfere, as in a bilocal arrival, this rule (3.30) gives such twin events a place of special significance in quantum mechanics.

3.4 Polar form of the bilocal velocity

It is well known that if we put the wavefunction into polar form as $\psi = \sqrt{\mathsf{P}}e^{i\theta}$, the formula for current density reduces to $\mathsf{j} = \mathsf{P}\mathsf{v}$, where $\mathsf{v} = \frac{\hbar}{\mathsf{m}}\nabla_{\mathsf{x}}\theta$ is interpreted as mean velocity (see *e.g.* [36, section 21-5]). This result is a special case of an expression for the displaced current densities $\mathsf{j}(xt, \pm\tau)$ (3.3), which we consider to be due to wavelike interference at locations 1 and 2 given by $q_1 = x - \frac{\tau}{2}$, $q_2 = x + \frac{\tau}{2}$. They are the final two terms of the total bicurrent density (3.18). Substituting into them the polar form of the wavefunction at the two locations, *i.e.*, $\psi_1 = \sqrt{\mathsf{P}_1}e^{i\theta_1}$ and $\psi_2 = \sqrt{\mathsf{P}_2}e^{i\theta_2}$, we find after a little calculus:

$$\mathsf{j}_{12} \equiv \mathsf{j}(xt, \tau) = \frac{\hbar}{m}\mathsf{P}_{12}\left(\frac{1}{2}\left[\nabla_x\theta_1 + \nabla_x\theta_2\right] + \frac{1}{2}\left[\nabla_x \ln\sqrt{\frac{\mathsf{P}_2}{\mathsf{P}_1}}\right]\right) = \mathsf{P}_{12}\mathsf{v}_{12}, \tag{3.31}$$

where $\mathsf{P}_{12} = \psi_1^*\psi_2 \equiv \mathsf{P}(xt, \tau)$ as defined by (3.2), and we define the wavelike velocity

$$\mathsf{v}_{12} \equiv \mathsf{v}(xt, \tau) = \frac{1}{2}\left[\mathsf{v}_1 + \mathsf{v}_2\right] + \frac{1}{2}\frac{\hbar}{m}\left[\nabla_x \ln\sqrt{\frac{\mathsf{P}_2}{\mathsf{P}_1}}\right]. \tag{3.32}$$

For a single location ($\tau = 0$), the second term on the right hand side of (3.31) vanishes and $\mathsf{j}_{12} = \mathsf{j}_1 = \mathsf{j}_2$. Similarly, by exchanging locations 1 and 2, we also have

$$\mathsf{j}_{21} \equiv \mathsf{j}(xt, -\tau) = \frac{\hbar}{m}\mathsf{P}_{21}\left(\frac{1}{2}\left[\nabla_x\theta_1 + \nabla_x\theta_2\right] + \frac{1}{2}\left[\nabla_x \ln\sqrt{\frac{\mathsf{P}_1}{\mathsf{P}_2}}\right]\right) = \mathsf{P}_{21}\mathsf{v}_{21} \tag{3.33}$$

$$\mathsf{v}_{21} \equiv \mathsf{v}(xt, -\tau) = \frac{1}{2}\left[\mathsf{v}_1 + \mathsf{v}_2\right] + \frac{1}{2}\frac{\hbar}{m}\left[\nabla_x \ln\sqrt{\frac{\mathsf{P}_1}{\mathsf{P}_2}}\right]. \tag{3.34}$$

The sum of the the displaced current densities is a real-valued, virtual current:

$$\mathsf{j}(xt,\tau)+\mathsf{j}(xt,-\tau) \;=\; \frac{\hbar}{m}\left(\left[\nabla_x\theta_1+\nabla_x\theta_2\right]\Re\mathsf{P}_{12}+\left[\nabla_x \ln\sqrt{\frac{\mathsf{P}_2}{\mathsf{P}_1}}\right]\Im\mathsf{P}_{12}\right) \quad (3.35)$$

where $\Re z = x$ and $\Im z = y$ denote the real and imaginary parts of any complex number $z = x + iy$. Note that in case $\theta_2 - \theta_1 = \frac{\pi}{2}$, or any odd multiple of $\frac{\pi}{2}$, $\mathsf{P}_{12} = \pm i\sqrt{\mathsf{P}_1\mathsf{P}_2}$, so that $\Re\mathsf{P}_{12} = 0$, and the first term on the right hand side of (3.35) vanishes. The total bicurrent density (3.18) is given by

$$\begin{aligned}
\bar{\mathsf{j}}(xt,\tau) \;&=\; \tfrac{\hbar}{m}\left\{\mathsf{P}_1\nabla_x\theta_1+\mathsf{P}_2\nabla_x\theta_2+\Re\mathsf{P}_{12}\cdot\left[\nabla_x\theta_1+\nabla_x\theta_2\right]+\Im\mathsf{P}_{12}\cdot\nabla_x\ln\sqrt{\frac{\mathsf{P}_2}{\mathsf{P}_1}}\right\}\\
&=\; \Bigg(\mathsf{P}_1\mathsf{v}_1+\mathsf{P}_2\mathsf{v}_2\\
&\quad +\sqrt{\mathsf{P}_1\mathsf{P}_2}\left\{\cos\left(\theta_2-\theta_1\right)\left[\mathsf{v}_1+\mathsf{v}_2\right]+\sin\left(\theta_2-\theta_1\right)\left[\frac{\hbar}{m}\nabla_x\ln\sqrt{\frac{\mathsf{P}_2}{\mathsf{P}_1}}\right]\right\}\Bigg)
\end{aligned} \quad (3.36)$$

Formulas (3.35) and (3.36) for the virtual and total bi-current density are true in general. They represent, respectively, the particle current density passing through both locations, and through one or both locations.

3.5 Path-fluctuation current density

Besides the bilocal current density j defined in (3.3), a second kind of bilocal current density k can be defined in this context:

$$\mathsf{k}(xt,\tau) \;=\; \tfrac{\hbar}{2mi}\left[\psi^*(x-\tfrac{\tau}{2},t)\nabla_{\frac{\tau}{2}}\psi(x+\tfrac{\tau}{2},t)-\psi(x+\tfrac{\tau}{2},t)\nabla_{\frac{\tau}{2}}\psi^*(x-\tfrac{\tau}{2},t)\right]. \quad (3.37)$$

We name this the path-fluctuation current density. The gradients are now partial derivatives with respect to $\frac{\tau}{2}$ instead of x. Thus, in case $\tau = 0$, the fluctuation current $\mathsf{k}(xt, 0)$ is an imaginary-valued vector. This follows because the right hand side of equation (3.37) reverses sign when conjugated and evaluated at $\tau = 0$, since $\left(\nabla_{\frac{\tau}{2}}\psi^*(x-\frac{\tau}{2}, t)\right)^*\Big|_{\tau=0} = -\left(\nabla_{\frac{\tau}{2}}\psi(x+\frac{\tau}{2}, t)\right)\Big|_{\tau=0}$. Also, since $\nabla_{\frac{\tau}{2}}\psi(x\pm\frac{\tau}{2}, t) = \pm\nabla_x\psi(x\pm\frac{\tau}{2}, t)$, we have an equivalent expression

$$\begin{aligned}
\mathsf{k}(xt, \tau) &= \tfrac{\hbar}{2mi}\left[\psi^*(x-\tfrac{\tau}{2}, t)\nabla_x\psi(x+\tfrac{\tau}{2}, t) + \psi(x+\tfrac{\tau}{2}, t)\nabla_x\psi^*(x-\tfrac{\tau}{2}, t)\right] \\
&= \tfrac{\hbar}{2mi}\nabla_x\psi^*(x-\tfrac{\tau}{2}, t)\psi(x+\tfrac{\tau}{2}, t) \\
&= \tfrac{\hbar}{2mi}\nabla_x\mathsf{P}(xt, \tau),
\end{aligned} \tag{3.38}$$

by the product rule for gradients. The path-fluctuation bicurrent density is proportional to the gradient (with respect to x) of the bilocal probability (3.2). Evaluated at $\tau = 0$, the right hand sides of equations (3.38) reverse sign when conjugated, so the bicurrent density of the second kind is again seen to be imaginary-valued in that case.

The bicurrent density j (3.3) of the first kind is real-valued at $\tau = 0$, where it reduces to the usual quantum-mechanical current. We have:

$$\begin{aligned}
\mathsf{j}(xt, \tau) &= \tfrac{\hbar}{2im}\left[\psi^*(x-\tfrac{\tau}{2}, t)\nabla_x\psi(x+\tfrac{\tau}{2}, t) - \psi(x+\tfrac{\tau}{2}, t)\nabla_x\psi^*(x-\tfrac{\tau}{2}, t)\right] \\
&= \tfrac{\hbar}{2im}\left[\psi^*(x-\tfrac{\tau}{2}, t)\nabla_{\frac{\tau}{2}}\psi(x+\tfrac{\tau}{2}, t) + \psi(x+\tfrac{\tau}{2}, t)\nabla_{\frac{\tau}{2}}\psi^*(x-\tfrac{\tau}{2}, t)\right] \\
&= \tfrac{\hbar}{2im}\nabla_{\frac{\tau}{2}}\mathsf{P}(xt, \tau).
\end{aligned} \tag{3.39}$$

We see that, up to an imaginary constant coefficient, the bicurrent density j (3.3) is the gradient with respect to $\frac{\tau}{2}$ of the bilocal probability (3.2). The usual quantum-mechanical current is this gradient evaluated at $\tau = 0$, multiplied by the constant. When conjugated and evaluated at $\tau = 0$, for the same reasons given in the previous paragraph, the first two expressions for j on the right hand side of (3.39) remain the same, and are thus real.

3.5.1 Polar form of the fluctuation current

Changing signs in the steps taken in section 3.4, to agree with formula (3.38), we find that the polar form of the fluctuation bicurrent density is

$$\begin{aligned}
\mathsf{k}_{12} \equiv \mathsf{k}(xt,\tau) &= \tfrac{\hbar}{2mi}\mathsf{P}_{12}\left(i\left[\nabla_x\theta_2 - \nabla_x\theta_1\right] + \left[\nabla_x \ln\sqrt{\mathsf{P}_2\mathsf{P}_1}\right]\right) = \mathsf{P}_{12}\mathsf{w}_{12} \quad (3.40)\\
&= \tfrac{\hbar}{2mi}\mathsf{P}_{12}\nabla_x\left(\ln\sqrt{\mathsf{P}_2\mathsf{P}_1} + i\left[\theta_2 - \theta_1\right]\right)\\
&= \tfrac{\hbar}{2mi}\mathsf{P}_{12}\nabla_x \ln \mathsf{P}_{12}\\
&= \tfrac{\hbar}{2mi}\nabla_x\mathsf{P}_{12}, \quad (3.41)
\end{aligned}$$

again, since we can write

$$\mathsf{P}_{12} = \exp\left\{\ln\sqrt{\mathsf{P}_2\mathsf{P}_1} + i\left[\theta_2 - \theta_1\right]\right\}, \quad (3.42)$$

and we define the wavelike velocity

$$\mathsf{w}_{12} \equiv \mathsf{w}(xt,\tau) \quad = \quad \tfrac{1}{2}\left[\mathsf{v}_2 - \mathsf{v}_1\right] + \tfrac{1}{2}\tfrac{\hbar}{mi}\left[\nabla_x \ln\sqrt{\mathsf{P}_2\mathsf{P}_1}\right]. \quad (3.43)$$

For a single location ($\tau = 0$), the first term on the right hand side of (3.40) and of (3.43) vanishes, and this bicurrent $\mathsf{k}_{12} = \mathsf{k}_1 = \mathsf{k}_2$, reducing to

$$\mathsf{k}_1 \equiv \mathsf{k}(xt,0) = \mathsf{P}_1 \cdot \tfrac{1}{2}\tfrac{\hbar}{mi}\nabla_x \ln \mathsf{P}_1 = \tfrac{1}{2}\tfrac{\hbar}{mi}\nabla_x\mathsf{P}_1. \quad (3.44)$$

Here we recognize the so-called osmotic velocity field [42]

$$\mathsf{w}_1 \equiv \mathsf{w}(xt, 0) = \tfrac{1}{2}\tfrac{\hbar}{mi}\nabla_x \ln \mathsf{P}_1 \tag{3.45}$$

of the particle at any single location. Now we can write the single current as $\mathsf{k}_1 = \mathsf{P}_1\mathsf{w}_1$.

By exchanging locations 1 and 2, we similarly have

$$\begin{aligned}
\mathsf{k}_{21} \equiv \mathsf{k}(xt, -\tau) &= \tfrac{\hbar}{mi}\mathsf{P}_{21}\left(i\tfrac{1}{2}\left[\nabla_x\theta_1 - \nabla_x\theta_2\right] + \tfrac{1}{2}\left[\nabla_x \ln\sqrt{\mathsf{P}_1\mathsf{P}_2}\right]\right) = \mathsf{P}_{21}\mathsf{w}_{21} && (3.46)\\
\mathsf{w}_{21} \equiv \mathsf{v}(xt, -\tau) &= \tfrac{1}{2}\left[\mathsf{v}_1 - \mathsf{v}_2\right] + \tfrac{1}{2}\tfrac{\hbar}{mi}\left[\nabla_x \ln\sqrt{\mathsf{P}_1\mathsf{P}_2}\right]. && (3.47)
\end{aligned}$$

The sum of the displaced current densities is imaginary-valued for any τ:

$$\mathsf{k}(xt, \tau) + \mathsf{k}(xt, -\tau) = \tfrac{\hbar}{mi}\left(\left[\nabla_x\theta_1 - \nabla_x\theta_2\right]\Im\mathsf{P}_{12} + \left[\nabla_x \ln\sqrt{\mathsf{P}_2\mathsf{P}_1}\right]\Re\mathsf{P}_{12}\right) \tag{3.48}$$

From formula (3.41), the total fluctuation bicurrent density is given by the sum of four parts

$$\begin{aligned}
\overline{\mathsf{k}}(xt, \tau) &= \left(\mathsf{k}_1 + \mathsf{k}_2 + \mathsf{k}_{12} + \mathsf{k}_{21}\right)\\
&= \tfrac{\hbar}{2mi}\nabla_x\left(\mathsf{P}_1 + \mathsf{P}_2 + \mathsf{P}_{12} + \mathsf{P}_{21}\right)\\
&= \tfrac{\hbar}{2mi}\nabla_x\overline{\mathsf{P}}(xt, \tau). && (3.49)
\end{aligned}$$

Formulas (3.40) and (3.49) for the displaced and total bi-current density (and the formulas in between) are true in general. They represent, respectively, the particle fluctuation current density passing through both locations, and through one or both locations.

3.5.2 Fluctuation current propagator

Since $\nabla^2_{\frac{\tau''}{2}}\psi(x''\pm\frac{\tau''}{2},t'') = \nabla^2_{x''}\psi(x''\pm\frac{\tau''}{2},t'')$, we can rewrite the characterizing equation of the Blue function in [25, section 8, equation (67)] (including the ΔV term that was omitted there) as

$$\left(\frac{\partial}{\partial t''} - \frac{1}{i\hbar}\Delta V\right) B(\tau'') + \nabla_{\frac{\tau''}{2}} \cdot \tilde{\mathbf{B}}(\tau'') \;=\; -2\delta(t''-t')\delta(x''-x'+\tfrac{\tau''}{2}-\tfrac{\tau'}{2}) \times\delta(x''-x'-\tfrac{\tau''}{2}+\tfrac{\tau'}{2}), \tag{3.50}$$

where we define the second Blue current density propagator

$$\tilde{\mathbf{B}}(x''t''\tau'';x't'\tau') \;=\; \frac{\hbar}{2mi}\left[G_1^*\nabla_{\frac{\tau''}{2}}G_2 - G_2\nabla_{\frac{\tau''}{2}}G_1^*\right]. \tag{3.51}$$

The propagator G is the Green function for the Schrödinger equation, and we put $G_1, G_2 = G(x''\pm\frac{\tau''}{2},t'';x'\pm\frac{\tau'}{2},t')$.

Likewise, the bilocal conservation equation (3.4) for the fluctuation current k has the same form again as in [25],

$$\left[i\hbar\frac{\partial}{\partial t''} - \Delta V(x''\tau''t'')\right]\mathsf{P}(x''\tau''t'') \;=\; -i\hbar\nabla_{\frac{\tau''}{2}}\cdot\mathsf{k}(x''\tau''t''). \tag{3.52}$$

The right-hand sides of equations (3.4) and (3.52) must be equal, because the left-hand sides are identical. This fact also follows from expressions (3.39) and (3.38) for the usual and fluctuation currents, since $\nabla_{x''}\cdot\nabla_{\frac{\tau''}{2}}\psi(x''\pm\frac{\tau''}{2},t'') = \nabla_{\frac{\tau''}{2}}\cdot\nabla_{x''}\psi(x''\pm\frac{\tau''}{2},t'')$.

Then, in a manner similar to that in [25, section 8], we obtain the formal expression for the fluctuation current kernel path integral,

$$\tilde{\mathbf{B}}(x''t''\tau'';x't'\tau') \quad = \quad \iint \dot{\boldsymbol{\tau}}'' e^{i\Delta S/\hbar}\mathcal{D}\mathbf{x}(t)\mathcal{D}\boldsymbol{\tau}(t), \tag{3.53}$$

where $\dot{\boldsymbol{\tau}}'' = \left(\tau'' - \tau_{N-1}\right)/\epsilon$, and the *displaced action* or *motion* is again the line integral

$$\Delta S[x(t),\tau(t)] \quad = \quad \int_{t'}^{t''} \left(m\dot{x}\dot{\tau} - \left[V(x+\tfrac{\tau}{2}) - V(x-\tfrac{\tau}{2})\right]\right) dt, \tag{3.54}$$

as defined in [25, equation (26)]. Lastly, modifying appendix B, we find the free-space propagator for the fluctuation current density,

$$\tilde{\mathbf{B}}_0^{\mu}(x''t''\tau'';x'\tau't') \quad = \quad \left(\tfrac{m}{2\pi\hbar T}\right)^{d} \frac{(\tau''-\tau')^{\mu}}{T} \exp\left\{\tfrac{im}{\hbar T}(x''-x')\cdot(\tau''-\tau')\right\} \tag{3.55}$$

$$\quad = \quad \bar{\boldsymbol{\tau}} B_0, \tag{3.56}$$

where $T = t'' - t'$ and $\bar{\boldsymbol{\tau}} = \left(\tau'' - \tau'\right)^{\mu}/T$ is the mean fluctuation, for components $\mu = 1, 2, \ldots, d$.

3.6 Probabilistic Schrödinger equation

The bilocal probability and current densities together satisfy the bicontinuity equation (3.4), as we have seen. Since we found that $\mathsf{j}(x\tau t) = \frac{\hbar}{2im}\nabla_{\frac{\tau}{2}}\cdot\mathsf{P}(x\tau t)$, in section 3.5, equation (3.39), we can rewrite equation (3.4) in a probabilistic Schrödinger form

$$\boxed{i\hbar\frac{\partial}{\partial t}\mathsf{P}(x\tau t) = \left[-\frac{\hbar^2}{2m}\nabla_x\nabla_{\frac{\tau}{2}} + \Delta V(x\tau t)\right]\mathsf{P}(x\tau t).} \tag{3.57}$$

for the bilocal probability density P. Here the familiar kinetic energy operator $-\frac{\hbar^2}{2m}\nabla_x^2$ is replaced by $-\frac{\hbar^2}{2m}\nabla_x\nabla_{\frac{\tau}{2}} = -\frac{\hbar^2}{2m}\nabla_{\frac{\tau}{2}}\nabla_x$. This operator is the product of two distinct momentum operators, $\hat{p}_x = -i\hbar\nabla_x$, for the central momentum, and $\hat{p}_\tau = -i\hbar\nabla_{\frac{\tau}{2}}$, for the relative bilocal displacement momentum or, for short, the separating momentum.

This equation decouples into two conjugate Schrödinger equations:

$$
\begin{aligned}
i\hbar\frac{\partial}{\partial t}\psi_a^*\psi_b(x\tau t) &= \left[-\frac{\hbar^2}{2m}\nabla_x\nabla_{\frac{\tau}{2}} + \Delta V(x\tau t)\right]\cdot\psi_a^*\psi_b \\
i\hbar\left(\psi_b\frac{\partial\psi_a^*}{\partial t} + \psi_a^*\frac{\partial\psi_b}{\partial t}\right) &= -\frac{\hbar^2}{2m}\Big[\psi_a^*\nabla_x\nabla_{\frac{\tau}{2}}\psi_b + \psi_b\nabla_x\nabla_{\frac{\tau}{2}}\psi_a^* \\
&\quad + \nabla_x\psi_a^*\cdot\nabla_{\frac{\tau}{2}}\psi_b + \nabla_{\frac{\tau}{2}}\psi_a^*\cdot\nabla_x\psi_b\Big] \\
&\quad + [V_b - V_a]\,\psi_a^*\psi_b. \\
-\psi_b\cdot\left(i\hbar\frac{\partial\psi_a}{\partial t}\right)^* + \psi_a^*\cdot i\hbar\frac{\partial\psi_b}{\partial t} &= -\psi_b\left(-\frac{\hbar^2}{2m}\nabla_x^2\psi_a^* + V_a\psi_a^*\right) \\
&\quad +\psi_a^*\left(-\frac{\hbar^2}{2m}\nabla_x^2\psi_b + V_b\psi_b\right), \qquad (3.58)
\end{aligned}
$$

since $\nabla_{\frac{\tau'}{2}}\psi(x'\pm\frac{\tau'}{2},t') = \pm\nabla_{x'}\psi(x'\pm\frac{\tau'}{2},t')$. Thus a displaced product of two wavefunctions,

$$\rho(x\tau t) = A\left[\psi_a^*(x-\tfrac{\tau}{2},t)\cdot\psi_b(x+\tfrac{\tau}{2},t)\right], \qquad (3.59)$$

and its complex conjugate, are solutions of (3.57). We conjecture that the solutions of this form (3.59) constitute a basis for the physical Hilbert space of all solutions $\rho(x\tau t)$ of (3.57).

3.6.1 Stationary solutions for fixed energy level differences

To solve equation (3.57) for time-independent ΔV by separation of variables, we put $\mathsf{P} = \rho(x,\tau)\mathsf{T}(t)$. Substituting this and dividing both sides by P, we have

$$i\hbar\frac{\dot{\mathsf{T}}(t)}{\mathsf{T}(t)} \quad = \quad \Delta E = -\frac{\hbar^2}{2m}\frac{\nabla_x \nabla_{\frac{\tau}{2}} \rho(x,\tau)}{\rho(x,\tau)} + \Delta V(x,\tau) \tag{3.60}$$

where the left and right hand sides must be a constant ΔE, because they are functions of different variables yet equal. The constant ΔE must also be real-valued, possibly negative, since the operators on either side are Hermitean (self-adjoint). Integrating the left-hand side over time, we have

$$\mathsf{T}(t) \quad = \quad T_0 e^{-i\Delta E t/\hbar}. \tag{3.61}$$

The right-hand side presents an eigenproblem,

$$\left[-\frac{\hbar^2}{2m}\nabla_x \nabla_{\frac{\tau}{2}} + \Delta V(x,\tau)\right]\rho(x,\tau) \quad = \quad \Delta E \rho(x,\tau). \tag{3.62}$$

For a uniform potential, $\Delta V = 0$ and the eigensolutions of (3.62) include the product of two different planewaves

$$\rho(x,\tau) \quad = \quad A e^{ik_a\cdot\left(x-\frac{\tau}{2}\right)} e^{-ik_b\cdot\left(x+\frac{\tau}{2}\right)}, \tag{3.63}$$

and its complex conjugate, for eigenvalue

$$\Delta E \quad = \quad -\hbar^2\left(|k_a|^2 - |k_b|^2\right)/2m, \tag{3.64}$$

and for wavenumber vectors k_a, k_b. Each eigenvalue is independent of τ. (We must discard as unphysical, the corresponding solutions for real exponents, since in that case $\rho \to \infty$ as $\pm x, \pm\tau \to \infty$.) The solution $\rho = \psi_-^* \psi_+ = e^{ik\left(x-\frac{\tau}{2}\right)} e^{-ik\left(x+\frac{\tau}{2}\right)} = e^{-ik\tau}$ requires $\Delta E = 0$, $k_a = k_b$.

3.6.2 Inner product space

To construct an abstract basis of functions of form (3.59), let $|a\rangle, |b\rangle, \ldots$ be stationary states of the usual kind, a complete set of eigenstates of the time-independent Schrödinger equation. In the position representation, the wavefunctions are $\psi_a(x) = \langle x\,|a\,\rangle$, $\psi_b(x) = \langle x\,|b\,\rangle, \ldots$ We introduce dyadic kets defined by

$$\begin{aligned} |a_\mp b_\pm\rangle &= |b_\pm\rangle\langle a_\mp| \\ &\sim \langle a\,|x\,\rangle \mathcal{D}^\dagger(\pm\tfrac{\tau}{2})\mathcal{D}(\mp\tfrac{\tau}{2})\langle x\,|b\,\rangle \\ &= \psi_a^*(x \mp \tfrac{\tau}{2}) \cdot \psi_b(x \pm \tfrac{\tau}{2}). \end{aligned} \tag{3.65}$$

The dyadic bras dual to these kets are the complex conjugates of the kets, defined by

$$\begin{aligned} \langle b_\pm a_\mp| &= |a_\mp\rangle\langle b_\pm| \\ &\sim \langle b\,|x\,\rangle \mathcal{D}^\dagger(\mp\tfrac{\tau}{2})\mathcal{D}(\pm\tfrac{\tau}{2})\langle x\,|a\,\rangle \\ &= \psi_b^*(x \pm \tfrac{\tau}{2}) \cdot \psi_a(x \mp \tfrac{\tau}{2}). \end{aligned} \tag{3.66}$$

The sign subscripts here signify that, in the position representation, the original states are translated by $\pm\frac{\tau}{2}$; *i.e.*, $|a_\pm\rangle \sim \psi_a(x \pm \frac{\tau}{2})$. Here the spatial translation operator $\mathcal{D}$, which uses Taylor series to translate the real-valued argument x of a complex-valued function (with no singular points on the real line) by a distance vector $\frac{\tau}{2}$, is given by $\mathcal{D}(\frac{\tau}{2}) = \exp\left\{-i\hat{p}_x \cdot \frac{\tau}{2}/\hbar\right\} = \exp\left\{-\nabla_x \cdot \frac{\tau}{2}\right\}$.

We define the inner product of two dyads by

$$\begin{aligned}
\langle b_\pm a_\mp \,| c_\mp d_\pm \rangle &= \iint \psi_b^*(x\pm\tfrac{\tau}{2})\psi_a(x\mp\tfrac{\tau}{2})\psi_c^*(x\mp\tfrac{\tau}{2})\psi_d(x\pm\tfrac{\tau}{2})\; dx\; d\tau \\
&= \int \psi_a(r)\psi_c^*(r)dr \cdot \int \psi_b^*(s)\psi_d(s)ds \\
&= \langle a\,|c\rangle^*\langle b\,|d\rangle \qquad (3.67)
\end{aligned}$$

where the integrals run from $-\infty$ to $+\infty$. It follows that this inner product is linear (lefthand scalars are conjugated) and has conjugate symmetry:

$$(\langle b_\pm a_\mp \,| c_\mp d_\pm \rangle)^* = \langle d_\pm c_\mp \,| a_\mp b_\pm \rangle. \qquad (3.68)$$

Since the substitution $\tau \leftarrow -\tau$ does not change the inner product integral (3.67), we have another symmetric property,

$$\langle b_\pm a_\mp \,| c_\mp d_\pm \rangle = \langle c_\pm d_\mp \,| b_\mp a_\pm \rangle. \qquad (3.69)$$

The norm induced by the inner product is given by

$$||a_\mp b_\pm\rangle|^2 = \langle b_\pm a_\mp \,| a_\mp b_\pm \rangle = |a|^2|b|^2 = 1, \qquad (3.70)$$

assuming that the original wavefunctions are normalized to begin with. Provided that $\langle a\,|c\rangle = 0$ or $\langle b\,|d\rangle = 0$ (*i.e.,* $a \perp c$ or $b \perp d$), then we also have orthonormal dyads:

$$\langle b_\pm a_\mp \,| c_\mp d_\pm \rangle = \langle a\,|c\rangle^*\langle b\,|d\rangle = 0. \qquad (3.71)$$

An operator $\Delta\mathcal{O}$ that acts on the dyadic states has matrix elements given by the expectation value

$$\begin{aligned}\langle b_{\pm}a_{\mp}\,|\Delta\mathcal{O}|\,c_{\mp}d_{\pm}\rangle &= \iint \psi_b^*(x{\pm}\tfrac{\tau}{2})\psi_a(x{\mp}\tfrac{\tau}{2})\cdot \\ &\qquad \Delta\mathcal{O}\psi_c^*(x{\mp}\tfrac{\tau}{2})\cdot\psi_d(x{\pm}\tfrac{\tau}{2})\;dx\;d\tau. \end{aligned} \tag{3.72}$$

In the case that the operator $\Delta\mathcal{O}$ has the form $\Delta\mathcal{O} = \mathcal{O}(x{+}\frac{\tau}{2}) - \mathcal{O}(x{-}\frac{\tau}{2})$, changing the sign of τ also changes that of $\Delta\mathcal{O}$, so we have

$$\langle b_{\mp}a_{\pm}\,|\Delta\mathcal{O}|\,c_{\pm}d_{\mp}\rangle = -\,\langle b_{\pm}a_{\mp}\,|\Delta\mathcal{O}|\,c_{\mp}d_{\pm}\rangle\,. \tag{3.73}$$

When we reverse the sign of τ, this of course reverses the label signs of the dyadic kets (3.65) and bras (3.66), but each represents the same physical dyadic state that it did before reversing the sign of τ. For this reason, we identify $|a_+b_-\rangle$ with $|a_-b_+\rangle$, and we identify $\langle b_-a_+|$ with $\langle b_+a_-|$. By convention, from now on we will always use the representative kets $|a_-b_+\rangle$ and their corresponding dual bras $\langle b_+a_-|$.

3.6.3 Multi-level time-dependent systems

Consider a multi-level system with a basis of discrete orthonormal states $|a\rangle, |b\rangle, |c\rangle, \ldots$ Let their respective energy levels be, in increasing order, $E_a, E_b, E_c, \ldots$ For the time-independent probabilistic Hamiltonian ΔH^0, we have dyadic eigenstates:

$$\Delta H^0|i_-j_+\rangle = \Delta E_{ij}|i_-j_+\rangle, \text{ for } i,j\in\{a,b,...\} \tag{3.74}$$

where $\Delta E_{ij} = \hbar^2(k_j^2 - k_i^2)/(2m)$. By equation (3.61), the dyadic stationary states propagate over time t as $|i_-j_+\rangle \exp\{-i\Delta E_{ij}t/\hbar\}$.

Now to ΔH^0 let us add a time-dependent perturbation $\Delta H^I(t)$, and solve the probabilistic Schrödinger equation (3.57):

$$(\Delta H^0 + \Delta H^I(t))\mathsf{P}(t) = i\hbar\frac{\partial \mathsf{P}}{\partial t}. \tag{3.75}$$

The method we use is similar to that normally used to solve the time-dependent Schrödinger equation for states that combine two or more energy levels, *e.g.*, as given in [43, Ch. 9]. We solve for the time-dependent coefficients $\mathsf{p}_{ji}(t)$ of the linear combination of dyadic states

$$\mathsf{P}(t) \quad = \quad \Sigma_{i,j\in\mathbb{A}}\ \mathsf{p}_{ji}(t)\cdot|i_- j_+\rangle e^{-i\omega^0_{ji}t}, \tag{3.76}$$

where the index set is $\mathbb{A} = \{a, b, c, ...\}$, and we put $\omega^0_{ji} = \Delta E_{ji}/\hbar$. Substituting this expression into (3.75), using (3.74), we obtain

$$\Delta H^I \mathsf{P}(t) \quad = \quad i\hbar\,\Sigma_{i,j\in\mathbb{A}}\ \dot{\mathsf{p}}_{ji}(t)\cdot|i_- j_+\rangle e^{-i\omega^0_{ji}t}. \tag{3.77}$$

Note that, since each coefficient p_{ji} is only a function of time t, and of no other variables that change with time, we have $\dot{\mathsf{p}}_{ji}(t) \equiv d\mathsf{p}_{ji}(t)/dt = \partial\mathsf{p}_{ji}(t)/\partial t + 0$. Premultiplying both sides by $\langle j'_+ i'_-|$, taking inner products and using orthonormality, we find

$$\Sigma_{i,j\in\mathbb{A}}\ \mathsf{p}_{ji}(t)\cdot\left\langle j'_+ i'_- \left|\Delta H^I\right| i_- j_+\right\rangle e^{-i\left[\omega^0_{ji}-\omega^0_{j'i'}\right]t} \quad = \quad i\hbar\dot{\mathsf{p}}_{j'i'}(t) \tag{3.78}$$

where $\Delta H^I = H^I(x + \frac{\tau}{2}, t) - H^I(x - \frac{\tau}{2}, t)$, for a typical interaction potential operator H^I having the form of a scalar multiplier. Then ΔH^I has matrix elements given by the expectation values

$$
\begin{aligned}
\langle b_+ a_- \,|\Delta H|\, c_- d_+\rangle &= \iint \psi_b^*(x{+}\tfrac{\tau}{2})\psi_a(x{-}\tfrac{\tau}{2})\cdot \\
&\qquad \Delta H \psi_c^*(x{-}\tfrac{\tau}{2})\cdot\psi_d(x{+}\tfrac{\tau}{2})\; dx\; d\tau \\
&= \int \psi_c^*(r)\psi_a(r)dr \int \psi_b^*(s)H^I(s,t)\psi_d(s)\; ds \\
&\quad - \int \psi_c^*(r)H^I(r,t)\psi_a(r)dr \int \psi_b^*(s)\psi_d(s)\; ds \\
&= \delta_{ca}H^I_{bd} - \delta_{bd}H^I_{ca}.
\end{aligned} \tag{3.79}
$$

Then (3.78) reduces to

$$
\Sigma_{i,j\in\mathbb{A}}\; \left[\delta_{ii'}H^I_{j'j} - \delta_{j'j}H^I_{ii'}\right] \mathsf{p}_{ji}(t)\cdot e^{-i\left[\omega^0_{ji}-\omega^0_{j'i'}\right]t} \;=\; i\hbar\dot{\mathsf{p}}_{j'i'}(t) \tag{3.80}
$$

or with some reindexing,

$$
\Sigma_{k\in\mathbb{A}}\left[H^I_{jk}e^{-i\omega^0_{jk}t}\mathsf{p}_{ki} - \;\mathsf{p}_{jk}H^I_{ki}e^{-i\omega^0_{ki}t}\right] \;=\; i\hbar\dot{\mathsf{p}}_{ji} \tag{3.81}
$$

In operator form, this is the von Neumann equation for the density-of-states operator p:

$$
[H,\mathsf{p}] \;=\; i\hbar\frac{\partial\mathsf{p}}{\partial t} \tag{3.82}
$$

after we replace the matrix elements $H^I_{ji}(t)e^{-i\omega^0_{ji}t}$ by H_{ji}. Usually this equation is derived *ad hoc* from the Schrödinger equation, using the product rule for derivatives as in *e.g.,* [44]; but here it follows directly from the probabilistic Schrödinger equation (3.57).

For two levels ($\mathbb{A} = \{a, b\}$), assuming $H^I_{aa} = H^I_{bb} = 0$, equation (3.80) comprises the usual equations of motion for the elements of the density-of-states matrix [45, section 2.7],

$$\begin{aligned} \dot{\mathsf{p}}_{ab}(t) = \dot{\mathsf{p}}^*_{ba}(t) &= \tfrac{-i}{\hbar} H^I_{ab} \left[\mathsf{p}_{bb}(t) - \mathsf{p}_{aa}(t)\right] \cdot e^{-i\omega^0_{ab} t} \\ \dot{\mathsf{p}}_{bb}(t) = -\dot{\mathsf{p}}_{aa}(t) &= \tfrac{-i}{\hbar} \left[H^I_{ba} \mathsf{p}_{ab}(t) \cdot e^{i\omega^0_{ab} t} - H^I_{ab} \mathsf{p}_{ba}(t) \cdot e^{-i\omega^0_{ab} t}\right] \end{aligned} \tag{3.83}$$

A well-known two-level example is the electric dipole interaction potential H^I for an atomic electron in an oscillating electric field. Using the rotating-wave approximation of Rabi, the two-level equations (3.83) become the optical Bloch equations [45, ch. 2].

We have introduced the probabilistic Schrödinger equation, a new equation of motion (3.57) for the bilocal probability density. It is a second-order partial differential equation that is equivalent to the Schrödinger equation for the wavefunction. Next we show how to include the electromagnetic potential in the new bilocal equation.

3.6.4 Charged Particle in an External Electromagnetic Field

Our final step is to incorporate the electromagnetic potentials into equation (3.57). A Lagrangian for a particle of charge e in an electromagnetic field with scalar electric potential ϕ and vector magnetic potential A is [1]:

$$L(q, \dot{q}) = \tfrac{1}{2} m\dot{q}^2 + \tfrac{e}{c}\dot{q} \cdot A(q,t) - e\phi(q,t). \tag{3.84}$$

As introduced in [25] and in chapter 2, the Blue function (probability propagator) can be represented as the double path integral

$$B(x''t''\tau''; x't'\tau') = \iint e^{i\Delta S[q(t),\tau(t)]/\hbar}\, \mathcal{D}q(t)\mathcal{D}\tau(t), \tag{3.85}$$

where the *displaced action* or *motion* ΔS is given by the line integral

$$\Delta S[q(t), \tau(t)] \quad = \quad \int_{t'}^{t''} \Delta L(q, \dot{q}, \tau, \dot{\tau})\, dt, \tag{3.86}$$

and given any function f, we denote its displaced difference by $\Delta f = \Delta f(q, \tau) = f(q + \frac{\tau}{2}) - f(q - \frac{\tau}{2})$, and its displaced sum by $\bar{f} = \bar{f}(q, \tau) = f(q + \frac{\tau}{2}) + f(q - \frac{\tau}{2})$. The difference of displaced Lagrangians now is

$$\begin{aligned}
\Delta L(q, \dot{q}, \tau, \dot{\tau}) &= L(q + \tfrac{\tau}{2}, \dot{q} + \tfrac{\dot{\tau}}{2}) - L(q - \tfrac{\tau}{2}, \dot{q} - \tfrac{\dot{\tau}}{2}) \\
&= m\dot{q} \cdot \dot{\tau} + \frac{e}{c}\dot{q} \cdot \Delta A(q, \tau, t) \\
&\qquad + \frac{e}{c}\dot{\tau}/2 \cdot \bar{A}(q, \tau, t) - e\Delta\phi(q, \tau, t).
\end{aligned} \tag{3.87}$$

A pair of Legendre transformations, replacing variables $\frac{\dot{\tau}}{2}$ and $\dot{q}$ by canonical momenta $p \equiv \frac{\partial \Delta L[q(t)]}{\partial \dot{\tau}/2} = 2m\dot{q} + \frac{e}{c}\bar{A}(q, \tau, t)$ and $\sigma \equiv \frac{\partial \Delta L[q(t)]}{\partial \dot{q}} = 2m\frac{\dot{\tau}}{2} + \frac{e}{c}\Delta A(q, \tau, t))$, produces a Hamiltonian as a function of the new variables,

$$\begin{aligned}
\Delta H(q, p, \tau, \sigma) &\equiv p \cdot \tfrac{\dot{\tau}}{2} + \sigma \cdot \dot{q} - \Delta L \\
&= m\dot{q} \cdot \dot{\tau} + e\Delta\phi \\
&= \frac{1}{2m}\left(p - \frac{e}{c}\bar{A}\right) \cdot \left(\sigma - \frac{e}{c}\Delta A\right) + e\Delta\phi
\end{aligned} \tag{3.88}$$

Now the probabilistic Schrödinger equation (3.57) becomes:

$$\boxed{i\hbar\frac{\partial}{\partial t}\mathsf{P}(q, \tau, t) = \left[-\frac{\hbar^2}{2m}\left(\nabla_q - \frac{ie}{\hbar c}\bar{A}\right)\left(\nabla_{\frac{\tau}{2}} - \frac{ie}{\hbar c}\Delta A\right) + e\Delta\phi\right]\mathsf{P}(q, \tau, t),} \tag{3.89}$$

for the bilocal probability density P of the charged particle, as defined in (3.2).

3.7 Conclusion

The bilocal picture of quantum mechanics that was initiated in [25] was expanded upon here. We used Born's probability rule to justify the bilocal interference term (3.2) as a virtual probability. We defined families of actual and virtual events, and proved that Born's rule implies that, while two states may interfere, three or more states do not mutually interfere.

We found that the bilocal picture sheds light on currents in quantum mechanics. There are two types of bilocal current density, j and k, whose polar form and related mean velocities were given. In the bilocal context, the definitions of both current types simplify. In the unilocal case, the two types become the usual current and a fluctuation current. Their respective mean velocity fields are the usual Bohm velocity and the imaginary (osmotic) velocity. Future work might address the ties that the bilocal quantum densities and currents may have with angular momentum and vortices [46].

From the bi-continuity equation, we obtained a new, probabilistic Schrödinger equation for the bilocal probability. For this bilocal equation, we constructed dyadic stationary states. From this equation, the von Neumann equation for the time-dependent density of multi-level states followed directly. Finally, we showed how to include the electromagnetic potentials in this bilocal equation.

Chapter 4: Bilocal current densities and mean trajectories in a Young interferometer with two Gaussian slits and two detectors

The recent single-photon double-slit experiment of Steinberg *et al.* [47], based on a weak measurement method proposed by Wiseman, showed that, by encoding the photon's transverse momentum behind the slits into its polarization state, the momentum profile can subsequently be measured on average, from a difference of the separated fringe intensities for the two circular polarization components. They then integrated the measured average velocity field, to obtain the average trajectories of the photons enroute to the detector array.

In this chapter, we propose a modification of their experiment, to demonstrate that the average particle velocities and trajectories change when the mode of detection changes. The proposed experiment replaces a single detector by a pair of detectors with a given spacing between them. The pair of detectors is configured so that it is impossible to distinguish which detector received the particle. The pair of detectors is then analogous to the simple pair of slits, in that it is impossible to distinguish which slit the particle passed through.

To establish the paradoxical outcome of the modified experiment, the theory and explicit three-dimensional formulas are developed for the bilocal probability and current densities, and for the average velocity field and trajectories as the particle wavefunction propagates in the volume of space behind the Gaussian slits. Examples of these predicted results are plotted. Implementation details of the proposed experiment are discussed.

4.1 Introduction

Young's double-slit experiment for photons or matter particles such as electrons or neutrons produces wave-like interference fringes on a screen behind the slits [45, 48–53]. The photon is free to behave as a wave passing through both slits or apertures. But paradoxically, if we treat the photon as a particle, it behaves as a particle. If by some means we identify which slit location the photon went through, the photon wave collapses into a particle that passes through at most one slit. The interference vanishes and only two intensity bumps remain behind the two slits on the screen. Refinements of this experiment, such as the quantum eraser and Wheeler's delayed choice experiment [51, 54–57], demonstrate this paradox in depth.

The recent double-slit interferometer experiment designed by Steinberg and carried out in the laboratory by his team using single photons may have been the first to demonstrate weak measurements of momenta (preselection) made for single photons enroute to strong measurements of location (postselection) for the photons detected as particles impinging on the separate pixels of a CCD screen [47, 58–60]. Having measured the momentum field of the photons behind the slits in this way, then they could compute the average trajectories of the photons. Since this experiment, Matzkin has proposed weak path measurements [61]. These paths are the semi-classical paths for which the action is near-stationary. They can differ from the mean paths inferred in the Steinberg experiment. Bliokh *et al.* showed that the quantum momentum density field in the experiment can be identified with the classical Poynting momentum density field [42]. Davidović *et al.* proposed varying the Steinberg experiment, by measuring the average momenta with the two slits covered by orthogonal polarizers. In this case, the photon carries an imprint of which slit it passed through (as well as of its transverse momentum) and the interference fringe disappears [62].

Chapter 3 [63] showed that quantum mechanics offers two ways to detect a particle, when we allow it to arrive as a wave at two locations as well as a particle at one location on the detecting screen. As a consequence, the particle trajectories inferred from the

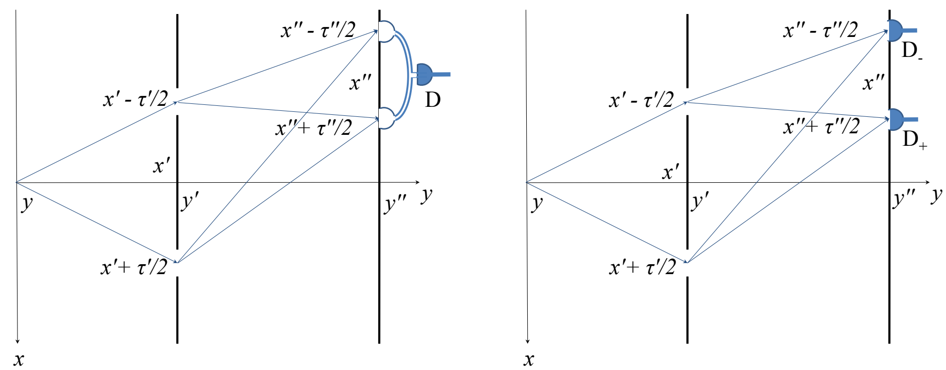

Figure 4.1: Double-slit, double-detector experiment configurations: (left) A pair of conjoined detectors, i.e., a two-port detector, allows wave-like arrivals of the particle. Just as which slits were passed through is ambiguous, so also is which detector port was entered. (right) For direct comparison, the two detectors are separated to count particle-like arrivals at each port. In this case, which port was entered is known.

weak momenta measurements of Steinberg *et al.* should be different for different detection modes. We are confronted with a new paradox of quantum mechanics: the average particle trajectories depend on how we configure the particle detectors.

4.1.1 Detecting wave-like arrivals in the double-slit interferometer experiment

A modified double-slit interferometer experiment is proposed in this chapter, to demonstrate that the average particle paths vary with the mode of detection. The experiment design employs a double or twin detector, which consists of two separated detectors that are conjoined to have a single output port, so that they sense the particle's impinging wavefront at two places at once (figure 4.1, left side). We will discuss possible implementations of this double detector in section 4.7. The interference fringes change as we vary only the detector spacing. As for any interferometer, an ambiguity always produces an interference term in the intensity distribution. In the proposed case, the ambiguity is not only that of "which slit?" did the particle pass through, but also that of "which detector?" did the particle impinge upon.

For comparison, the detectors placed at the two locations may be configured as independent, distinct units (figure 4.1, right side). In this case, which detector received the particle is known. The detector alternatives are distinguishable, or unambiguous, and there is no wavefront interference. Accordingly, we have a different probability of arrival and detection for each arrangement of two detectors.

We assume throughout this chapter that the detectors have perfect efficiency, so that every particle that arrives at a detector is detected and counted. It is worth noting (even if almost self-evident) that the appropriate detector for a particle arrival event must conform spatially to the kind of event we want it to detect. The detector must not filter out or get in the way of the arriving particle. If the particle arrives at a single location, the usual single detector placed at the location receives it as a particle, and faithfully counts the number of arrivals of this particle-like kind. If the particle arrives at one or both of two places, the bilocal twin detector receives it as a wave, and likewise faithfully counts the number of arrivals of this wavelike kind.

4.1.2 Bilocal picture of quantum mechanics

To propagate the probability and current densities for the double slits and double detectors in closed form, it is convenient to use a bilocal equivalent of the Schrödinger picture, which was introduced in chapter 3 and in [25][63]. To make this chapter self-contained, we briefly review its basic elements here, as follows.

Consider a quantum-mechanical particle whose state is spatially represented by a wavefunction $\psi(x)$. We begin with the *displaced* (bilocal) probability density of simultaneous arrival at time t' at two places $q_1', q_2' = x' \pm \frac{\tau'}{2}$,

$$\mathsf{P}(x't', \tau') \quad = \quad \psi^*(x' - \tfrac{\tau'}{2}, t')\psi(x' + \tfrac{\tau'}{2}, t'). \tag{4.1}$$

It is complex-valued and thus is only a quasi-probability density; but for spacing $\tau' = 0$ it reduces to the real-valued probability of arrival $|\psi(x', t')|^2$. It has an associated displaced (bilocal) current density

$$\mathsf{j}(x't',\tau') = \frac{\hbar}{2im}\left[\psi^*(x'-\tfrac{\tau'}{2},t')\nabla_{x'}\psi(x'+\tfrac{\tau'}{2},t') \right.$$
$$\left. -\psi(x'+\tfrac{\tau'}{2},t')\nabla_{x'}\psi^*(x'-\tfrac{\tau'}{2},t')\right]. \tag{4.2}$$

The bilocal probability and current densities in equations (4.1) and (4.2) together satisfy a continuity equation,

$$\left[i\hbar\frac{\partial}{\partial t'} - \Delta V(x'\tau't')\right]\mathsf{P}(x'\tau't') = -i\hbar\nabla_{x'}\cdot\mathsf{j}(x'\tau't'), \tag{4.3}$$

where we define

$$\Delta V(x',\tau',t') = V\left(x'+\tfrac{\tau'}{2},t'\right) - V\left(x'-\tfrac{\tau'}{2},t'\right) \tag{4.4}$$

and V is the possibly time-dependent potential. This equation (4.3) was shown in [25] to be equivalent to the Schrödinger equation. Both equations employ the energy and momentum operators, but equation (4.3) is a first order equation instead of second order.

The solution of the Schrödinger equation at time $t' \geq t$ is

$$\psi(x't') = \int dx \;\; G(x't';xt)\psi(xt), \tag{4.5}$$

for a Green function G, given as a path integral in [1]. The solution of the bilocal continuity equation (4.3) at time $t' \geq t$ is

$$\mathsf{P}(x't', \tau') = \iint dx\, d\tau\ B(x't'\tau'; xt\tau)\mathsf{P}(xt, \tau) \tag{4.6}$$

$$\mathsf{j}(x't', \tau') = \iint dx\, d\tau\ \mathbf{B}(x't'\tau'; xt\tau)\mathsf{P}(xt, \tau), \tag{4.7}$$

for Blue functions $B, \mathbf{B}$, given as path integrals in [25].

If there is no potential field ($V = 0$), the free Green propagator is [1]

$$\begin{aligned} G_0(x't'; xt) &= \langle x't' \,| xt \rangle \\ &= \left(\tfrac{m}{2\pi i\hbar T}\right)^{\frac{3}{2}} \exp\left\{\tfrac{im}{2\hbar T}|x' - x|^2\right\}. \end{aligned} \tag{4.8}$$

where $T = t' - t$ is the elapsed time. The free Blue probability propagator is [25]

$$B_0(x't'\tau'; xt\tau) = \left(\tfrac{m}{2\pi\hbar T}\right)^3 \exp\left\{\tfrac{im}{\hbar T}(x' - x) \cdot (\tau' - \tau)\right\}, \tag{4.9}$$

and the free current propagator is $\mathbf{B}_0 = \mathbf{v}B_0^0$, where $\mathbf{v}_k = \frac{(x'-x)_k}{T}$ for $k = 1, 2, 3$ [63]. In this paper, we will need only the free Blue propagators.

4.1.3 Probability theory for the wavefunction of a particle

We have just seen that, to propagate the wavefunction's real-valued probability density into the future, it is necessary and sufficient to operate upon the complex-valued probability density (4.1) given at the present time t [25]. The integral operator with its four-component Blue kernel acts on (4.1), to give the future probability and current density. In this sense, the displaced probability density (4.1) provides operational closure. Its central role in probability propagation suggests that it should have physical meaning. Its real part (times two) may be interpreted as a signed, *virtual probability* of self-interference, which occurs

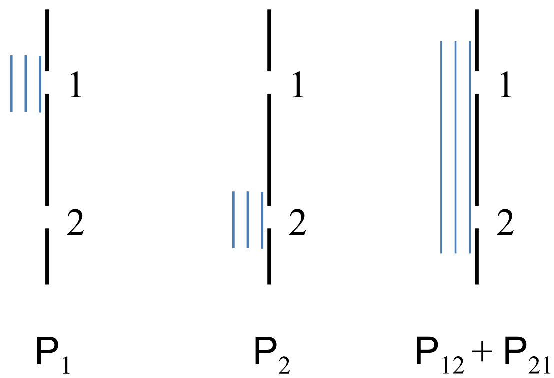

Figure 4.2: Bilocal events, for locations 1 and 2 at time t, and a particle depicted as a wavefront: (left) particle arrives at 1 with probability P_1; (center) particle arrives at 2 with probability P_2; (right) particle arrives at both 1 and 2 (wavelike arrival) with virtual probability $\mathsf{P}_{12} + \mathsf{P}_{21}$. The combined event of arrival at 1 or 2 or both has probability given by the sum $\bar{\mathsf{P}}_{1,2} = \mathsf{P}_1 + \mathsf{P}_2 + (\mathsf{P}_{12} + \mathsf{P}_{21})$, equation (3.15). The event of wavelike arrival at both locations (right) is considered to be a virtual event, which occurs only with the single-location events. If, by some means, we can determine which location the particle passed through, the virtual probability vanishes (i.e., $(\mathsf{P}_{12} + \mathsf{P}_{21}) = 0$, resulting in equation (3.13)). In this paper, we solve for these probability densities, as well as the current densities j and mean velocities v associated with these events.

during the wavefunction's collapse to produce the observed probability of detection.

For any two locations 1 and 2, given by coordinates $q_1, q_2 = x \pm \frac{\tau}{2}$, there are four ways for the particle to arrive in one or both locations at once, as shown in figure 2. It may behave like a particle, arriving at either place (left side and center of figure 2). The quantum-mechanical particle may also behave like a wave, arriving at both places simultaneously (right side of figure 2). This arrival may occur in two ways, oriented in a (1,2) or (2,1) sense.

For two single (independent) detectors, the associated total probability element $\overline{\mathsf{P}}(x \pm \frac{\tau}{2}, t)\mathrm{d}^3\mathrm{x}$ to arrive (and be detected) at either (not both) of the two locations, each with volume element $\mathrm{d}^3\mathrm{x}$, is given by

$$\overline{\mathsf{P}}(x \pm \tfrac{\tau}{2}, t)\, \mathrm{d}^3\mathrm{x} = \mathsf{P}(x + \tfrac{\tau}{2}, t, 0)\mathrm{d}^3\mathrm{x} + \mathsf{P}(\mathrm{x} - \tfrac{\tau}{2}, \mathrm{t}, 0)\mathrm{d}^3\mathrm{x} \tag{4.10}$$

$$= \left|\psi(x + \tfrac{\tau}{2})\right|^2 \mathrm{d}^3\mathrm{x} + \left|\psi(\mathrm{x} - \tfrac{\tau}{2})\right|^2 \mathrm{d}^3\mathrm{x}. \tag{4.11}$$

From now on, we denote a two-detector probability density with an overline. For a double detector, the associated total probability $\overline{\mathsf{P}}(x \pm \frac{\tau}{2}, t)\mathrm{d}^3\mathrm{x}$ to arrive and be detected at one or both locations is given by

$$\begin{aligned} \overline{\mathsf{P}}(x \pm \tfrac{\tau}{2}, t)\mathrm{d}^3\mathrm{x} &= \mathsf{P}(x + \tfrac{\tau}{2}, t, 0)\mathrm{d}^3\mathrm{x} + \mathsf{P}(\mathrm{x} - \tfrac{\tau}{2}, \mathrm{t}, 0)\mathrm{d}^3\mathrm{x} \\ &\quad + \mathsf{P}(xt, \tau)\mathrm{d}^3\mathrm{x} + \mathsf{P}(\mathrm{xt}, -\tau)\mathrm{d}^3\mathrm{x} \qquad (4.12) \\ &= \left|\psi(x + \tfrac{\tau}{2}) + \psi(x - \tfrac{\tau}{2})\right|^2 \mathrm{d}^3\mathrm{x} \geq 0. \qquad (4.13) \end{aligned}$$

Of the four probabilities summed above, we of course recognize the first two from equation (4.10), as those of arriving at a single location. The last two probabilities in the sum (4.12) represent wavelike, bilocal presence of the object. As a conjugate pair, their sum is the real part of (4.1) (times two) and may be negative. But in absolute value this quantity never exceeds the sum of the first two probabilities for the usual particle-like, unilocal presence of the object at one of the two locations. An argument is made in chapter 3 [63] to justify calling this quantity a virtual probability.

Given an array of multiple detectors, there are of course many possible ways to arrange them so that subsets of them are conjoined detectors, and others are kept as single detector units. For example, multiple detectors may all be conjoined. For a single particle detected in any of K locations $x_k = \bar{x} + \tau_k$, for $k = 1, 2, 3, \ldots, K$, about their mean location $\bar{x}$, when all detectors are conjoined, the total probability of detection at any one of these locations (particle-like detection), or at multiple co-locations (wavelike detection) at time t is given by:

$$\overline{\mathsf{P}}(x_1, \ldots, x_K, t)\mathrm{d}^3\mathrm{x} = \left|\tfrac{1}{\sqrt{K}}\left[\psi(x_1) + \psi(x_2) + \cdots + \psi(x_K)\right]\right|^2 \cdot K\mathrm{d}^3\mathrm{x}. \qquad (4.14)$$

This formula also applies to one detector, whose aperture is considered to be divided into K equal parts, each of volume $\mathrm{d}^3\mathrm{x}$.

4.1.4 Chapter overview

In this chapter, we develop complete closed-form formulas for the three-dimensional probability and current density, and the mean velocity field in the recent two-slit experiment of Steinberg *et al.* [47]. Formulas provide flexibility, and physical insight that we may miss when we begin with numerical computing. These formulas enable us to predict the results of modifying the detectors in this experiment.

The outline of the rest of this chapter is as follows: The integrals that propagate the bilocal probability and current densities for both particle-like and wave-like detection are set up in section 4.2, including the aperture function for the two Gaussian slits. These integrals are then evaluated in sections 4.3 and 4.4. Mean velocities and trajectories are computed in sections 4.5 and 4.6. Details of the proposed experiment are covered in section 4.7. We conclude in section 4.8.

4.2 Propagation path integrals and the Gaussian slit model

4.2.1 Two path legs in succession

To propagate through the slits, and find the final probability and current density arriving at the double detector, we will use a two-kernel integral, as we explain now. We can propagate in two path legs or stages in succession. We split the time interval $[0, t'']$ at the time t' when the particle arrives at the slits, and likewise split the path integral kernel into two parts, using the property that

$$B(x''t''\tau''; x_0\tau) \quad = \quad \iint dx'\, d\tau'\; B(x''t''\tau''; x't'\tau')B(x't'\tau'; xt\tau). \tag{4.15}$$

This property follows from the path integral for the Blue function, given by equation (24) in [25]. This property will allow us to insert an aperture or window function to represent the two slits at the time t', to restrict the possible paths from source to detector to those passing through the twin slits.

The current blue function $\mathbf{B}$ satisfies a similar, but mixed, completeness property that follows from its path integral expressed by equation (74) in [25]:

$$\mathbf{B}(x''t''\tau''; x_0\tau) \quad = \quad \iint dx'\, d\tau'\, \mathbf{B}(x''t''\tau''; x't'\tau')B(x't'\tau'; xt\tau). \tag{4.16}$$

For the potential-free case, with $\mathbf{B} = \mathbf{v}''B_0$, the key difference in splitting this current propagator (versus splitting the probability propagator (4.15)) is that the final endpoint velocity factor $\mathbf{v}''$ only occurs in the later path segment.

4.2.2 Gaussian slits

For a realistic model, we use two circular gaussian slits. This model was implemented in the double-slit experiment of Steinberg *et al.* by two fiber-launched gaussian beams. In their experiment, the twin beams were produced by passing a gaussian beam of single photons through an in-fiber beamsplitter [47].

To obtain the aperture function for the two gaussian slits, consider any pair of points $q, \tilde{q}$ of passage through the middle screen of either side of figure 4.1. The two-variable transformation $q, \tilde{q} = x \pm \frac{\tau}{2}$ has unity Jacobian. We saw in section 4.1 that the x, τ parameters for the Blue integral specify four alternative path pairs that the particle may thread through one or both passage points.

For our two-leg paths, the particle entering one of the slits in the screen will pass *through* the slit with a gaussian probability-of-passage amplitude, $g_q(q_0, b^2) = \frac{1}{\sqrt{2\pi}b}\exp\left\{-\frac{1}{2}\left(\frac{q-q_0}{b}\right)^2\right\}$, specified by its mean q_0 and variance b^2.(This amplitude is an approximation of unity [21], whose limit as $b \to 0$ is the delta function $\delta\left(q - q_0\right)$. The passage-probability variance after squaring is $b^2/2$, for an effective r.m.s. half-width parameter of $0.707b$.)

To model the experiment of [47], we assume a circular slit aperture, so that the passage probability for the x and y components of q independently has this distribution with variance

$b^2/2$ along both dimensions. Since the slit is 2-dimensional, it does not affect passage along the z direction. We model the z component of passage probability as uniformly 1 along the q_z axis. This may be regarded as as an unnormalized gaussian probability density with infinite variance, i.e. its exponent is always 0.

It follows that the passage probabilities for x and τ also have gaussian distributions in the plane of the slit. The variance of $x = \frac{1}{2}(q + \tilde{q})$ and of $\frac{\tau}{2} = \frac{1}{2}(q - \tilde{q})$ are both $b^2/2$ (in each direction, x and y). Let $s = 2$ be the number of finite dimensions defining the slits. Now we replace each delta function in the point-slit aperture formula of example 3 of [25] by its corresponding gaussian. That is, we replace each one-dimensional delta of form $\delta(x - x^0)$ by a gaussian of form $\frac{1}{\sqrt{2}} g_x(x^0)$. This yields the aperture function for a pair of gaussian circular slits:

$$\begin{aligned}
\alpha(x, \tau) &= g_x(x') \cdot \left(g_{\frac{\tau}{2}}(\tfrac{\tau'}{2}) + g_{\frac{\tau}{2}}(-\tfrac{\tau'}{2}) \right) + g_{\frac{\tau}{2}}(0) \cdot \left(g_x([x' - \tfrac{\tau'}{2}]) + g_x([x' + \tfrac{\tau'}{2}]) \right) \\
&= \left(\frac{1}{2\pi b^2} \right)^s e^{-\frac{1}{b^2}(x - x')^2} \left[e^{-\frac{1}{b^2}\left(\frac{\tau - \tau'}{2}\right)^2} + e^{-\frac{1}{b^2}\left(\frac{\tau + \tau'}{2}\right)^2} \right] \\
&\quad + \left(\frac{1}{2\pi b^2} \right)^s e^{-\frac{1}{b^2}\left(\frac{\tau}{2}\right)^2} \left[e^{-\frac{1}{b^2}\left(x - \left[x' - \frac{\tau'}{2}\right]\right)^2} + e^{-\frac{1}{b^2}\left(x - \left[x' + \frac{\tau'}{2}\right]\right)^2} \right]. \qquad (4.17)
\end{aligned}$$

Another way to derive this aperture formula (4.17) is to begin with the sum of the two gaussians $g_q(x' \pm \frac{\tau'}{2}, b^2)$. This sum is the relative probability amplitude of passage through either or both slits, given arrival at the slits. We insert this sum, as the Green aperture amplitude factor, inside both the left and right copies of the Green integral in equation (10) of [25]. We multiply both sums and get four pairs of exponential products. After substituting $r, s = x \pm \frac{\tau}{2}$ into the exponents there, we can add the exponents in pairs. Then the Blue aperture function equation (4.17) follows from squaring and rearranging the exponents.

4.3 The interference pattern

We take the general double-endpoint case of arbitrary detector spacing τ'', as shown on the left side of figure 4.1. The Blue propagation integral (4.6) takes the particle over its first leg to any double destination x', τ' at time t': $\mathsf{P}(x't', \tau') = B_0(x't'\tau; x'00) = \left(\frac{m}{2\pi\hbar t'}\right)^3 \exp\left\{\frac{i}{\hbar}\left[m\frac{x'-x^0}{t'}\right] \cdot [\tau' - 0]\right\}$. Then after the second leg, by the completeness relation (4.15, the interference fringe pattern or final probability density is given by the Blue propagation integral

$$\mathsf{P}(x''t'', \tau'') = \iint d\hat{x}\, d\hat{\tau}\; B_0(x''t''\tau''; \hat{x}t'\hat{\tau})\alpha(\hat{x}, \hat{\tau})\mathsf{P}(\hat{x}t', \hat{\tau}). \tag{4.18}$$

The aperture function α given by (4.17) has four terms, so the propagation integral (4.18) breaks into four, which we will integrate in this section. Each of the four Gaussian integrals results in a probability density over the final screen with its own unique meaning. The first integral is:

$$\begin{aligned}
\mathsf{P}^{(12)} \quad = \quad & \left(\frac{1}{2\pi b^2}\right)^s \left(\frac{m}{2\pi\hbar t'}\right)^d \left(\frac{m}{2\pi\hbar T}\right)^d \\
& \times \iint d\hat{x}\, d\hat{\tau}\; \exp\left\{-\frac{1}{b^2}\left(\hat{x} - x'\right)^2\right\} \cdot \exp\left\{-\frac{1}{b^2}\left[\tfrac{1}{2}\left(\hat{\tau} - \tau'\right)\right]^2\right\} \\
& \quad \times \exp\left\{\frac{i2m}{\hbar T}\left(\hat{x} - x' + (x' - x'')\right) \cdot \tfrac{1}{2}\left(\hat{\tau} - \tau' + (\tau' - \tau'')\right)\right\} \\
& \quad \times \exp\left\{\frac{i2m}{\hbar t'}\left(\hat{x} - x' + (x' - x^0)\right) \cdot \tfrac{1}{2}\left(\hat{\tau} - \tau' + (\tau' - \tau^0)\right)\right\}
\end{aligned} \tag{4.19}$$

The last two exponents above have been prepared for a change of variables. Substituting x

for $\hat{x} - x'$ and τ for $\hat{\tau} - \tau'$, then $\frac{\tau}{2}$ for τ, and using $x^0 = \tau^0 = (0,0,0)$, we find

$$\begin{aligned} \mathsf{P}^{(12)} \quad = \quad & 2^d \left(\frac{1}{2\pi b^2}\right)^s \left(\frac{m}{2\pi\hbar t'}\right)^d \left(\frac{m}{2\pi\hbar T}\right)^d \iint dx\, d\tfrac{\tau}{2}\ \exp\left\{-\frac{1}{b^2}x^2\right\} \cdot \exp\left\{-\frac{1}{b^2}\left(\tfrac{\tau}{2}\right)^2\right\} \\ & \times \exp\left\{\frac{i2m}{\hbar T}\left[x - (x'' - x')\right] \cdot \tfrac{1}{2}\left[\tau - (\tau'' - \tau')\right]\right\} \\ & \times \exp\left\{\frac{i2m}{\hbar t'}\left[x + x'\right] \cdot \tfrac{1}{2}\left[\tau + \tau'\right]\right\} \end{aligned} \tag{4.20}$$

The factor $1/b^2$ in the gaussian exponents in the first line of equation (4.20) above applies only to their x and y exponents, for the circular slit. In their z gaussian exponents, this factor is replaced by 0, making the z-component exponentials 1. (To model a slit which has x-width b, but which is open along the entire y-axis, we would similarly just replace the y-gaussian density by 1.)

We can convert equation (4.20) into a gaussian integral in $2d$ dimensions. The exponent of the integrand separates into a sum of $d = 3$ two-dimensional quadratic forms:

$$-\tfrac{1}{2}v_k \cdot A_k \cdot v_k + i\left(u_k^{(12)} + w_k^{(12)}\right) \cdot v_k + i\tfrac{1}{2}u_k^{(12)} \cdot B \cdot u_k^{(12)} + i\tfrac{1}{2}w_k^{(12)} \cdot B' \cdot w_k^{(12)}, \tag{4.21}$$

where we use the Einstein summation convention to sum the forms for $k = 1,2,3$ (for $d = 3$ dimensions of space). Each two-dimensional form may be integrated separately, by the Fubini theorem. Here $v_k = (x, \frac{\tau}{2})_k$, A_k is a 2×2 matrix, $B = \frac{\hbar T}{2m}\sigma_1 = \frac{\hbar T}{2m}\begin{pmatrix} 0 & 1 \\ 1 & 0 \end{pmatrix}$, $B' = \frac{\hbar t'}{2m}\sigma_1$, and $u_k^{(12)}$ and $w_k^{(12)}$ are constant vectors. In our case the quadratic form is specified by

$$
\begin{aligned}
A_k &= 2 \cdot \begin{bmatrix} \frac{1}{b^2} & -\frac{im}{\hbar T}\gamma \\ -\frac{im}{\hbar T}\gamma & \frac{1}{b^2} \end{bmatrix} = 2 \cdot \begin{bmatrix} \frac{1}{b^2} & -\frac{i\gamma m}{\hbar T} \\ -\frac{i\gamma m}{\hbar T} & \frac{1}{b^2} \end{bmatrix} \\
u_k^{(12)} &= -\frac{2m}{\hbar T} \cdot \begin{bmatrix} \frac{1}{2}(\tau'' - \tau') \\ (x'' - x') \end{bmatrix}_k \\
w_k^{(12)} &= \frac{2m}{\hbar t'} \cdot \begin{bmatrix} \frac{1}{2}(\tau' - \tau^0) \\ (x' - x^0) \end{bmatrix}_k .
\end{aligned} \tag{4.22}
$$

For $k = 3$, we must take the limit of A_k as $b \to \infty$, as we explain soon. As a shorthand, we define the ubiquitous constant

$$\gamma \equiv \left(1 + \frac{T}{t'}\right) = \frac{t''}{t'}. \tag{4.23}$$

Since the last two terms $i\frac{1}{2}u_k^{(12)} \cdot Bu_k^{(12)}$ and $i\frac{1}{2}w_k^{(12)} \cdot B'w_k^{(12)}$ of this form (4.21) are constant, we can take them outside the integral. Put $J_k^{(12)} = u_k^{(12)} + w_k^{(12)}$. The gaussian integral that remains has the closed form [17, 66, 67]

$$\iint d\hat{x}\, d\frac{\hat{\tau}}{2}\ \exp\left\{-\tfrac{1}{2}v_k \cdot A_k v_k + iJ_k^{(12)} v_k\right\} = \left(\frac{2\pi}{\sqrt{\det A_k}}\right)^d \exp\left\{-\tfrac{1}{2}J_k^{(12)} \cdot A_k^{-1} J_k^{(12)}\right\} \tag{4.24}$$

For our application,

$$
\begin{aligned}
A_k^{-1} &= \frac{2}{\det A_k} \begin{bmatrix} \frac{1}{b^2} & \frac{im}{\hbar T}\gamma \\ \frac{im}{\hbar T}\gamma & \frac{1}{b^2} \end{bmatrix} \\
\det A_k &= 4 \cdot \left(\frac{1}{b^4} + \left[\frac{m}{\hbar T}\gamma \right]^2 \right) = \left(\frac{2m}{\hbar T b} \right)^2 \left[\left(\frac{\hbar T}{mb} \right)^2 + b^2\gamma^2 \right] \\
J_k^{(12)} &= u_k^{(12)} + w_k^{(12)} = \quad -\frac{2m}{\hbar T} \cdot \begin{bmatrix} \frac{1}{2}\left(\tau'' - \tau'\gamma\right) \\ \left(x'' - x'\gamma\right) \end{bmatrix}. \qquad (4.25)
\end{aligned}
$$

Therefore, applying the coefficient of $J_k^{(12)}$ twice to A_k^{-1} cancels part of $\det A_k$:

$$
\begin{aligned}
\left(\frac{2m}{\hbar T} \right)^2 A_k^{-1} &= \frac{2}{(\Delta x)^2} \begin{bmatrix} 1 & i\frac{mb^2}{\hbar T}\gamma \\ i\frac{mb^2}{\hbar T}\gamma & 1 \end{bmatrix} \\
(\Delta x)^2 &= \left(\frac{\hbar T}{mb} \right)^2 + b^2\gamma^2, \quad \sqrt{\det A_k} = \frac{2m\Delta x}{\hbar T b}. \qquad (4.26)
\end{aligned}
$$

This is the formula for A_k^{-1} for both the x and y-components of the form. For the z-component, we need the limit of A_k^{-1} as $b^{-2} \to 0$ in equation (4.25):

$$
\begin{aligned}
\left(\frac{2m}{\hbar T} \right)^2 A_z^{-1} &= \frac{2}{\gamma^2} \begin{bmatrix} 0 & i\frac{m}{\hbar T}\gamma \\ i\frac{m}{\hbar T}\gamma & 0 \end{bmatrix} \\
\sqrt{\det A_z} &= \frac{2m\gamma}{\hbar T}. \qquad (4.27)
\end{aligned}
$$

Since this limit exists, we can apply the integral formula (4.24) even for the z-component ($k = 3$), for which the gaussian slit function leaves the diagonal of A_z empty (0's).

Collecting the terms, we get the first probability of four:

$$\mathsf{P}^{(12)} = C \exp\left\{-\tfrac{1}{2} J_k^{(12)} \cdot A_k^{-1} J_k^{(12)} + i\tfrac{1}{2}\left(u_k^{(12)} \cdot B u_k^{(12)} + w_k^{(12)} \cdot B' w_k^{(12)}\right)\right\} \quad (4.28)$$

where the Einstein convention is used, and the normalizing constant is

$$\begin{aligned} C &= 2^d \cdot \frac{2\pi}{\gamma} \frac{\hbar T}{2m} \left(\frac{2\pi}{\Delta x} \frac{\hbar T b}{2m} \frac{1}{2\pi b^2}\right)^s \left(\frac{m}{2\pi\hbar t'} \frac{m}{2\pi\hbar T}\right)^d \\ &= \frac{2\pi}{\gamma} \left(\frac{\hbar T}{m}\right)^{s+1} \left(\frac{1}{b\Delta x}\right)^s \left(\frac{m}{2\pi\hbar t'} \frac{m}{2\pi\hbar T}\right)^d . \end{aligned} \quad (4.29)$$

The second integral of the four is like the first, but the mean value $-\tau'$ replaces τ' in the aperture gaussian. Since $\frac{\tau'}{2}$ enters the integral in the second piece only to define the slit center displacement $\frac{\tau'}{2}$, we immediately have for the slit center at $x' + \frac{\tau'}{2}$ the similar result

$$\mathsf{P}^{(21)} = C \exp\left\{-\tfrac{1}{2} J_k^{(21)} \cdot A_k^{-1} J_k^{(21)} + i\tfrac{1}{2}\left(u_k^{(21)} \cdot B u_k^{(21)} + w_k^{(21)} \cdot B' w_k^{(21)}\right)\right\} \quad (4.30)$$

by replacing $\frac{\tau'}{2} \leftarrow -\frac{\tau'}{2}$ in formulas (4.22) to define $u_k^{(21)}, w_k^{(21)}, J_k^{(21)}$.

The third integral is

$$\begin{aligned} \mathsf{P}^{(1)} = \; & \left(\frac{1}{2\pi b^2}\right)^s \left(\frac{m}{2\pi\hbar t'}\right)^d \left(\frac{m}{2\pi\hbar T}\right)^d \iint d\hat{x}\, d\hat{\tau} \\ & \exp\left\{-\frac{1}{b^2}\left(\hat{x} - \left[x' - \tfrac{\tau'}{2}\right]\right)^2\right\} \cdot \exp\left\{-\frac{1}{b^2}\left(\tfrac{\hat{\tau}}{2} - 0\right)^2\right\} \\ & \times \exp\left\{\frac{im}{\hbar T}\left(\hat{x} - \left[x' - \tfrac{\tau'}{2}\right] + (\left[x' - \tfrac{\tau'}{2}\right] - x'')\right) \cdot (\hat{\tau} - \tau''))\right\} \\ & \times \exp\left\{\frac{im}{\hbar t'}\left(\hat{x} - \left[x' - \tfrac{\tau'}{2}\right] - \left(x^0 - \left[x' - \tfrac{\tau'}{2}\right]\right)\right) \cdot \left(\hat{\tau} - \tau^0\right)\right\} \end{aligned} \quad (4.31)$$

Substituting x for $\hat{x} - \left[x' - \frac{\tau'}{2}\right]$, then $\frac{\tau}{2}$ for $\hat{\tau}$, we have

$$\begin{aligned}
\mathsf{P}^{(1)} \quad = \quad & 2^d \left(\frac{1}{2\pi b^2}\right)^s \left(\frac{m^2}{4\pi^2\hbar^2 t' T}\right)^d \iint dx\, d\tfrac{\tau}{2}\; \exp\left\{-\frac{1}{b^2}x^2\right\} \cdot \exp\left\{-\frac{1}{b^2}\left(\tfrac{\tau}{2}\right)^2\right\} \\
& \times \exp\left\{\frac{i2m}{\hbar T}\left(x - \left(x'' - \left[x' - \tfrac{\tau'}{2}\right]\right)\right) \cdot \tfrac{1}{2}\left(\tau - \tau''\right)\right\} \\
& \times \exp\left\{\frac{i2m}{\hbar t'}\left(x - \left(x^0 - \left[x' - \tfrac{\tau'}{2}\right]\right)\right) \cdot \tfrac{\tau}{2}\right\} \qquad (4.32)
\end{aligned}$$

The exponent of this third integrand is again the quadratic form

$$-\tfrac{1}{2}v_k \cdot A_k \cdot v_k + i\left(u_k^{(1)} + w_k^{(1)}\right) \cdot v_k + i\tfrac{1}{2}\left(u_k^{(1)} \cdot B \cdot u_k^{(1)} + w_k^{(1)} \cdot B' \cdot w_k^{(1)}\right), \qquad (4.33)$$

with the same A_k, B, B' and Δx. But now $u_k^{(1)}, w_k^{(1)}, J_k^{(1)}$ are given by

$$\begin{aligned}
u_k^{(1)} &= -\frac{2m}{\hbar T} \cdot \begin{bmatrix} \frac{\tau''}{2} \\ x'' - \left[x' - \frac{\tau'}{2}\right] \end{bmatrix}_k \\
w_k^{(1)} &= -\frac{2m}{\hbar t'} \cdot \begin{bmatrix} \frac{\tau}{2}^0 \\ x^0 - \left[x' - \frac{\tau'}{2}\right] \end{bmatrix}_k \\
J_k^{(1)} &= u_k^{(1)} + w_k^{(1)} \\
&= -\frac{2m}{\hbar T} \cdot \begin{bmatrix} \frac{\tau''}{2} \\ x'' - \left[x' - \frac{\tau'}{2}\right]\gamma \end{bmatrix}_k . \qquad (4.34)
\end{aligned}$$

Collecting the terms once more, we have the third probability (1)

$$\begin{aligned}
\mathsf{P}^{(1)} &= C\exp\left\{-\tfrac{1}{2}J_k^{(1)}\cdot A_k^{-1}J_k^{(1)} + i\tfrac{1}{2}\left(u_k^{(1)}\cdot B\cdot u_k^{(1)} + w_k^{(1)}\cdot B'\cdot w_k^{(1)}\right)\right\} \\
&= C\exp\left\{-\tfrac{1}{2}J_k^{(1)}\cdot A_k^{-1}J_k^{(1)} + i\tfrac{1}{2}u_k^{(1)}\cdot B\cdot u_k^{(1)}\right\} \qquad (4.35)
\end{aligned}$$

Because $\tau^0 = (0,0,0)$, we have $w_k^{(1)}\cdot B'\cdot w_k^{(1)} = 0$.

Since $\frac{\tau'}{2}$ enters the integral in equation (4.31) only to define the slit center $x' - \frac{\tau'}{2}$, we immediately have for the slit center at $x' + \frac{\tau'}{2}$ the similar and fourth result

$$\mathsf{P}^{(2)} = C\exp\left\{-\tfrac{1}{2}J_k^{(2)}\cdot A_k^{-1}J_k^{(2)} + i\tfrac{1}{2}u_k^{(2)}\cdot Bu_k^{(2)}\right\}, \qquad (4.36)$$

by replacing $\frac{\tau'}{2} \leftarrow -\frac{\tau'}{2}$ in formulas (4.34) to define $u_k^{(2)}, w_k^{(2)}, J_k^{(2)}$.

The four parts of equation (4.18) have been evaluated as formulas (4.28), (4.30), (4.35) and (4.36). Their sum is the actual interference pattern

$$\begin{aligned}
\mathsf{P}(x''t'',\tau'') &= \iint d\hat{x}\,d\hat{\tau}\;\alpha(\hat{x},\hat{\tau})B_0(x''t''\tau'';\hat{x}t'\hat{\tau})\mathsf{P}(\hat{x}t',\hat{\tau}) \\
&= \mathsf{P}^{(12)} + \mathsf{P}^{(21)} + \mathsf{P}^{(1)} + \mathsf{P}^{(2)}. \qquad (4.37)
\end{aligned}$$

Each part has a meaning as a probability: one for each slit by itself, and a conjugate pair of interference probabilities. For a single slit, the aperture function has only one term, the third term of equation (4.17) for the lower slit, or the fourth term for the upper slit. Thus the propagation integrals $\mathsf{P}^{(1)}$ and $\mathsf{P}^{(2)}$ each represent the diffraction pattern for a single gaussian slit, the lower and upper slits, respectively.

What are the first two aperture terms in equation (4.17), and the two densities that result from them, $\mathsf{P}^{(12)}$ and $\mathsf{P}^{(21)}$? These aperture terms signify wavelike passage through both slits. In turn, the corresponding densities are complex conjugates, whose sum $\mathsf{P}^{(12)} + \mathsf{P}^{(21)}$ is a real, though possibly negative, virtual probability of wavelike passage through both slits and subsequent interference. However, as we have seen, the total sum (4.37) gives us the nonnegative probability of arrival at the screen, whose statistics accumulate as an interference fringe. Figure 4.4 below displays the entire probability density surface over the x-z plane with $y = 0$ for the double slit, single detector Steinberg experiment reported in [47].

4.3.1 Example: single detector in one dimension

As an example, we examine these four probabilities for twin Gaussian slits in the usual case of a single detector, i.e. for $\tau'' = 0$. Consider the single slit patterns $\mathsf{P}^{(1)}$ and $\mathsf{P}^{(2)}$ first. In this case, the imaginary term $iu_k^{(1)} \cdot Bu_k^{(1)}$ in equation (4.35) vanishes. The imaginary parts in $J_k^{(1)} \cdot A_k^{-1} J_k^{(1)}$ also vanish, since we can write it in the simple form

$$J_k^{(1)} \cdot A_k^{-1} J_k^{(1)} = \begin{bmatrix} 0 \\ X \end{bmatrix} \cdot \begin{bmatrix} 1 & ib^2\beta \\ ib^2\beta & 1 \end{bmatrix} \begin{bmatrix} 0 \\ X \end{bmatrix} = X^2.$$

Here we label the second component of $J^{(1)}$ in equation (4.34) as $X = \left(x'' - \left[x' - \frac{\tau'}{2}\right]\gamma\right)$, where $\gamma = 1 + T/t'$. The same result occurs for $J^{(2)}$, but for $-\tau'$ instead of $+\tau'$. Using these algebraic facts, for $\tau'' = 0$ and one dimension $d = 1, s = 1$ we have

$$\mathsf{P}^{(1,2)}(x'') = \frac{1}{\pi b^2} \frac{mb}{2\pi\hbar\Delta x t'} \exp\left\{ -\frac{1}{(\Delta x)^2} \left(x'' - \left[x' \pm \frac{\tau'}{2} \right] \gamma \right)^2 \right\}. \tag{4.38}$$

This is in agreement with the formula for the single-slit gaussian diffraction pattern for $d = 1$ given in [1] (The formula there in [1] excludes the normalizing factor $\frac{1}{\pi b^2}$, and here it is translated into our notation) :

$$\mathsf{P}^{(1)}(X'') \quad = \quad \frac{mb}{2\pi\hbar\Delta x t'} \exp\left\{ -\frac{1}{(\Delta x)^2} \left(x'' - \left[x' \pm \tfrac{\tau'}{2} \right] - VT \right)^2 \right\}, \tag{4.39}$$

where $V = \left(x' \pm \frac{\tau'}{2} \right)_1 / t' = \pm\tau_1/2t'$ is the mean tranverse first-leg velocity to the upper or lower slit, respectively. So VT is the projected mean transverse second-leg distance, based on first-leg velocity. We may also interpret $X'' = \left(x'' - \left[x' \pm \frac{\tau'}{2} \right] \right)_1$ as the gaussian distance the particle traveled away from the respective slit center during the second leg of its trip.

For reference in the next section, we also obtain the current for this example in the usual way. Formula (4.39) is derived in [1, pp.50-51] from the wavefunction amplitude for one gaussian slit (1D case):

$$\begin{aligned}
\psi^{(1)}(X'') \quad &= \quad \sqrt{\frac{m}{2\pi i\hbar}} \left(t' + T + it'T\frac{\hbar}{mb^2} \right)^{-\frac{1}{2}} \\
&\quad \times \exp\left\{ \frac{im}{2\hbar} \left(\frac{X''^2}{T} + V^2 t' \right) + \frac{m^2}{2\hbar^2 T^2} \frac{(X'' - VT)^2}{(im/\hbar)\,(1/t' + 1/T) - 1/b^2} \right\} \\
&= \quad \sqrt{\frac{mb}{2\pi i\hbar t'}} \left(b\gamma + i\frac{\hbar T}{mb} \right)^{-\frac{1}{2}} \\
&\quad \times \exp\left\{ \frac{im}{2\hbar T} \left(X''^2 + V^2 t' T \right) - \left(1 + i\frac{mb^2}{\hbar T}\gamma \right) \frac{(X'' - VT)^2}{2(\Delta x)^2} \right\}
\end{aligned} \tag{4.40}$$

From this, we obtain the one-dimensional transverse current density from one slit:

$$
\begin{aligned}
\mathsf{j}^{(1)}(X'') &= \frac{\hbar}{2mi}\left(\psi^*(X'')\partial_{X''}\psi(X'') - \psi(X'')\partial_{X''}\psi^*(X'')\right) \\
&= \frac{1}{T}\left(X'' - \frac{b^2\gamma}{(\Delta x)^2}(X'' - VT)\right) \\
&\quad \times \frac{mb}{2\pi(\Delta x)\hbar t'}\exp\left\{-\tfrac{1}{2}\left(\tfrac{X''-VT}{\Delta x}\right)^2\right\} \\
&= \frac{1}{T}\left(x''\left(1 - \frac{b^2\gamma}{(\Delta x)^2}\right) - \left[x' - \tfrac{\tau'}{2}\right]\left(1 - \frac{b^2\gamma^2}{(\Delta x)^2}\right)\right) \\
&\quad \times \frac{mb}{2\pi(\Delta x)\hbar t'}\exp\left\{-\tfrac{1}{2}\left(\tfrac{X''-VT}{\Delta x}\right)^2\right\}. \qquad (4.41)
\end{aligned}
$$

Feynman showed that $(\Delta x)^2$, the mean-squared width of the single-slit diffraction pattern $\mathsf{P}(x'')$, contains a quantum correction to the classical width[1] . We can rewrite formula (4.26) as the variance of a sum of two independent random variables, $(\Delta x)^2 = (\Delta x_1)^2 + (\Delta x_2)^2$. The extra term is $(\Delta x_2)^2 = \left(\frac{\hbar T}{mb}\right)^2$. The width $\Delta x_1 = b\gamma$ that we see in the other term in formula (4.26) represents our uncertainty in position at the slit. Initially, at the slit at time t', the uncertainty is b. After a time interval T seconds after the time t' of passage through the slit, the width b has spread classically (by rectilinear motion projected using the first leg speed V) by the factor $\gamma = \left(1 + \frac{T}{t'}\right) = \frac{t''}{t'}$. The extra quantum correction is a random variable that represents a momentum uncertainty $\Delta p = m\Delta v$, where Δv is given by $\Delta x_2 = \frac{\hbar T}{mb} = \Delta v \cdot T$. So the quantum correction approximately obeys the Heisenberg uncertainty relation $\Delta x_1 \cdot \Delta p = \hbar$ [1].

Next we examine the interference probability of wavelike travel out of both Gaussian slits followed by arrival at a single detector; that is, the case of detector separation $\tau'' = 0$.

Consider $\mathsf{P}^{(12)}$. Expanding equation (4.28) for $\tau''=0, d=1, s=1$, we get

$$\begin{aligned}\mathsf{P}^{(12)}(x'') &= \frac{1}{\pi b^2}\cdot\frac{mb}{2\pi\hbar\Delta x t'} \\ &\quad \times\exp\left\{-\frac{1}{(\Delta x)^2}\left([x''-x'\gamma]^2+\left[\tfrac{\tau'}{2}\gamma\right]^2-i\tfrac{2m}{\hbar T}\left[x''-x'\gamma\right]\left[\tfrac{\tau'}{2}\right]\left[b^2\gamma-(\Delta x)^2\right]\right)\right\}\end{aligned} \tag{4.42}$$

and $\mathsf{P}^{(21)}(x'')$ is the complex conjugate of this. Now we add all four parts (given by equations (4.42) and (4.38)) for the single detector case with $d=1, s=1$, to obtain the total interference fringe formula for two slits,

$$\begin{aligned}\bar{\mathsf{P}}(x'') &= \frac{m}{\pi^2\hbar b\Delta x t'}\times\exp\left\{-\frac{1}{(\Delta x)^2}\left([x''-x'\gamma]^2+\left[\tfrac{\tau'}{2}\gamma\right]^2\right)\right\} \\ &\quad \times\left(\cosh\left\{\tfrac{2}{(\Delta x)^2}\left[x''-x'\gamma\right]\left[\tfrac{\tau'}{2}\gamma\right]\right\}\right. \\ &\qquad \left.+\cos\left\{\tfrac{2m}{\hbar T}\left[x''-x'\gamma\right]\left[\tfrac{\tau'}{2}\right]\left[1-\left(\tfrac{b}{\Delta x}\right)^2\gamma\right]\right\}\right).\end{aligned} \tag{4.43}$$

Here we recognize the exponential as the centered gaussian envelope shaping the cosine fringe pattern, raised by a $\cosh\geq 1$. The fringe pattern for two slits and a single detector with parameters consistent with the Steinberg experiment [47] is shown in figure 4.3. As indicated, the one-dimensional pattern is plotted twice, as computed from formula (4.43) and computed as a slice of the three-dimensional formula (4.37) with detector separation $\tau''=0$. The plots are in good agreement with the experimental fringe pattern observed in [47].

For small slit width b, we have $\left[1-\left(\frac{b}{\Delta x}\right)^2\gamma\right]\approx 1$, so that the cosine argument becomes approximately $\frac{2m}{\hbar T}\left[x''-x'\right]\left[\frac{\tau'}{2}\right]$, which matches that of the cosine in the double point-slit, single detector formula (48) of [25]. At the same time, as $b\to 0$, the variance $(\Delta x)^2/2$ of

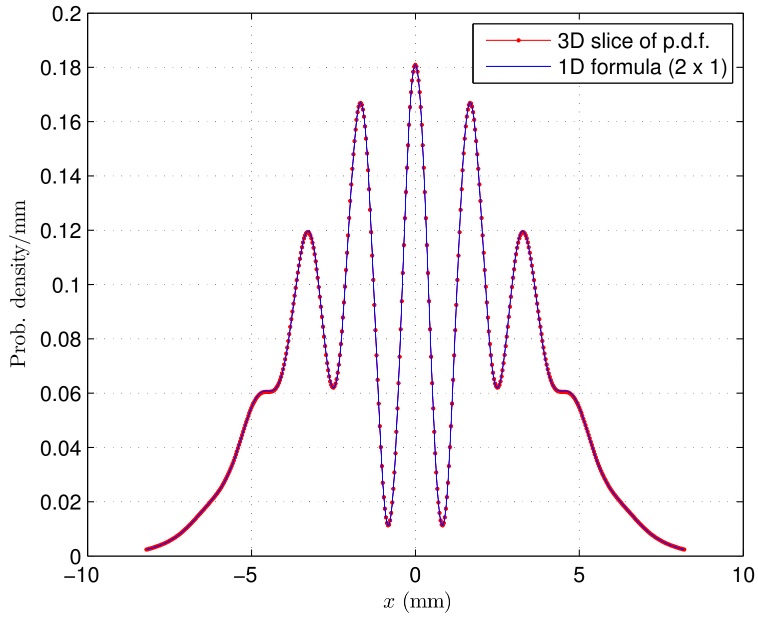

Figure 4.3: Interference pattern at distance $z = 8.2m$ behind the slits for the Steinberg double gaussian slit experiment with single-pixel CCD detector. The photon wavelength was $\lambda = 943$nm, slit spacing $\tau' = 4.69$mm, gaussian beam waist e^{-2} radius 0.608mm. Single photons were used, showing photon self-interference.

the gaussian envelope here becomes infinitely wide. This makes the cosh $\downarrow 1$, which also agrees with formula (48) of [25], which has no single-slit diffraction envelope, i.e. it is a constant, flat envelope [24].

4.4 The current density field from two gaussian slits

To get the current density for the double gaussian slit, we operate upon the probability density departing from the slits with the free current propagator $\mathbf{v}B_0$ as the kernel. As in equation (4.37), there are four aperture terms to integrate. The mean velocity vector $\mathbf{v} = \frac{(x''-x)}{T}$ now appears in the integral:

$$\begin{aligned} \mathsf{j}(x''t'', \tau'') &= \iint d\hat{x}\, d\hat{\tau}\ \alpha(\hat{x}, \hat{\tau}) \tfrac{(x''-\hat{x})}{T} B_0(x''t''\tau''; \hat{x}t'\hat{\tau}) \mathsf{P}(\hat{x}t', \hat{\tau}) \\ &= \mathsf{j}^{(12)} + \mathsf{j}^{(21)} + \mathsf{j}^{(1)} + \mathsf{j}^{(2)}. \end{aligned} \tag{4.44}$$

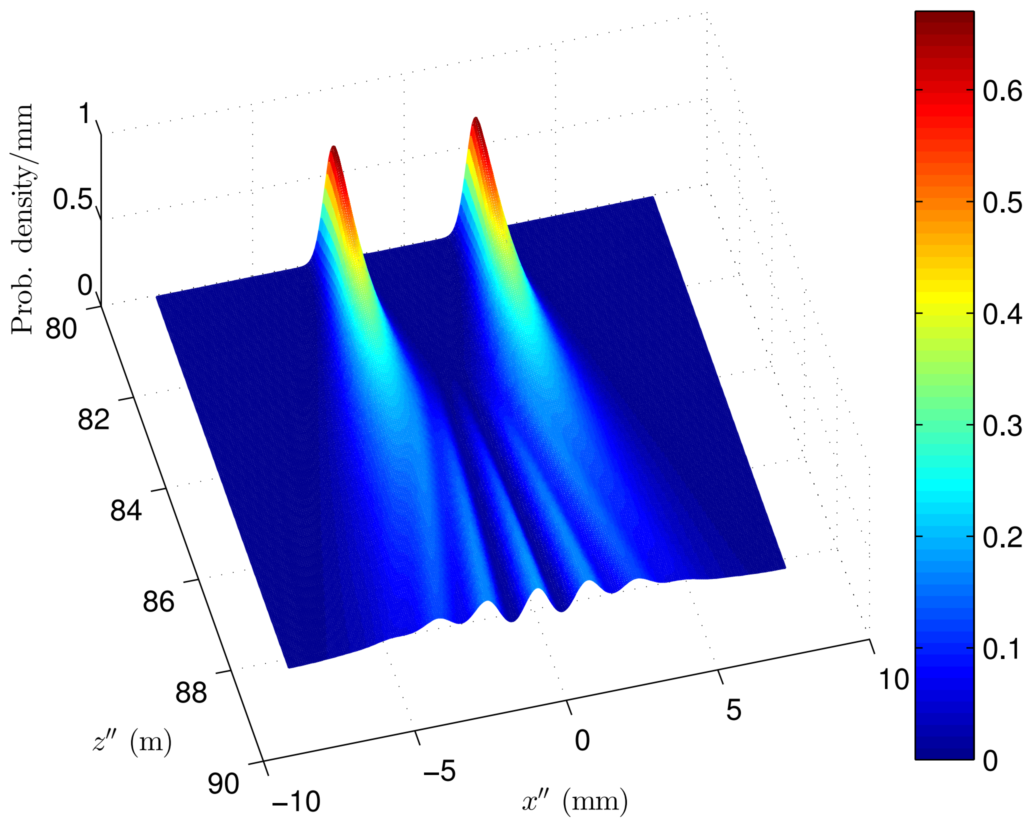

Figure 4.4: Complete interference surface (probability density) for the Steinberg double gaussian slit experiment with single-pixel CCD detector ($\tau'' = 0$), for $\lambda = 943$nm, slit spacing $\tau' = 4.69$mm, slits positioned at $z' = 80$m, gaussian beam waist e^{-2} radius 0.608mm. Single photons were used, showing photon self-interference. This plot is in close agreement with the measured probability density in [47, Fig.4].

To evaluate the integral (4.44), the standard trick is to differentiate both sides of equation (4.24) by J_k [17,66,67]. We differentiate each of the four probabilities. We begin with the first one. First we multiply both sides of equation (4.24) by the factor $C \exp\left\{i\frac{1}{2}\left(u_k^{(12)} \cdot Bu_k^{(12)} + w_k^{(12)} \cdot B'w_k^{(12)}\right)\right\}$, to restore the whole probability $\mathsf{P}^{(12)}$. On the left side, differentiating pulls down the factor $iv_k = i(x, \frac{\tau}{2})^t$ inside the integral (4.24). (However, this actually corresponds to the factor $i(x-x', \frac{1}{2}(\tau-\tau'))^t$ inside the original Blue integral for $\mathsf{P}^{(12)}$, *after* we substituted x for $x-x'$ and τ for $\tau-\tau'$ to bring the integral into the form (4.20). The latter form was repackaged into the standard quadratic form (4.24) which we are differentiating. So we will need to adjust in some way to get $(x''-x)$ inside the integral (4.44). But it turns out that this adjustment happens automatically, as we will see shortly.) On the right side of equation (4.24), differentiating by $J_k^{(12)}$ gives us the answer:

$$\begin{aligned}
\partial \mathsf{P}^{(12)}/\partial J_k^{(12)} &= \\
\tfrac{T}{i}\mathcal{J}^{(12)} &= C\left(-A_k^{-1}J_k^{(12)} + iBu_k^{(12)}\right) \\
&\qquad \times \exp\left\{-\tfrac{1}{2}J_k^{(12)} \cdot A_k^{-1}J_k^{(12)} + i\tfrac{1}{2}\left(u_k^{(12)} \cdot Bu_k^{(12)} + w_k^{(12)} \cdot B'w_k^{(12)}\right)\right\} \\
&= \left(-A_k^{-1}J_k^{(12)} + iBu_k^{(12)}\right)\mathsf{P}^{(12)}, \qquad (4.45)
\end{aligned}$$

where for each $k = 1,2,3$ we define $\mathcal{J}_k = (\mathsf{j}_k, \mathsf{k}_k)^t$.We have not used the τ-current density k_k that appears here:

$$\begin{aligned}
\mathsf{k}(x''t'', \tau'') &= \iint d\hat{x}\, d\hat{\tau}\ \alpha(\hat{x}, \hat{\tau})\frac{\left(\frac{1}{2}(\tau''-\tau')\right)}{T}B_0(x''t''\tau''; \hat{x}t'\hat{\tau})\mathsf{P}(\hat{x}t', \hat{\tau}) \\
&= \mathsf{k}^{(12)} + \mathsf{k}^{(21)} + \mathsf{k}^{(1)} + \mathsf{k}^{(2)}.
\end{aligned}$$

This osmotic current density is defined and developed in section 3.5 and in section 5 of [63].

Since $u_k = J_k - w_k$, we remember that u_k depends on J_k. We choose J_k and w_k as the two independent variables. Suppressing the space index k for a moment, we have used $\partial u_j / \partial J_{j'} = \delta_{jj'}$ for both components of J, i.e. for $j, j' = 1, 2$.

Differentiating by J_k also "pulls down" the term $iBu_k^{(12)}\mathsf{P}^{(12)}$ on both sides above. This term adjusts the differentiated integral on the left-hand side above so that we get the x-current j_k of $\mathcal{J}_k$. This is how it happens: As we noted, the top (x-current) component actually corresponds to "bringing down" the factor $x - x'$ by differentiating inside the original integral for $\mathsf{P}^{(12)}$. To change this into the factor $-(x'' - x) = (x - x') - (x'' - x')$ inside the integral, we simply subtract the constant multiple $(x'' - x')\mathsf{P}^{(12)}$. But this is exactly what the additive term $iBu_k^{(12)}$ does for us on the left-hand side, since $iBu_k^{(12)} = -i \begin{bmatrix} (x'' - x') \\ \frac{1}{2}(\tau'' - \tau') \end{bmatrix}_k$.

Clearly a similar adjustment also happens in the bottom (τ-current) component on the left hand side.

Therefore, multiplying both sides of equation (4.45) by $\frac{i}{T}$, we have

$$
\begin{aligned}
\mathcal{J}_k^{(12)} &= \frac{1}{T}\left(\begin{bmatrix} (x'' - x') \\ \frac{1}{2}(\tau'' - \tau') \end{bmatrix}_k + \frac{1}{(\Delta x)^2} \begin{bmatrix} \frac{i\hbar T}{m}\frac{1}{2}(\tau'' - \tau'\gamma) - b^2\gamma(x'' - x'\gamma) \\ -b^2\frac{1}{2}(\tau'' - \tau'\gamma) + \frac{i\hbar T}{m}\gamma(x'' - x'\gamma) \end{bmatrix}_k \right) \mathsf{P}^{(12)}, \\
& \qquad \text{for} \quad k = 1, 2; \\
&= \frac{1}{T}\left(\begin{bmatrix} (x'' - x') \\ \frac{1}{2}(\tau'' - \tau') \end{bmatrix}_k - \frac{1}{\gamma} \begin{bmatrix} (x'' - x'\gamma) \\ \frac{1}{2}(\tau'' - \tau'\gamma) \end{bmatrix}_k \right) \mathsf{P}^{(12)}, \quad \text{for} \quad k = 3.
\end{aligned} \tag{4.46}
$$

We can rewrite the x-current (the upper component) as

$$
\begin{aligned}
\mathsf{j}_k^{(12)} &= \begin{cases} \left(\frac{x_k''}{T}\left(1-\frac{b^2\gamma}{(\Delta x)^2}\right) - \frac{x_k''}{T}\left(1-\frac{b^2\gamma^2}{(\Delta x)^2}\right) + \frac{i\hbar}{m(\Delta x)^2}\frac{1}{2}(\tau''-\tau'\gamma)_k\right)\mathsf{P}^{(12)}, & k=1,2 \\ \left(\frac{x_k''}{T}\left(1-\frac{1}{\gamma}\right)\right)\mathsf{P}^{(12)}, & k=3 \end{cases} \\
&= \begin{cases} \left(\frac{x_k''}{t''}\left(1+\frac{\hbar^2 t'T}{(mb\Delta x)^2}\right) - \frac{x_k'}{T}\left(\frac{\hbar^2 T^2}{(mb\Delta x)^2}\right) + \frac{i\hbar}{m(\Delta x)^2}\frac{1}{2}(\tau''-\tau'\gamma)_k\right)\mathsf{P}^{(12)}, & k=1,2 \\ \left(\frac{x_k''}{t''}\right)\mathsf{P}^{(12)}, & k=3 \end{cases} \\
&= \begin{cases} \left(\frac{x_k''}{t''} + \frac{\hbar^2 t'T}{(mb\Delta x)^2}\left(\frac{x_k''}{t''}-\frac{x_k'}{t'}\right) + \frac{i\hbar}{m(\Delta x)^2}\frac{1}{2}(\tau''-\tau'\gamma)_k\right)\mathsf{P}^{(12)}, & k=1,2 \\ \left(\frac{x_k''}{t''}\right)\mathsf{P}^{(12)}, & k=3. \end{cases}
\end{aligned} \tag{4.47}
$$

Note that for the y-component above ($k=2$), there is no slit displacement, i.e. $\tau_2''=\tau_2'=0$, so the imaginary part vanishes. The last two steps above involve some algebra (the identity $1-\frac{1}{\gamma(a+1)} = \left[1+\frac{1}{\gamma(a+1)-1}\right]^{-1}$, for $\gamma \neq 0$ and any number $a \neq -1$, may be of use). The result for $\mathsf{j}^{(21)}(x''t'', \tau'')$ is similar, with the sign of τ_1' reversed to $-\tau_1'$. So, for a single detector ($\tau''=0$), the two interference currents $\mathsf{j}^{(12)}$ and $\mathsf{j}^{(21)}$ sum to a real number ($\pm$).

We compute the third part of the current in a similar way. The gradient of the third probability (4.35) is

$$
\begin{aligned}
\partial \mathsf{P}^{(1)}/\partial J_k^{(1)} &= \\
\tfrac{T}{i}\mathcal{J}^{(1)} &= C\left(-A_k^{-1}J_k^{(1)} + iBu_k^{(1)}\right) \\
&\quad \times \exp\left\{-\tfrac{1}{2}J_k^{(1)}\cdot A_k^{-1}J_k^{(1)} + i\tfrac{1}{2}u_k^{(1)}\cdot Bu_k^{(1)}\right\} \\
&= \left(-A_k^{-1}J_k^{(1)} + iBu_k^{(1)}\right)\mathsf{P}^{(1)}
\end{aligned} \tag{4.48}
$$

In this case, we have $iBu_k^{(1)} = -i \begin{bmatrix} (x'' - \left[x' - \frac{\tau'}{2}\right]) \\ \frac{1}{2}(\tau'') \end{bmatrix}_k$. The absorbed term $iBu_k^{(1)}\mathsf{P}^{(1)}$ again adjusts the differentiated integral on the left-hand side above to give the x-current j_k of $\mathcal{J}_k$. The top (x) component in equation (4.48) now corresponds to "bringing down" $x - \left[x' - \frac{\tau'}{2}\right]$ by differentiating inside the original integral for $\mathsf{P}^{(1)}$ after we substituted x for $x - \left[x' - \frac{\tau'}{2}\right]$. To get the factor $x - x'' = x - \left[x' - \frac{\tau'}{2}\right] - (x'' - \left[x' - \frac{\tau'}{2}\right])$, we would simply add the constant multiple $(x'' - \left[x' - \frac{\tau'}{2}\right])\mathsf{P}^{(1)}$ to the above. But the term $iBu_k^{(1)}\mathsf{P}^{(1)}$ is there to accomplish this for us.

Therefore, multiplying both sides of equation (4.48) by $\frac{i}{T}$, we have

$$\begin{aligned} \mathcal{J}_k^{(1)} &= \begin{bmatrix} \mathsf{j}_k^{(1)} \\ \mathsf{k}_k^{(1)} \end{bmatrix} \\ &= \frac{1}{T}\left(\begin{bmatrix} x'' - \left[x' - \frac{\tau'}{2}\right] \\ \frac{1}{2}\tau'' \end{bmatrix}_k + \frac{1}{(\Delta x)^2} \begin{bmatrix} \frac{i\hbar T}{m}\frac{1}{2}\tau'' - b^2\gamma(x'' - \left[x' - \frac{\tau'}{2}\right]\gamma) \\ -b^2\gamma\frac{1}{2}\tau'' + \frac{i\hbar T}{m}(x'' - \left[x' - \frac{\tau'}{2}\right]\gamma) \end{bmatrix}_k \right)\mathsf{P}^{(1)} \\ &\quad \text{for } \ k = 1, 2; \\ &= \frac{1}{T}\left(\begin{bmatrix} x'' - \left[x' - \frac{\tau'}{2}\right] \\ \frac{1}{2}\tau'' \end{bmatrix}_k - \frac{1}{\gamma} \begin{bmatrix} x'' - \left[x' - \frac{\tau'}{2}\right]\gamma \\ \frac{1}{2}\tau'' \end{bmatrix}_k \right)\mathsf{P}^{(1)}, \qquad k = 3. \end{aligned} \tag{4.49}$$

We can rewrite the x-current vector (the upper component above) as

$$\mathsf{j}_k^{(1)} = \begin{cases} \left(\frac{x_k''}{T} \left(1 - \frac{b^2\gamma}{(\Delta x)^2}\right) - \frac{\left[x_k' - \frac{\tau'}{2}\right]_k}{T} \left(1 - \frac{b^2\gamma^2}{(\Delta x)^2}\right) + \frac{i\hbar}{m(\Delta x)^2} \frac{1}{2}\tau_k'' \right) \mathsf{P}^{(1)}, \\ \qquad \text{for } \ k = 1, 2; \\ \left(\frac{x_k''}{T} \left(1 - \frac{1}{\gamma}\right)\right) \mathsf{P}^{(1)}, \qquad k = 3 \end{cases}$$

$$= \begin{cases} \left(\frac{x_k''}{t''} + \frac{\hbar^2 t' T}{(mb\Delta x)^2} \left(\frac{x_k''}{t''} - \frac{\left[(x' - \frac{\tau'}{2})_k\right]}{t'} \right) + \frac{i\hbar}{m(\Delta x)^2} \frac{1}{2}\tau_k'' \right) \mathsf{P}^{(1)}, & k = 1, 2 \\ \left(\frac{x_k''}{t''} \right) \mathsf{P}^{(1)}, & k = 3. \end{cases} \tag{4.50}$$

Note we can check that the first expression above with $\tau'' = 0$ equals the current formula (4.41) that we derived from the one-dimensional single-slit wavefunction. We have continuity at the slits: as $T = t'' - t' \to 0$, $t'' \to t'$, and $\Delta x \to b$, so at time t' the current exiting the slits is $\frac{x_k'}{t'}$. This equals the current entering the slits, as an easy calculation shows. Again, for the y-component of the current above ($k = 2$), there is no slit displacement, i.e. $\tau_2'' = \tau_2' = 0$, so only the first term remains. (In fact, in the central x-z plane through $y'' = y' = 0$, the y-components of the current terms are all 0.) The result for $\mathsf{j}^{(2)}(x''t'', \tau'')$ is similar, with the sign of τ' reversed to $-\tau'$. For a single detector ($\tau'' = 0$), the two single-slit currents $\mathsf{j}^{(1)}$ and $\mathsf{j}^{(2)}$ are both real numbers ($\pm$).

4.4.1 Twin detector fringe patterns and current densities

We now have, in closed-form, all four pieces of the probability and current densities *departing* from one or both of the two slits, propagated out to two locations at time t''. Their respective sums give the displaced probability of arrival density and the associated current density:

$$\mathsf{P}(x''t'', \tau'') = \mathsf{P}^{(12)} + \mathsf{P}^{(21)} + \mathsf{P}^{(1)} + \mathsf{P}^{(2)} \tag{4.51}$$

$$\mathsf{j}(x''t'', \tau'') = \mathsf{j}^{(12)} + \mathsf{j}^{(21)} + \mathsf{j}^{(1)} + \mathsf{j}^{(2)}. \tag{4.52}$$

However, once more, there are four ways to *arrive* at one or both of the two locations $x'' \pm \frac{\tau''}{2}$. To complete the recipe, we evaluate the *total* probability and current densities arriving at the twin detectors. Then we can obtain the mean bilocal velocity from the current-to-probability density ratio. The total probability $\overline{\mathsf{P}}(x'' \pm \frac{\tau''}{2}, t'')$ to arrive and be detected at one or both locations is given by the relation (3.15):

$$\begin{aligned} \overline{\mathsf{P}}(x'' \pm \tfrac{\tau''}{2}, t'') &= \mathsf{P}(x'' + \tfrac{\tau''}{2}, t'', 0) + \mathsf{P}(x'' - \tfrac{\tau''}{2}, t'', 0) \\ &\quad + \mathsf{P}(x''t'', \tau'') + \mathsf{P}(x''t'', -\tau'') \\ &= \left| \left[\psi(x'' + \tfrac{\tau''}{2}) + \psi(x'' - \tfrac{\tau''}{2}) \right] \right|^2 \geq 0. \end{aligned} \tag{4.53}$$

The total bicurrent $\bar{\mathsf{j}}(x'' \pm \frac{\tau''}{2}, t'')$ is a new quantity, defined by

$$\begin{aligned} &\bar{\mathsf{j}}(x'' \pm \tfrac{\tau''}{2}, t'') \\ &= \frac{\hbar}{2mi} \Big\{ \left[\psi(x'' + \tfrac{\tau''}{2}) + \psi(x'' - \tfrac{\tau''}{2}) \right]^* \nabla_{x''} \left[\psi(x'' + \tfrac{\tau''}{2}) + \psi(x'' - \tfrac{\tau''}{2}) \right] \\ &\qquad - \left[\psi(x'' + \tfrac{\tau''}{2}) + \psi(x'' - \tfrac{\tau''}{2}) \right] \nabla_{x''} \left[\psi(x'' + \tfrac{\tau''}{2}) + \psi(x'' - \tfrac{\tau''}{2}) \right]^* \Big\} \qquad (4.54) \\ &= \mathsf{j}(x'' + \tfrac{\tau''}{2}, t'', 0) + \mathsf{j}(x'' - \tfrac{\tau''}{2}, t'', 0) + \mathsf{j}(x''t'', \tau'') + \mathsf{j}(x''t'', -\tau''). \qquad (4.55) \end{aligned}$$

The expression for total bicurrent splits into a sum of two usual currents (one at each location) and two conjugate displaced currents of form (4.2) for simultaneous, wavelike arrival at both locations. This sum (4.55) of four currents is analogous to the sum (4.53) for total probability for arrival at one or both detectors. (The total bicurrent easily extends to a total multicurrent, impinging on an array of many detector pairs located about their center x''. We replace the wavefunction sum $\left[\psi(x'' + \frac{\tau''}{2}) + \psi(x'' - \frac{\tau''}{2})\right]$ by the sum $\sum_{k=1}^{K} [\psi(x'' + \tau_k''/2) + \psi(x'' - \tau_k''/2)]$ everywhere inside the total current expression defined above.) Computationally, we merely evaluate the formulas (4.51) and (4.52) at the four (x'', τ'') values, and take the two sums.

Figure 4.5 below displays the double slit, double detector probability densities for constant slit spacing, and three detector spacings. For direct comparison at each detector spacing, we include the double detector with both distinguishable and indistinguishable detectors. The former just consists of two separate detector units, so we consider the probability that the particle arrives at one or the other detector. The latter is the ambiguous twin detector, with the same spacing as the unambiguous detector pair. In this situation, we consider the total probability (4.53) that the particle arrives at one or the other detector, or both. These probability densities are clearly different for unambiguous and ambiguous detector pairs. (As we discuss below, these densities have been renormalized to 1 for every z-section, to model the photon.)

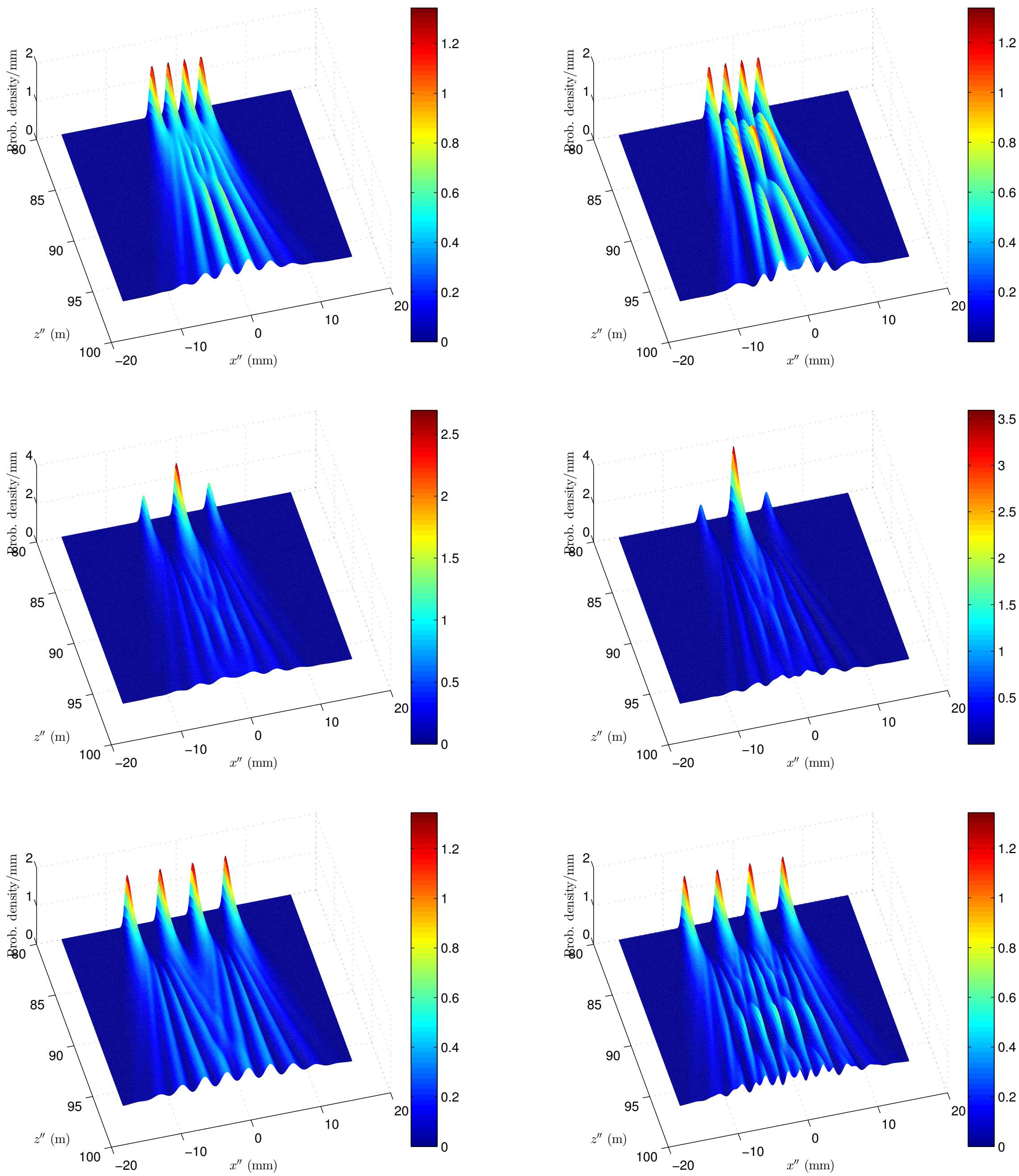

Figure 4.5: Probability density surface for the *modified* Steinberg double gaussian slit experiment, having a twin detector, for wavelength $\lambda = 943$nm, slit spacing $\tau' = 4.69$mm, gaussian beam waist e^{-2} radius 0.608mm. The probability densities for arrival at one of two locations (left side) and at one or both locations (right side) are somewhat different. The plots are shown for three twin detector spacings, given as a multiple of the slit spacing τ': $\tau'' = \frac{1}{2}\tau'$ (top row), $\tau'' = \tau'$ (middle row), and $\tau'' = 2\tau'$ (bottom row).

4.5 Mean velocity field

The mean velocity field for the double-slit, double-detector experiment is given by the ratio of the total "one-or-both detector, one-or-both slit" current to probability density:

$$
\begin{aligned}
\overline{\mathsf{v}}(x''t'',\tau'') &= \bar{\mathsf{j}}(x''t'',\tau'')/\overline{\mathsf{P}}(x''t'',\tau'') && (4.56)\\
&= \Big[\mathsf{P}(x''+\tfrac{\tau''}{2},t'',0)\cdot\mathsf{v}(x''+\tfrac{\tau''}{2},t'',0)+\mathsf{P}(x''-\tfrac{\tau''}{2},t'',0)\cdot\mathsf{v}(x''-\tfrac{\tau''}{2},t'',0)\\
&\quad +\ \mathsf{P}(x''t'',\tau'')\cdot\mathsf{v}(x''t'',\tau'')+\mathsf{P}(x''t'',-\tau'')\cdot\mathsf{v}(x''t'',-\tau'')\Big]\\
&\quad /\ \Big[\mathsf{P}(x''+\tfrac{\tau''}{2},t'',0)+\mathsf{P}(x''-\tfrac{\tau''}{2},t'',0)\\
&\quad +\ \mathsf{P}(x''t'',\tau'')+\mathsf{P}(x''t'',-\tau'')\Big] && (4.57)
\end{aligned}
$$

from the total equations (4.53) and (4.55). The second, expanded expression (4.57) above shows that the velocity $\overline{\mathsf{v}}$ is an average velocity for arrival at one or both of the two detectors.

Note that the common normalizing constant C of $\mathsf{P}(x''t'',\tau'')$ cancels in this ratio (4.56). The z-component ($k=3$) of the velocity field reduces to

$$
\begin{aligned}
\mathsf{v}_3(x''t'',\tau'') &= \mathsf{j}_3(x''t'',\tau'')/\mathsf{P}(x''t'',\tau'')\\
&= \frac{x_3''}{t''}. && (4.58)
\end{aligned}
$$

It is appropriate to contrast this mean velocity field (4.56) for two conjoined detectors with that for two separate detectors having the same spacing τ'' but distinguishable particle arrivals:

$$\mathsf{v}(x''t'', \tau'') = \frac{\mathsf{j}(x'' + \frac{\tau''}{2}, t'', 0) + \mathsf{j}(x'' - \frac{\tau''}{2}, t'', 0)}{\mathsf{P}(x'' + \frac{\tau''}{2}, t'', 0) + \mathsf{P}(x'' - \frac{\tau''}{2}, t'', 0)} \tag{4.59}$$

$$\begin{aligned} &= \Big[\mathsf{P}(x'' + \tfrac{\tau''}{2}, t'', 0)\mathsf{v}(x'' + \tfrac{\tau''}{2}, t'', 0) \\ &\quad + \mathsf{P}(x'' - \tfrac{\tau''}{2}, t'', 0)\mathsf{v}(x'' - \tfrac{\tau''}{2}, t'', 0)\Big] \\ &\quad / \Big[\mathsf{P}(x'' + \tfrac{\tau''}{2}, t'', 0) + \mathsf{P}(x'' - \tfrac{\tau''}{2}, t'', 0)\Big]. \end{aligned} \tag{4.60}$$

In this case, the detector that sensed the particle is known, and the interference terms in formula (4.57) vanish. In the experiment of Steinberg *et al.*, we can construct this velocity field (4.60) from the measured single-detector values $\mathsf{P}(x'' \pm \frac{\tau''}{2}, t'', 0)$ and $\mathsf{v}(x'' \pm \frac{\tau''}{2}, t'', 0)$.

The current density and mean velocity formulas we have developed for the double gaussian slit and double detector are easy to compute. Examples of mean transverse (x) velocity profiles for cases with and without distinguishable detectors are contrasted in figure 4.6.

4.6 Mean trajectories for single and double detector

Next we will integrate the equation of motion $\dot{\mathbf{x}} = \mathsf{v}$ for the double gaussian slit. Our geometry as in figure 4.1 places the source before the slits at a finite distance, with free-space propagation into the slit. Published trajectories do not include this pre-slit source geometry, *e.g.* those in [47, 62, 64, 65]. The experiment of Steinberg *et al.* employed what we may regard as "parallel gaussian headlamps," twin parallel beams that issue from an in-fiber beamsplitter and then spread. Thus our trajectories are somewhat different. But when the source is a long distance in front of the slits, e.g. 80m, the beams from the slits align so that they are almost parallel. The parameter $\gamma = 1 + T/t'$ determines the twin beam alignment. As $t' \to \infty$, $\gamma \to 1$ and the beams become parallel.

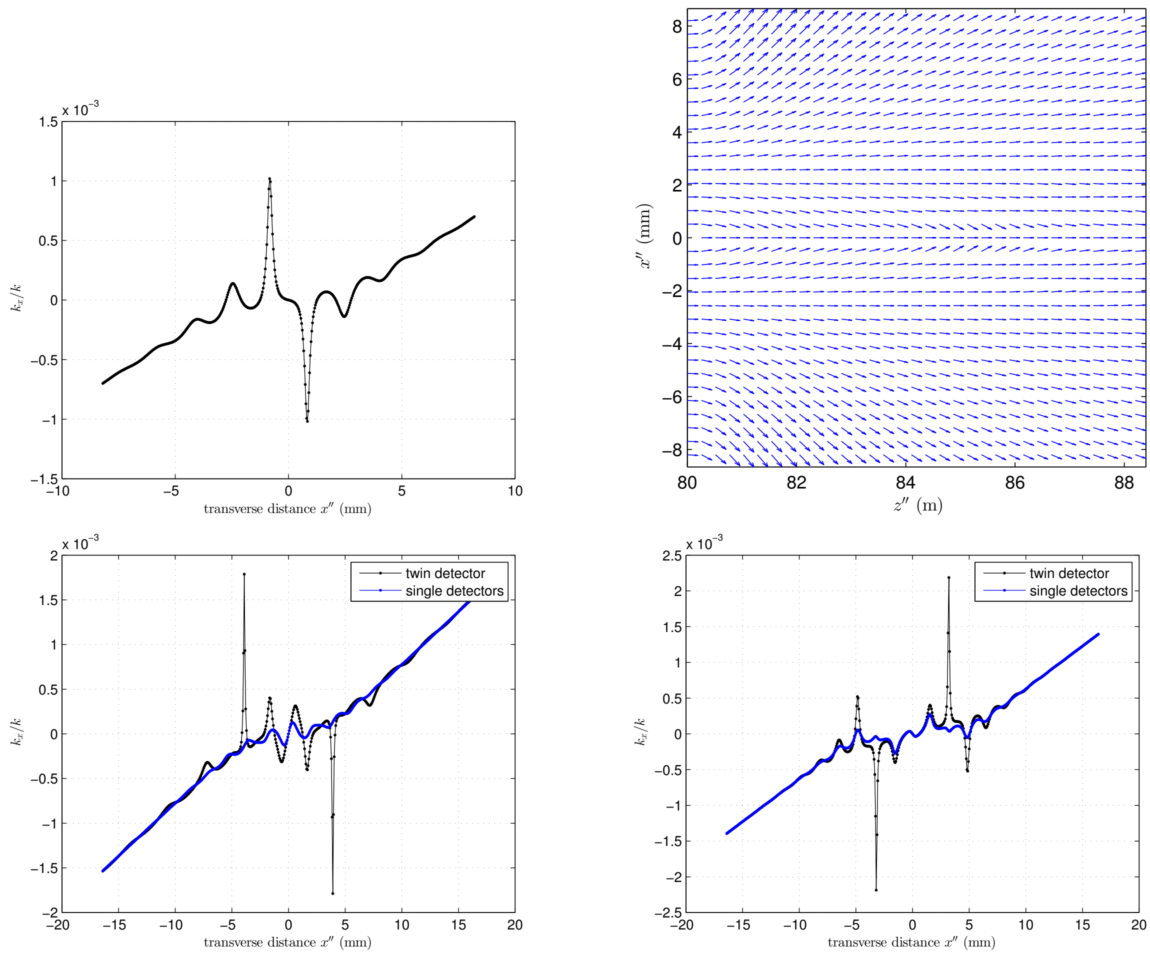

Figure 4.6: Normalized transverse (x) momentum profiles for the Steinberg double gaussian slit experiment measured across the single-pixel CCD detector (top row), and across a twin-pixel detector (bottom row), for wavelength $\lambda = 943$nm, slit spacing $\tau' = 4.69$mm, gaussian beam waist e^{-2} radius 0.608mm. The detection plane for the momentum profiles is fixed at a distance $z'' - z' = 8.2$m behind the slits in the $z' =$80m plane. The top left plot is in close agreement with the transverse momentum profile measured in Fig.2D of [47]. The top right "quiver" plot depicts the entire corresponding velocity field behind the slits for the single detector experiment, of which the top left profile is a slice (taken at z''=88.2m). The bottom row shows the transverse momentum profiles for the same experiment, only modified with double detectors spaced apart by a distance equal to half the slit spacing ($\tau'' = \frac{1}{2}\tau'$, lower left), and to the slit spacing ($\tau'' = \tau'$, lower right). On each side, for a given detector spacing, the momentum profiles for two arrival modes are compared. The blue profile is that measured for particle-like arrival at one of two locations (single detectors, distinguishable detection mode) and the black profile is that for wavelike arrival at one or both locations (twin detector, indistinguishable detection mode).

4.6.1 Converting from massive particle to photon

To adapt the formulas from the previous sections to an experiment with photons, we convert from a massive particle with arbitrary momentum to a spin-0 photon. The photon has zero rest mass. The photonic particle is now constrained to move on the light cone, with speed c and some definite momentum $p = \hbar k = \hbar\omega/c$ and energy $E = pc = \hbar\omega$. The photon thus has an effective kinetic mass m given by

$$m = p/c = \hbar k/c. \tag{4.61}$$

Therefore, we replace an expression such as $m/(\hbar T)$ by $k/(cT) = k/R$, where $R = cT$ is the distance the photon travels in time T. Our spatial geometry is given as in figure 4.1, with parameters selected to match the Steinberg experiment configuration. The new parameter τ'' defines the double-detector spacing. We now fix the passage time t' when the photon passes through any point $x' \pm \frac{\tau'}{2}$ in the transverse slit, and the arrival time t'' when the photon arrives at any point $x'' \pm \frac{\tau''}{2}$ on the transverse screen. Doing this, we are actually scanning the wavefunction at light speed from left to right, viewing it as a wavefront $f\left(t'' - z''/c\right)$, ignoring all values except those at light-like coordinates.

Since the geometric center-to-center distance $\hat{R} = |x'' - x'|$ varies transversely across the screen, fixing the times this way imposes an approximation. This approximation will be good when the double experiment design is very narrow and long (e.g., 16mm $\times$ 8m in [47]).

The probability and current density formulas for a particle with mass are functions of space and time. In particular, time always appears in the normalizing coefficients. A lightlike particle (confined to move on a spacetime light cone) is certain to arrive at a time T somewhere on a spherical shell of radius $R = cT$. So we must numerically renormalize the particle probability density over each shell, to get a density snapshot at a fixed moment in time that sums to 1.

4.6.2 Example trajectories

Figures 4.7 and 4.8 below show the computed mean trajectories for the 2×1 (double slit, single detector) case configured as in the Steinberg experiment [47], and for corresponding 2×2 (double slit, double detector) cases, respectively. The 2×1 mean trajectories agree well with those computed from measured tranverse momentum slices by the experiment team in [47, figure 3]. For the 2×2 cases in figure 4.8 the slit spacing is again kept constant, and three detector spacings are selected. For direct comparison at each detector spacing, we include results for the double detector with both distinguishable and indistinguishable detectors, displayed on the left and right hand sides of figure 4.8, respectively. (We could compare the trajectories for twin detectors on the right side of figure 4.8 with those for a single detector in figure 4.7. (We could ignore the plots on the left side of figure 4.8.) But this comparison would not provide a direct contrast between trajectories for the same two detectors, conjoined as a twin detector vs. separated as two single detectors; that is, between trajectories integrated over the velocity fields with and without interference terms, as in (4.57) and (4.60), respectively.) The distinguishable case consists of two separate detector units, so we consider the probability that the particle arrives at one or the other detector. There is no chance of wavelike arrival at both locations. The indistinguishable case is that of the ambiguous twin detector with the same spacing as the unambiguous detector pair. In this situation, we consider the probability that the particle arrives at one or the other detector, or both. Wavelike arrival at both locations is permitted.

As shown in figure 4.8, the trajectories of the ambiguous twin detector are noticeably different from those of the unambiguous double detector. This presents a paradox: installing a twin detector changes the mean trajectories! In a classical view, we would expect the trajectory enroute to the detectors to remain unaltered by a change in how the two detectors are connected together.

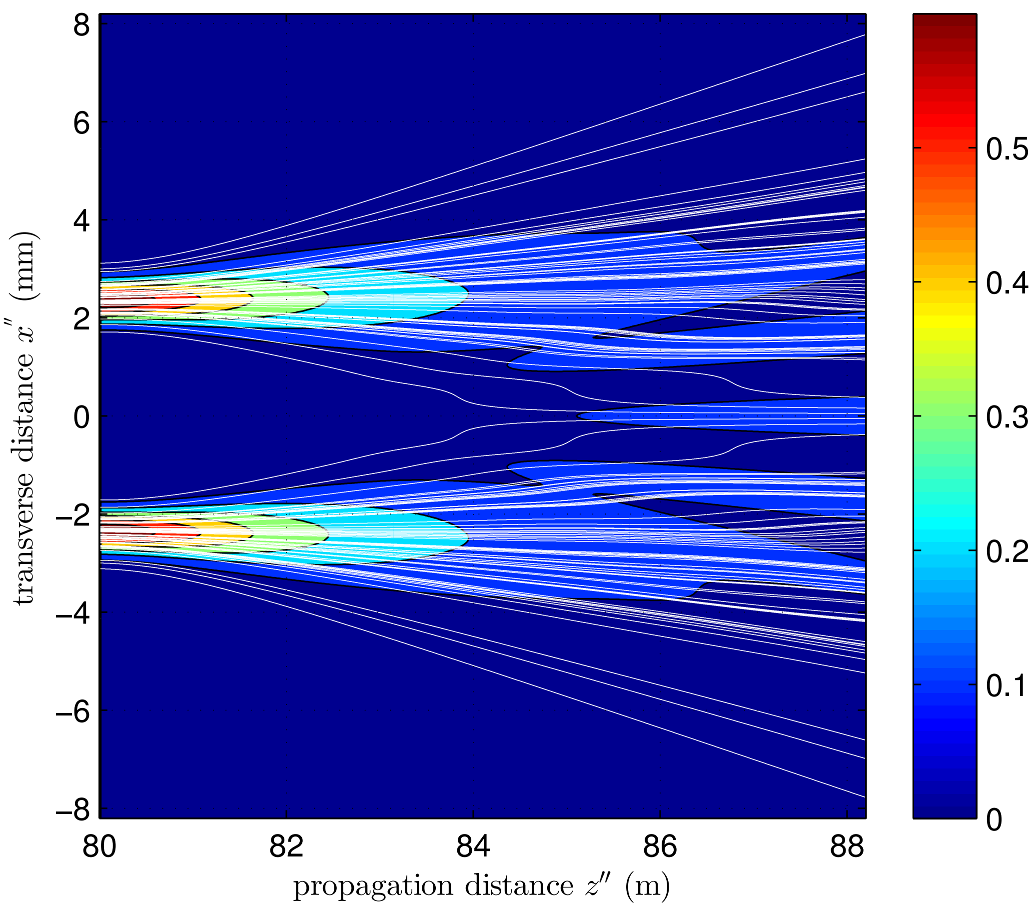

Figure 4.7: Mean trajectories (white plots) issuing from the double gaussian slit for the Steinberg-Wiseman experiment with single-pixel CCD detector ($\tau'' = 0$), for $\lambda = 943$nm, slit spacing $\tau' = 4.69$mm, gaussian beam waist e^{-2} radius 0.608mm. The trajectories are overlaid upon the color contour plot of the probability density. Single photons were used, showing photon self-interference. These plots agree well with those inferred from weak momentum measurements in [47].

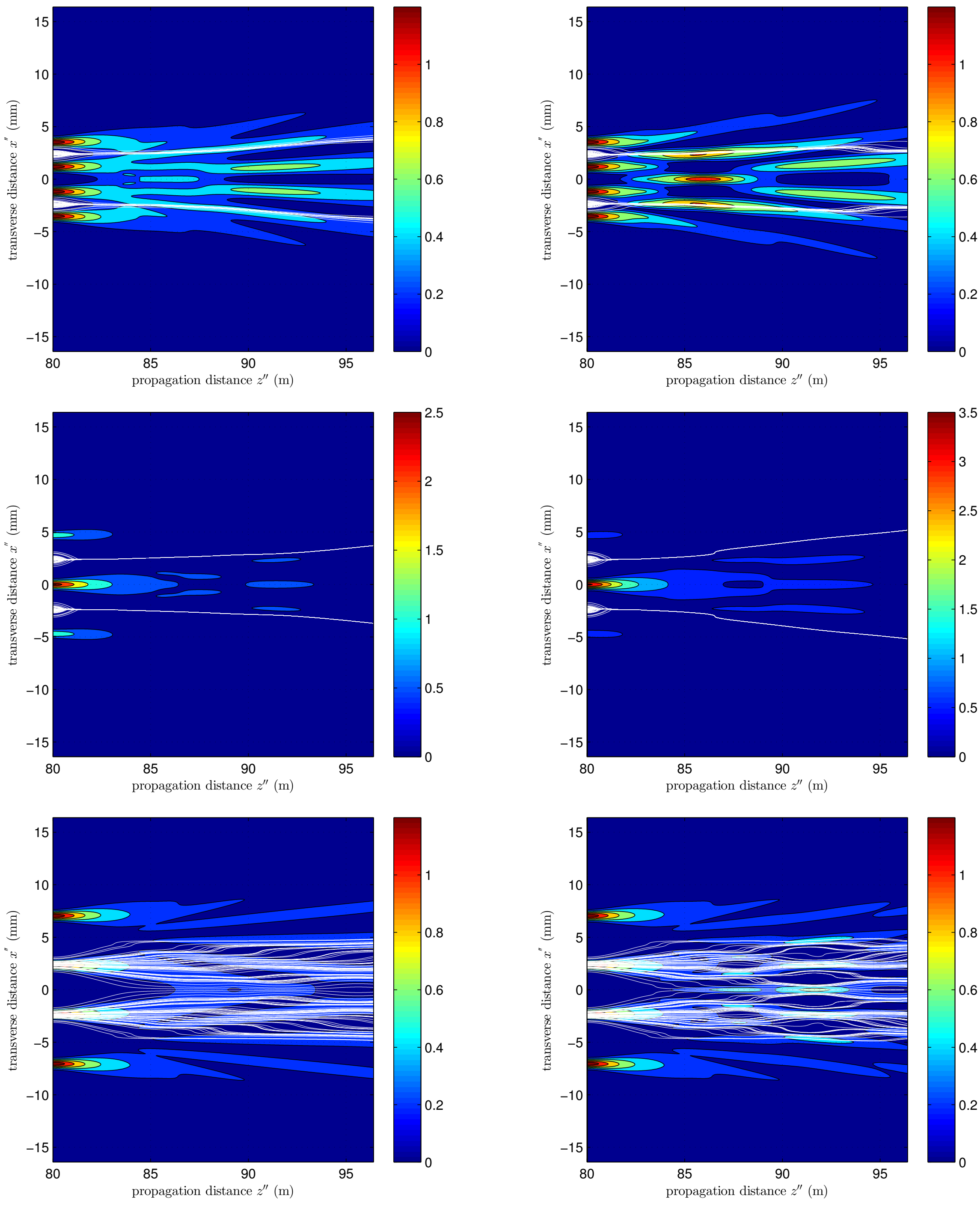

Figure 4.8: Mean trajectories (white plots) issuing from the double gaussian slit in the Steinberg-Wiseman experiment modified with a twin detector, for $\lambda = 943$nm, slit spacing $\tau' = 4.69$mm, gaussian beam waist e^{-2} radius 0.608mm. Each row of plots is for a different detector spacing (from top to bottom, $\tau'' = \frac{1}{2}\tau', \tau', 2\tau'$). The left and right plots in each row are for particle-like and wavelike arrival modes, respectively. *The mean trajectories for arrival at one of two locations (left column) and at one or both locations (right column) are somewhat different*, a counterintuitive result of merely modifying the detector mode. This is the main finding of this paper. The trajectories are overlaid upon the color contour plot of the respective probability density for the distinguishable (left) and indistinguishable (right) detector pair at each spacing τ''.

4.7 Modified Young-Steinberg experiment using twin detectors - a proposal

The two-point mean velocity field, as plotted in figure 4.6, can be measured weakly and post-selected, in much the same way that Steinberg *et al.* did in their experiment [47]. The only modification required is to replace the single detector by a twin detector. The twin detector has two collection ports at separate locations, connected to give the same detection response to a particle that enters through one or both of the ports. The twin detector is designed so that, even in principle, it is impossible to distinguish through which of the two ports (one or both of them) the particle entered. In section 3.3.1, we considered different ways to implement the twin detector. Thus we would implement a double detector in each of the two columns which receive the polarized beam displacer RHC and LHC beam components. The rest of the experiment would be unchanged. The velocity field could then be integrated (as is also done here) to produce the mean trajectories for the twin-detector version of the experiment.

4.7.1 The modified experiment

To show that the double slit experiment of Steinberg *et al.*[47] can be carried out with a twin detector, let us briefly review the experiment setup. In [47], the two slits 4.67mm apart (x) are located at the front of a runway 8.2m long (z). The photon is finally detected by a cooled CCD array oriented parallel with the x-y plane and placed at various z positions along the runway. Near the slits, a calcite crystal first takes a weak measurement of the photon as it passes through with a variable transverse momentum component $\hbar k_x$. The crystal is aligned with its optic axis in the x-z plane such that it imparts a wavenumber-dependent phase change $\varphi_k = \zeta k_x/k$ to the photon, where $\zeta = 373.5 \pm 3.4$. That is, it rotates the photon's prepared polarization state from $\psi_0^p = \frac{1}{\sqrt{2}}\left(|H\rangle + |V\rangle\right)$ to $\psi^p = \frac{1}{\sqrt{2}}\left(e^{-i\varphi_k/2}|H\rangle + e^{i\varphi_k/2}|V\rangle\right)$. (Here horizontal (H) is in the x-direction, vertical (V) is in the y-direction. We express the right-hand circular (RHC) and left-hand circular (LHC) polarization states as $|R\rangle = \frac{1}{\sqrt{2}}(|H\rangle + i|V\rangle) = e^{i\pi/4}\frac{1}{\sqrt{2}}\left(e^{-i\pi/4}|H\rangle + e^{i\pi/4}|V\rangle\right)$, and $|L\rangle = \frac{1}{\sqrt{2}}(|H\rangle - i|V\rangle)$.) Before the photon reaches the CCD detector array at the other end of the runway, a beam displacer passes its right-hand circular component without change, but deflects its left-hand circular component in the y-direction. The displaced components of the wavefunction modulate (multiply) it by the respective factors

$$\begin{aligned}
\langle\psi^p|R\rangle &= e^{i\pi/4}\cos\left(\varphi_{k(x)}/2 - \pi/4\right) = \tfrac{e^{i\pi/4}}{\sqrt{2}}\left(\cos\varphi_{k(x)}/2 + \sin\varphi_{k(x)}/2\right) \\
\langle\psi^p|L\rangle &= e^{i\pi/4} i \sin\left(\varphi_{k(x)}/2 - \pi/4\right) = \tfrac{e^{-i\pi/4}}{\sqrt{2}}\left(\cos\varphi_{k(x)}/2 - \sin\varphi_{k(x)}/2\right). \quad (4.62)
\end{aligned}$$

The squared amplitudes or intensities

$$\begin{aligned}
I_R = |\langle\psi^p|R\rangle|^2|\psi|^2 = \mathsf{P}_R(x'', t'') &= \tfrac{1}{2}\left(1 + \sin\varphi_{k(x)}\right)\mathsf{P}(x'', t'') \\
I_L = |\langle\psi^p|L\rangle|^2|\psi|^2 = \mathsf{P}_L(x'', t'') &= \tfrac{1}{2}\left(1 - \sin\varphi_{k(x)}\right)\mathsf{P}(x'', t'') \quad (4.63)
\end{aligned}$$

are proportional to the photon count received by the CCD detector array along the x-axis for separate pixel columns at $y = 0$ and $y = y_0$, respectively. Their sum is $1{\cdot}\mathsf{P}(x'', t'')$; their difference is $\sin\varphi_{k(x)}\mathsf{P}(x'', t'')$. The ratio gives us the mean transverse momentum for the particle if it arrives at horizontal coordinate x in the CCD plane [47]:

$$\frac{k_x}{k} = \frac{1}{\zeta}\varphi_{k(x)} = \frac{1}{\zeta}\sin^{-1}\left(\frac{I_R - I_L}{I_R + I_L}\right). \quad (4.64)$$

For the modified experiment with twin detectors at locations 1 and 2 given by $x_1, x_2 = x'' \pm \frac{\tau''}{2}$, formula (4.64) estimates the average value $\overline{k}_{x''}$ defined by (4.57). It is based on the proportional polarization phase shifts (weak measurements) $\varphi_{\overline{k}_x}$. That is, $\hbar\overline{k}_{x''}$ is the average transverse momentum of a large number of photons that will be received and detected (post-selected) about the transverse position coordinate x'', the midpoint or center of the twin detectors (in both y-columns). Classically, of course, for $y = k_y = 0$, the photon travels a distance $r = \sqrt{x^2 + z^2}$, so $x = x_0 + r \cdot k_x/k \approx x_0 + z \cdot k_x/k$ is nearly a linear function of k_x for $x \ll z$. The transverse wavenumber profile plots, easily converted to velocity profiles, will be different with the twin detector, as predicted in figure 4.6. But the method of the modified experiment would remain the same as that of the original.

To contrast the measured twin-detector velocity field (4.56) with the closest equivalent single-detector velocity field, we chose formula (4.59). It is the mean velocity field we would obtain for no interference between the twin detectors. As noted earlier, we can recover this velocity field by means of formula (4.60), from the measured single-detector intensity and velocity values, as in the original experiment, for the pair of detector locations.

4.8 Conclusion

The bilocal picture of quantum mechanics [25][63] was used here to carry out closed-form calculations for both the experiment of Steinberg *et al.* [47], and its twin-detector version. Formulas were developed for bilocal probability and current densities, and bilocal mean velocities.

The point of the modified Steinberg experiment proposed here is that, when we measure the average path of a photon, that path depends on the kind of detector used. Is it a pair of single (particle-like) detectors, or a conjoined double (wave-like) detector, that counts each photon? The path depends on the detector configuration, as we have shown in some detail. What happens is that the conjoined detector admits the interference terms in both the spatial and current densities. These terms alter the average velocity field as seen by the pair of separate detectors. The changed local velocities, in turn, deflect the average path of the particle issuing from any initial point in the plane of the slits.

The conjoined double detector itself is quite different from the single detectors used in other quantum experiments such as those of Brown-Twiss and Hong-Ou-Mandel, which correlate or count photon coincidences from the outputs of two single (distinguishable) detectors [48, 50, 51]. Therefore, interesting effects could result from modifying other experiments to use a conjoined double detector.

In summary, we have shown from closed-form formulas that the proposed, modified Steinberg experiment should verify that the mean velocity field and resulting particle paths are not unique, but are relative to the frame of detection that is chosen [69].

Chapter 5: Light-pulse atom interferometry

In this chapter, we consider light-pulse atom interferometry, an example of matter wave interferometry. In chapter 3 we derived the density-of-states equations of motion from the probabilistic Schrödinger equation. Here we apply these to model Raman transitions stimulated by a pair of laser beams. To do this, we reduce the density-of-states equations for a three-level atom to the density-of-states equations for an effective two-level system. The two-level system enables us to model the effect on the atom of short pulses from the pair of lasers tuned close to atomic state transition frequencies.

It is well-known that a timed sequence of $\pi/2, \pi, \pi/2$ laser pulses creates an atomic analogy to a Mach-Zehnder interferometer, shown in figure 5.1. The interference pattern is measured in momentum space, for various detunings of the laser wavenumber differences. For each detuning, the atomic cloud is prepared in the ground state and the light pulses are applied. A final tuned light pulse reads out the number of atoms that Raman-transitioned to the excited state.

5.1 Density-of-states equations for stimulated three-level atom transitions

Consider a three-level atom, whose energy levels are shown in figure 5.2. The atom is placed in two laser beams that counter-propagate along the z direction. The lasers can be turned on for a short pulse duration τ, then off again. Suppose the atom initially has momentum component $p - \hbar k_{1L}$ in the direction of the laser beams. After it absorbs a photon of energy

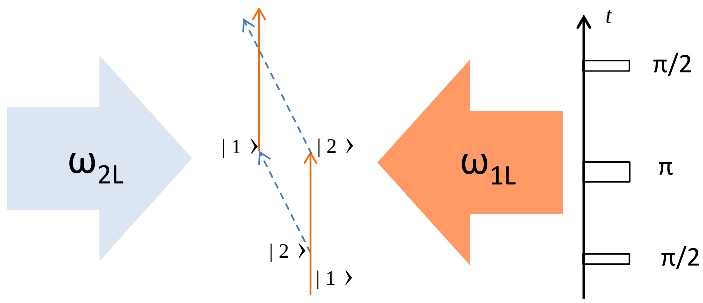

Figure 5.1: Schematic of a light-pulse atom interferometer. The atom (one of a cloud of alkali metal atoms) moves as a superposition of two internal energy states $|1\rangle$ and $|2\rangle$ in a Raman field of two counterpropagating laser beams at frequencies ω_{1L} and ω_{2L}. The two internal states are also associated with different external center-of-mass momenta, as shown by the solid or dashed path followed in state $|1\rangle$ or $|2\rangle$, respectively. Three pulses from both lasers together are applied in sequence to the atom, for time durations $\tau/2, \tau, \tau/2$. The pulses produce internal amplitude phase changes of $\pi/2, \pi, \pi/2$ radians, respectively. The π pulse exchanges the two states, including their momenta! During each pulse, the atom is stimulated to absorb a photon and emit a photon horizontally, and it recoils to conserve external momentum during the Raman transition. Thus the atomic center-of-mass of one of the states receives two impulse quanta $\pm\hbar k_{1L}$ and $\pm\hbar k_{2L}$, one from each laser beam. (The atom separates into two distinct centers of mass, whose paths are drawn here.) The three Raman pulses respectively have effects analogous to a beamsplitter, twin mirrors, and a beamcombiner in an optical Mach-Zehnder interferometer. [After Moler *et al.* [70].]

$\hbar\omega_{1L}$, the atom goes from state $|1, p - \hbar k_{1L}\rangle$ to state $|3, p\rangle$. Then after the excited atom is stimulated by a photon of energy $\hbar\omega_{2L}$, it emits another photon of the same energy and direction, going down one quantum to state $|2, p + \hbar k_{2L}\rangle$. For any initial momentum parameter p, these three states can be thought of as a closed momentum family.

5.1.1 Raman transitions become Rabi transitions

A three-level Raman transition reduces to a two-level model, by means of an adiabatic approximation to eliminate the intermediate high level $|3\rangle$. The amplitude c_3 becomes a function of the other two, when we set $\dot{c}_3 \approx 0$. This applies for a perturbing field detuned from the atom's transition frequency, in which case there is no spontaneous emission. Then the two-level Schrödinger equation has an exact solution for the Rabi rotating-wave approximation to a sinusoidal perturbing field which oscillates at frequency ω. For given momentum $\mathbf{p}$, and effective electric or magnetic dipole approximation for the two-level

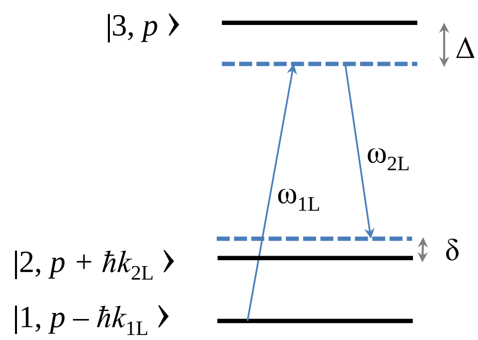

Figure 5.2: Three energy level Raman transition for two counterpropagating laser beams at radian frequencies ω_{1L} and ω_{2L}. Laser detuning parameters are shown as offsets Δ and δ. [After Moler *et al.* [70].]

interaction energy, the wavefunction is

$$|\Psi_p(t)\rangle \quad = \quad c_1(p,t)\,|1, p - \hbar k_{1L}\rangle + c_2(p,t)\,|2, p + \hbar k_{2L}\rangle + c_3(p,t)\,|3, p\rangle. \tag{5.1}$$

The Hamiltonian for this three-level atom of mass M is [70]

$$H \quad = \quad \frac{p^2}{2M} + \hbar\omega_{31}|3\rangle\langle 3| + \hbar\omega_{21}|2\rangle\langle 2| + H_{int}, \tag{5.2}$$

where the interaction energy for an atomic electric dipole with mean separating moment $\mathbf{d}$ is

$$H_{int} \quad = \quad -\mathbf{d}\cdot\mathbf{E}(x,t), \tag{5.3}$$

and the (Raman) electric field is

$$\mathbf{E}(x,t) \quad = \quad \frac{1}{2}\mathbf{E}_1 e^{ik_{1L}x - i\omega_{1L}t} + \frac{1}{2}\mathbf{E}_2 e^{-ik_{2L}x - i\omega_{2L}t} + \text{c.c.}, \tag{5.4}$$

for counterpropagating laser beams' electric fields $\mathbf{E}_1$ and $\mathbf{E}_2$.

We assume that $\mathbf{E}_1$ only couples $|1\rangle$ and $|3\rangle$, and that $\mathbf{E}_2$ only couples $|2\rangle$ and $|3\rangle$ [70].

The one-photon Rabi frequencies Ω_1 and Ω_2 are given by the matrix elements:

$$\Omega_k = -\langle k|\mathbf{d} \cdot \mathbf{E}_k|3\rangle/2\hbar, \quad k = 1,2 \tag{5.5}$$

so the interaction energy becomes

$$H_{int} = \hbar\Omega_1^* e^{ik_{1L}x - i\omega_{1L}t}|3\rangle\langle 1| + \hbar\Omega_2^* e^{-ik_{2L}x - i\omega_{2L}t}|3\rangle\langle 2| + \text{c.c.}. \tag{5.6}$$

The Hamiltonian matrix for this closed family of three momenta is then given by [70]

$$H = \begin{bmatrix} \frac{(p-\hbar k_{1L})^2}{2M} & 0 & \hbar\Omega_1 e^{i\omega_{1L}t} \\ 0 & \frac{(p+\hbar k_{2L})^2}{2M} + \hbar\omega_{21} & \hbar\Omega_2 e^{i\omega_{2L}t} \\ \hbar\Omega_1^* e^{-i\omega_{1L}t} & \hbar\Omega_2^* e^{-i\omega_{2L}t} & \frac{p^2}{2M} + \hbar\omega_{31} \end{bmatrix}. \tag{5.7}$$

Note that the stationary Hamiltonian is given here by the diagonal elements, and the time-varying perturbation is given by the off-diagonal electronic dipole-laser (L) interaction elements. Using notation similar to that of (3.74), we replace ω_{ji}^0 by $\Delta E_{ji}/\hbar = \frac{(p-\hbar k_{jL})^2}{2M\hbar} - \frac{(p-\hbar k_{iL})^2}{2M\hbar} + \omega_{ji}^0$, to propagate the atom's stationary states, given by both its center-of-mass kinetic energy for momentum eigenvalues and its internal energy level eigenvalues. Here we take $k_{3L} = 0$, and $\omega_{ij}^0 = -\omega_{ji}^0$ for levels $i < j$. Then writing out the von Neumann equation (3.82) for three levels, we have six equations for the density-of-states p_{ij} (usually denoted in textbooks as ρ_{ij})

$$\begin{aligned}
\dot{\mathsf{p}}_{11} &= -i\Omega_1 e^{i\omega_{1L}t} e^{-i\Delta E_{31}t/\hbar} \mathsf{p}_{31} + \text{c.c.} && \text{(5.8a)} \\
\dot{\mathsf{p}}_{12} &= -i\Omega_1 e^{i\omega_{1L}t} e^{-i\Delta E_{31}t/\hbar} \mathsf{p}_{32} + i\Omega_2^* e^{-i\omega_{2L}t} e^{-i\Delta E_{23}t/\hbar} \mathsf{p}_{13} && \text{(5.8b)} \\
\dot{\mathsf{p}}_{13} &= -i\Omega_1 e^{i\omega_{1L}t} e^{-i\Delta E_{31}t/\hbar} [\mathsf{p}_{33} - \mathsf{p}_{11}] + i\Omega_2 e^{i\omega_{2L}t} e^{-i\Delta E_{32}t/\hbar} \mathsf{p}_{12} && \text{(5.8c)} \\
\dot{\mathsf{p}}_{22} &= -i\Omega_2 e^{i\omega_{2L}t} e^{-i\Delta E_{32}t/\hbar} \mathsf{p}_{32} + \text{c.c.} && \text{(5.8d)} \\
\dot{\mathsf{p}}_{23} &= -i\Omega_2 e^{i\omega_{2L}t} e^{-i\Delta E_{32}t/\hbar} [\mathsf{p}_{33} - \mathsf{p}_{22}] + i\Omega_1 e^{i\omega_{1L}t} e^{-i\Delta E_{31}t/\hbar} \mathsf{p}_{21} && \text{(5.8e)} \\
\dot{\mathsf{p}}_{33} &= -i\Omega_1^* e^{-i\omega_{1L}t} e^{i\Delta E_{31}t/\hbar} \mathsf{p}_{13} \; - i\Omega_2^* e^{-i\omega_{2L}t} e^{i\Delta E_{32}t/\hbar} \mathsf{p}_{23} + \text{c.c.} && \text{(5.8f)}
\end{aligned}$$

We can define the laser detunings off-transition by $\Delta = \Delta E_{31}/\hbar - \omega_{1L}$ for the transition $|1, p - \hbar k_{1L}\rangle \to |3, p\rangle$, and $\delta = \Delta E_{12}/\hbar - (\omega_{2L} - \omega_{1L})$ for the transition $|1, p - \hbar k_{1L}\rangle \to |2, p - \hbar k_{2L}\rangle$. Note that

$$\begin{aligned}
\Delta &= \omega_{31} - \omega_{1L} + p \cdot k_{1L}/m - \hbar k_{1L}^2/2m && \text{(5.9a)} \\
\delta &= (\omega_{1L} - \omega_{2L}) - \left[\omega_{12} + p \cdot (k_{1L} - k_{2L})/m + \hbar(k_{1L}^2 - k_{2L}^2)/2m\right]. && \text{(5.9b)}
\end{aligned}$$

The three phase terms in square brackets above represent hyperfine (spin-spin) splitting ω_{12} (for example), Doppler shift of the laser field due to atomic motion, and recoil energy, respectively. The atomic recoils are due to momentum transfers from absorption and emission of atomic photons stimulated by the laser pulses. Between pulses, the c.m. velocity for each state does not change, unless another external field is also present then. These detunings are shown in figure 5.2.

In terms of these detunings, $\Delta + \delta = \Delta E_{32}/\hbar - \omega_{2L}$ is the detuning for the transition

$|2, p - \hbar k_{2L}\rangle \to |3, p\rangle$. Then we rewrite these equations (5.8a)-(5.8f) as

$$\dot{\mathsf{p}}_{11} = -i\Omega_1 e^{-i\Delta t}\mathsf{p}_{31} + \text{c.c.} \tag{5.10a}$$

$$\dot{\mathsf{p}}_{12} = -i\Omega_1 e^{-i\Delta t}\mathsf{p}_{32} + i\Omega_2^* e^{i(\Delta+\delta)t}\mathsf{p}_{13} \tag{5.10b}$$

$$\dot{\mathsf{p}}_{13} = -i\Omega_1 e^{-i\Delta t}\left[\mathsf{p}_{33} - \mathsf{p}_{11}\right] + i\Omega_2 e^{-i(\Delta+\delta)t}\mathsf{p}_{12} \tag{5.10c}$$

$$\dot{\mathsf{p}}_{22} = -i\Omega_2 e^{-i(\Delta+\delta)t}\mathsf{p}_{32} + \text{c.c.} \tag{5.10d}$$

$$\dot{\mathsf{p}}_{23} = -i\Omega_2 e^{-i(\Delta+\delta)t}\left[\mathsf{p}_{33} - \mathsf{p}_{22}\right] + i\Omega_1 e^{-i\Delta t}\mathsf{p}_{21} \tag{5.10e}$$

$$\dot{\mathsf{p}}_{33} = -i\Omega_1^* e^{i\Delta t}\mathsf{p}_{31} - i\Omega_2^* e^{i(\Delta+\delta)t}\mathsf{p}_{32} + \text{c.c.} \tag{5.10f}$$

For $\Delta \gg \Omega_1, \Omega_2, \delta$, we can use an adiabatic approximation to eliminate the densities p_{3k} that involve state $|3, p\rangle$. We assume the density elements change at a slow rate compared to Δ. Then we can easily integrate equations (5.10c,5.10e,5.10f) over time to get

$$\mathsf{p}_{13} = \frac{\Omega_1}{\Delta} e^{-i\Delta t}\left[\mathsf{p}_{33} - \mathsf{p}_{11}\right] - \frac{\Omega_2}{\Delta} e^{-i(\Delta+\delta)t}\mathsf{p}_{12} \tag{5.11a}$$

$$\mathsf{p}_{23} = \frac{\Omega_2}{\Delta} e^{-i(\Delta+\delta)t}\left[\mathsf{p}_{33} - \mathsf{p}_{22}\right] - \frac{\Omega_1}{\Delta} e^{-i\Delta t}\mathsf{p}_{21} \tag{5.11b}$$

$$\mathsf{p}_{33} = -\frac{\Omega_1^*}{\Delta} e^{i\Delta t}\mathsf{p}_{13} - \frac{\Omega_2^*}{\Delta} e^{i(\Delta+\delta)t}\mathsf{p}_{23} + \text{c.c.} \tag{5.11c}$$

Substituting (5.11a) and (5.11b) into (5.10b) gives

$$\begin{aligned} \dot{\mathsf{p}}_{12} = & -i\Omega_1 e^{-i\Delta t}\left[\frac{\Omega_2^*}{\Delta} e^{i(\Delta+\delta)t}\left[\mathsf{p}_{33} - \mathsf{p}_{22}\right] - \frac{\Omega_1^*}{\Delta} e^{i\Delta t}\mathsf{p}_{12}\right] \\ & + i\Omega_2^* e^{i(\Delta+\delta)t}\left[\frac{\Omega_1}{\Delta} e^{-i\Delta t}\left[\mathsf{p}_{33} - \mathsf{p}_{11}\right] - \frac{\Omega_2}{\Delta} e^{-i(\Delta+\delta)t}\mathsf{p}_{12}\right] \end{aligned}$$

or

$$\dot{\mathsf{p}}_{12} = i\frac{\Omega_1\Omega_2^*}{\Delta}e^{i\delta t}\left[\mathsf{p}_{22}-\mathsf{p}_{11}\right]+i\left[\frac{|\Omega_1|^2}{\Delta}-\frac{|\Omega_2|^2}{\Delta}\right]\mathsf{p}_{12}. \tag{5.12}$$

Substituting (5.11a) into (5.10a), and (5.11b) into (5.10d), we find that

$$\dot{\mathsf{p}}_{11} = i\frac{\Omega_1\Omega_2^*}{\Delta}e^{i\delta t}\mathsf{p}_{21}+\text{c.c.} \tag{5.13a}$$

$$\dot{\mathsf{p}}_{22} = i\frac{\Omega_1^*\Omega_2}{\Delta}e^{-i\delta t}\mathsf{p}_{12}+\text{c.c.} = -\dot{\mathsf{p}}_{11} \tag{5.13b}$$

Thus, we have obtained effective two-level density-of-states equations (5.12), (5.13a) and (5.13b). Normally this reduction from three to two levels is done using the corresponding amplitude equations [70][71].

For stimulated Raman transitions from state $|1\rangle$ to $|2\rangle$ via state $|3\rangle$, the population density of state 3 should be empty. We can show that the density of state 3 is nearly zero, still assuming a large detuning Δ. Substituting (5.11a) and (5.11b) into (5.11c), we have

$$\begin{aligned}\mathsf{p}_{33} &= -\frac{|\Omega_1|^2}{\Delta^2}\left[\mathsf{p}_{33}-\mathsf{p}_{11}\right]+\frac{\Omega_1^*\Omega_2}{\Delta^2}e^{-i\delta t}\mathsf{p}_{12}-\frac{|\Omega_2|^2}{\Delta^2}\left[\mathsf{p}_{33}-\mathsf{p}_{22}\right]+\frac{\Omega_2^*\Omega_1}{\Delta^2}e^{i\delta t}\mathsf{p}_{21}+\text{c.c.}\\ &= 2\left\{-\frac{|\Omega_1|^2}{\Delta^2}\left[\mathsf{p}_{33}-\mathsf{p}_{11}\right]+\frac{\Omega_1^*\Omega_2}{\Delta^2}e^{-i\delta t}\mathsf{p}_{12}-\frac{|\Omega_2|^2}{\Delta^2}\left[\mathsf{p}_{33}-\mathsf{p}_{22}\right]+\frac{\Omega_2^*\Omega_1}{\Delta^2}e^{i\delta t}\mathsf{p}_{21}\right\}\end{aligned} \tag{5,14a}$$

which we solve for p_{33}:

$$\begin{aligned}\mathsf{p}_{33} &= \left[\frac{|\Omega_1|^2}{\Delta}\mathsf{p}_{11}+\frac{|\Omega_2|^2}{\Delta}\mathsf{p}_{22}+\left(\frac{\Omega_2^*\Omega_1}{\Delta}e^{i\delta t}\mathsf{p}_{21}+\text{c.c.}\right)\right]\Big/\left[\frac{\Delta}{2}+\frac{|\Omega_1|^2}{\Delta}+\frac{|\Omega_2|^2}{\Delta}\right]\\ &\approx 0.\end{aligned} \tag{5.15}$$

We have eliminated state 3 by adiabatic approximation, reducing the three-level density-of-states equations to a set of effective two-level equations for the densities involving only the first two states. For the atoms initially prepared in state $|1, p - \hbar k_{1L}\rangle$, *i.e.*, $\mathsf{p}_{11}(0) = 1$, these equations (5.12), (5.13a) and (5.13b) have solutions at time τ as a function of momentum p [70]

$$\mathsf{p}_{11}(p,\tau) = \cos^2\left(\frac{\omega\tau}{2}\right) + \frac{1}{\omega^2}\left[\frac{|\Omega_1|^2}{\Delta} - \frac{|\Omega_2|^2}{\Delta} - \delta\right]^2 \sin^2\left(\frac{\omega\tau}{2}\right) \tag{5.16a}$$

$$\mathsf{p}_{22}(p,\tau) = \left(\frac{2|\Omega_1^*\Omega_2|}{\omega\Delta}\right)^2 \sin^2\left(\frac{\omega\tau}{2}\right) \tag{5.16b}$$

$$\begin{aligned}\mathsf{p}_{12}(p,\tau) &= \left\{\cos\left(\frac{\omega\tau}{2}\right) - \frac{i}{\omega}\left[\frac{|\Omega_1|^2}{\Delta} - \frac{|\Omega_2|^2}{\Delta} - \delta\right]\sin\left(\frac{\omega\tau}{2}\right)\right\} \\ &\quad \times \frac{i}{\omega}\frac{2|\Omega_1^*\Omega_2|}{\Delta}\sin\left(\frac{\omega\tau}{2}\right)e^{-i\delta\tau},\end{aligned} \tag{5.16c}$$

where

$$\omega^2 = \left[\frac{\Omega_1^2}{\Delta} - \frac{\Omega_2^2}{\Delta} - \delta\right]^2 + \left(\frac{2|\Omega_1^*\Omega_2|}{\Delta}\right)^2 \tag{5.17}$$

Here δ (5.9b), Δ (5.9a), and thus everything else, is a function of initial momentum p. The more general two-level solutions for arbitrary initial density-of-states are similar but lengthier, so we do not record them here.

To construct a wavepacket that models the atom cloud as an ensemble, suppose the initial momenta of the atoms are Gaussian distributed, with amplitude density $g(p) = \pi^{-1/4}\sigma_p^{-1/2}\exp\left\{-\frac{(p-p_0)^2}{2\sigma_p^2}\right\}$, normalized so that $\int |g(p)|^2 dp = 1$. Here $\sigma_p = \sqrt{2Mk_BT}$, as for a shifted Maxwell-Boltzmann distribution. Then the population densities for atomic states $|1, p - \hbar k_{1L}\rangle$ and $|2, p + |\hbar k_{2L}\rangle$ are given by $|g(p)|^2\mathsf{p}_{11}$ and $|g(p)|^2\mathsf{p}_{22}$, respectively, with (5.16a) and (5.16b). Plots of these two population probability densities, as a function

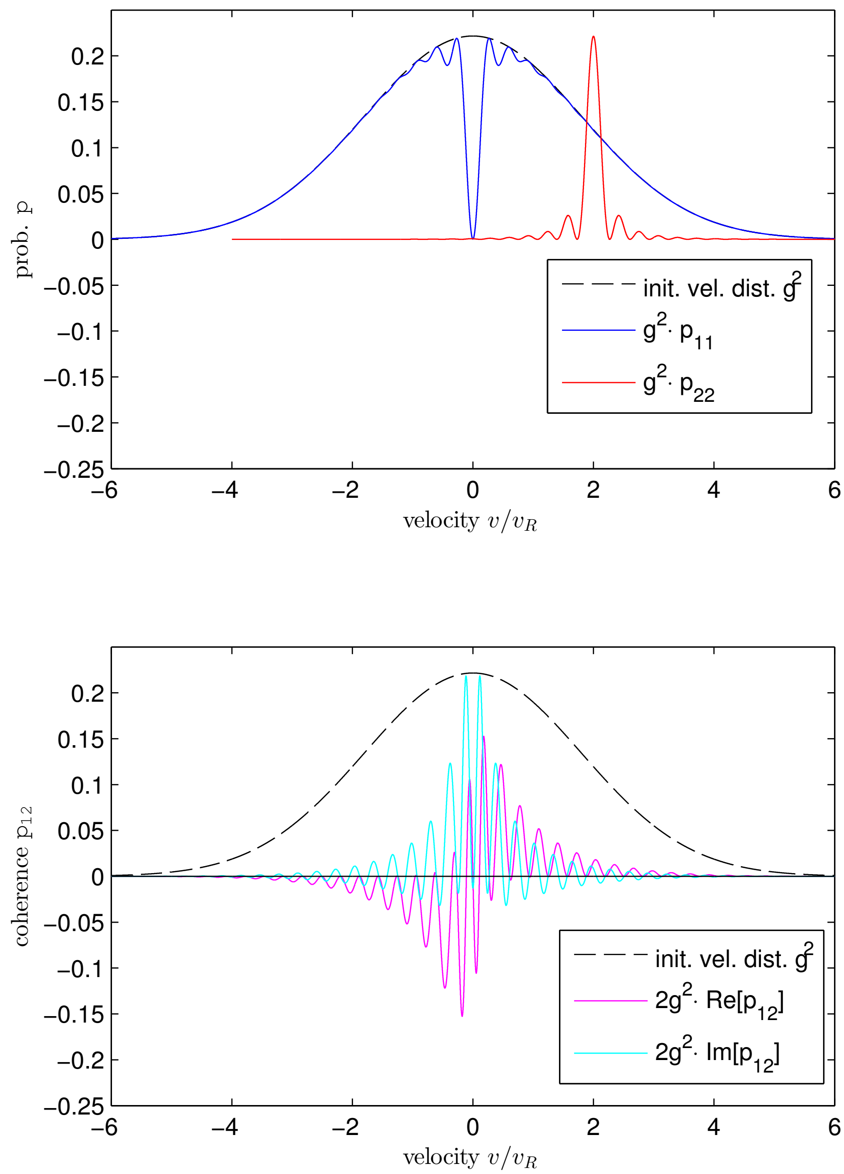

Figure 5.3: Probability densities p_{11} and p_{22} (upper plots) for atomic states $|1, p - \hbar k_{1L}\rangle$ and $|2, p + \hbar k_{2L}\rangle$ after a π pulse, for initial state $|1\rangle$ momentum density width $\sigma_p = 3.6 m v_R/\sqrt{2}$, Raman field wavenumbers $k_{1L} \approx k_{2L} = k = m v_R$, Raman pulse duration $\tau = 10/k v_R$, and effective two-photon Rabi frequency $|\Omega_1^* \Omega_2|/\Delta = 0.16 k v_R$. Note that the atoms in state $|2\rangle$ have been selected from a narrow velocity range after the pulse. They have also been boosted by $2\hbar k$, about twice the one-photon recoil momentum. [After Moler *et al.* [70].] The lower plots show the two-state coherence p_{12}.

of atomic c.m. velocity, scaled in units of the Raman one-photon recoil velocity v_R, are shown for the atoms initially in state $|1\rangle$ after a π-pulse in the top plots of figure 5.3. In the lab, the $|1\rangle \to |2\rangle$ transition detuning δ (5.9b) can be varied. The plots of the population densities as a function of total detuning δ are almost the same as those in the figure, without the initial Gaussian momentum envelope.

The lower plots of figure 5.3 show twice the real and imaginary plots of the coherence p_{12} between the two states.

5.2 The atomic Mach-Zehnder interferometer

To see the analogy with the Mach-Zehnder interferometer, as depicted in figure 5.1, we now use the amplitude formulas, as given in [70], to propagate the atomic states. We approximate these formulas by assuming $\frac{|\Omega_1|^2}{\Delta} \approx \frac{|\Omega_2|^2}{\Delta}$, and $\omega \approx \frac{2|\Omega_1^*\Omega_2|}{\Delta}$. Then the amplitude propagation formulas simplify to linear combinations involving phasors, as follows [72]:

After a $\pi/2$ pulse of $\tau/2$ seconds, for fixed effective Rabi frequency ω, we have

$$\begin{aligned} c_{1,\mathbf{p}}(t+\tau/2) &= \frac{1}{\sqrt{2}}\left(c_{1,\mathbf{p}}(t) - ie^{i\phi(t)}c_{2,\mathbf{p}+2\hbar\mathbf{k}}(t)\right) \\ c_{2,\mathbf{p}+2\hbar\mathbf{k}}(t+\tau/2) &= \frac{1}{\sqrt{2}}\left(-ie^{-i\phi(t)}c_{1,\mathbf{p}}(t) + c_{2,\mathbf{p}+2\hbar\mathbf{k}}(t)\right). \end{aligned} \tag{5.18}$$

Here we have attached the atom's associated c.m. momentum horizontal component, e.g. an initial horizontal momentum $\mathbf{p}$, as a subscript to the atom's internal electronic state amplitudes c_1 and c_2. After a π pulse of τ seconds,

$$\begin{aligned} c_{1,\mathbf{p}}(t+\tau) &= -ie^{i\phi(t)}c_{2,\mathbf{p}+2\hbar\mathbf{k}}(t) \\ c_{2,\mathbf{p}+2\hbar\mathbf{k}}(t+\tau) &= -ie^{-i\phi(t)}c_{1,\mathbf{p}}(t). \end{aligned} \tag{5.19}$$

Between pulses, the amplitude coefficients do not change with time. The two superposed laser fields are at frequencies ω_{1L}, ω_{2L}, respectively. For approximate electric dipole interaction potentials, the phase function $\phi(t)$ for both of the states is given with respect to an arbitrary start time t_0 by $\phi(t) = \int_{t_0}^{t} \delta(t')dt'$.

Now we can model the effect of a sequence of pulses applied in succession. Suppose the atom is prepared in the ground state at the initial time $t = 0$, with $c_{1,\mathbf{p}} = 1$ and $c_{2,\mathbf{p}} = 0$. We apply a sequence of $\pi/2, \pi$, and $\pi/2$ pulses, at times $0, T + \tau/2$ and $2T + 3\tau/2$, respectively. We apply the first pulse at time $t_1 = 0$, producing a superposition of states, given by relations (5.18) as:

$$\begin{aligned} c_{1,\mathbf{p}}(\tau/2) &= \frac{1}{\sqrt{2}} \\ c_{2,\mathbf{p}+2\hbar\mathbf{k}}(\tau/2) &= -i\frac{1}{\sqrt{2}}e^{-i\phi(t_1)}. \end{aligned} \tag{5.20}$$

This pulse thus has an effect analogous to that of a 50:50 beamsplitter.

Next, the π pulse is applied at $t_2 = T + \tau/2$. By relations (5.19), this pulse exchanges the amplitude coefficients of the states, and the corresponding linear momenta:

$$\begin{aligned} c_{1,\mathbf{p}+2\hbar\mathbf{k}}(t_2 + \tau) &= -ie^{i\phi(t_2)}c_{2,\mathbf{p}+2\hbar\mathbf{k}}(\tau/2) = \frac{1}{\sqrt{2}}e^{i(\phi(t_2)-\phi(t_1))} \\ c_{2,\mathbf{p}}(t_2 + \tau) &= -ie^{-i\phi(t_2)}c_{1,\mathbf{p}}(\tau/2) = -i\frac{1}{\sqrt{2}}e^{-i\phi(t_2)}. \end{aligned} \tag{5.21}$$

This effect is analogous to that of a pair of mirrors.

After another delay of T seconds, at time $t_3 = 2T + 3\tau/2$, the last $\pi/2$ pulse is applied.

After this pulse, the coefficients become:

$$\begin{aligned}
c_{1,\mathbf{p}}(t_3+\tau/2) &= \frac{1}{\sqrt{2}}\Big(c_{1,\mathbf{p}}(t_3) - ie^{i\phi(t_3)}c_{2,\mathbf{p}+2\hbar\mathbf{k}}(t_3)\Big) \\
&= \frac{1}{2}e^{+i(\phi(t_2)-\phi(t_1))} - \frac{1}{2}e^{i(\phi(t_3)-\phi(t_2))} \\
&= \frac{1}{2}e^{+i(\phi(t_2)-\phi(t_1))}\cdot\Big(1 - e^{i(\phi(t_3)-2\phi(t_2)+\phi(t_1))}\Big) \qquad (5.22a)
\end{aligned}$$

$$\begin{aligned}
c_{2,\mathbf{p}+2\hbar\mathbf{k}}(t_3+\tau/2) &= \frac{1}{\sqrt{2}}\Big(-ie^{-i\phi(t_3)}c_{1,\mathbf{p}}(t_3) + c_{2,\mathbf{p}+2\hbar\mathbf{k}}(t_3)\Big) \\
&= -i\frac{1}{2}e^{-i(\phi(t_3)-\phi(t_2)+\phi(t_1))} - i\frac{1}{2}e^{-i\phi(t_2)} \\
&= -i\frac{1}{2}e^{-i\phi(t_2)}\cdot\Big(1 + e^{-i(\phi(t_3)-2\phi(t_2)+\phi(t_1))}\Big). \qquad (5.22b)
\end{aligned}$$

The factors in parentheses on the right hand sides of (5.22a) and (5.22b) clearly contain a sine and cosine of the accumulated phase, respectively. They represent interference between the atomic states recombined by the final $\pi/2$ pulse.

The interference pattern is a function of detuning frequency δ, as well as any phase shifts caused by interaction with an external gravity field or magnetic field gradient, or by platform rotation. For example, in a vertical gravity field with local acceleration g, the additional phase due to the field accumulates over time t as $\Delta\phi = -(k_{1L} - k_{2L})\cdot gt^2$ [72].

To measure an external magnetic field gradient $\partial B/\partial x$ (*e.g.*, due to local mineral deposits in the earth), the atomic interferometer configuration in figure 5.1 can be modified to use copropagating instead of counterpropagating Raman lasers [73]. The magnetic number m splitting states of the alkali metal atom (*e.g.*, ^{85}Rb) are now present in a superposed ambient magnetic field, and we have magnetic dipole interaction with the laser beams. Then our formulas in this section apply as before, when we reverse the sign of wavenumber k_{2L} to agree with that of k_{1L}.

The two Raman frequencies ω_{1L}, ω_{2L}, for either direction of propagation, can be produced from one source laser frequency by using a polarizing beamsplitter and passing one or both resulting beams through an electro-optic modulator to shift their respective frequencies by *e.g.,* $\sim \pm 1$ GHz, as needed. Using one source laser keeps the Raman beams coherent and reduces sensitivity to the source beam frequency stability.

A final readout pulse projects the wavefunction onto one state, such as the upper state $|2\rangle$. This pulse is tuned on-resonance, and results in fluorescent decay as spontaneously emitted photons scatter uniformly in all directions. The latter can be detected to the side of the laser beams, and recorded for various detunings to measure the interference pattern.

5.3 Conclusion

In this chapter, we have applied the probabilistic Schrödinger equation from chapter 3 to develop the density-of-states equations for a three-level atom interacting with oscillating electromagnetic fields of two counter- or co-propagating lasers that stimulate two-photon Raman transitions in the atom, as in a light-pulse atom interferometer. By adiabatic approximation, we reduced these equations to effective two-level equations for the Raman transitions, which can be solved. By detuning the lasers from the resonant transition frequencies of the atom's excited intermediate state, the Raman transitions avoid the spontaneous decay present in a two-level atom interferometer. We also described the phasor approximation for how the two state amplitudes propagate, to demonstrate the well-known analogy between this and a Mach-Zehnder interferometer.

Chapter 6: Conclusions

A bilocal picture of standard quantum mechanics has been presented in this dissertation. This picture brings out the inherently bilocal aspects of quantum mechanics that appear when we try to propagate probability densities rather than amplitudes. Contemporary experiments have been analyzed using the new bilocal picture. It has been applied to recent three-slit tests of the Born rule, to propose a modified version of the Steinberg experiment using a twin detector, and to light-pulse atom interferometry.

In greater retrospective detail, we may enumerate the highlights of this dissertation:

- A new path integral for probability-current propagation was introduced, a "sum over all [twin] path histories". (The twin paths in this integral are expressed symmetrically, in terms of a central path with equal plus and minus displacements for each time.) It is shown that the propagator kernel reduces approximately to the simple form $e^{-i\mathbf{p}\cdot\boldsymbol{\tau}/\hbar}$, which is exact for a particle moving in a quadratic potential. Here $\mathbf{p}$ is the initial (central) momentum of the particle for a given pair of paths, and $\boldsymbol{\tau}$ is their arbitrary initial path displacement or separation.

- Four Blue propagator examples were given, including that for the quantum harmonic oscillator, and calculations for double-slit interferometer experiments that become simple using natural symmetry of propagation paths.

- The quantum bicontinuity equation was derived from the new path integral, showing its equivalence to the Schrödinger equation.

- For the first time, how to obtain the Weyl-Wigner theory for expectation values from ordinary quantum mechanics was shown, by demonstrating that the Wigner quasi-density is an expression of wavefunction probability propagation.

- The Wigner density was generalized naturally in terms of these path integrals, which is a physically meaningful way to extend it beyond the quadratic Lagrangian of the quantum harmonic oscillator.

- The Blue function property like that of a Green function [1] was derived, and path-integral expressions for a complete probability-and-current four-vector propagator in configuration and in phase space were obtained.

- A perturbation theory for the new propagators was initiated, including a closed-form first-order perturbation integral.

- A new symbol for path integrals, having the form $\int \mathcal{D}x(t)$, was introduced to avoid confusion with other integrals.

- A probability theory to include signed values for interference events was introduced. A new probability identity was introduced to show that at most two events can interfere together at once in quantum mechanics.

- A twin detector concept was introduced to permit interfering wavelike bilocal arrivals of a particle to be detected. Three ways to implement the twin detector were discussed, including the Michelson stellar interferometer. (This inspired Ramsey's molecular beam method with separated oscillating fields, which is related to light-pulse atom interferometry.)

- Bilocal forms of the usual current density and the path-fluctuation (osmotic) current density, were identified. Simple formulas were found for them, in terms of the bilocal probability density.

- A probabilistic Schrödinger equation was found for the bilocal probability density.

- The energy-difference eigenvalues and dyadic eigenstates for solving this equation were derived.

- The von Neumann density-of-states equation was shown to follow directly from the probabilistic Schrödinger equation.
- The bilocal probability framework was applied to recent three-slit experimental tests of the Born rule.
- The bilocal probability and current densities were computed in closed form formulas to obtain average paths for a proposed modified version of the Steinberg experiment that would use a twin detector.
- The von Neumann density-of-states equations for a three-level atom were adiabatically reduced to effective two-level equations, and applied to light-pulse atom interferometry.

These are the principal results of this dissertation.

Appendix A: Blue functions as path integrals in phase space

For a path integral involving a more general Lagrangian, we consider paths in phase (x, p) space. Let any path of the particle(s) from $x'p'$ at time t' to $x''p''$ at time t'' be given at N time increments $\epsilon = T/N$, as $x_0 = x', x_1, x_2, \ldots, x_N = x''$. Here $x_n = x(n\epsilon), n = 1, 2, 3, \ldots,$ and $T = t'' - t'$. The path integral expression in phase space for the Green function propagator is given by [16] [17]:

$$\begin{aligned} G(x''t''; x't') &= \iint \mathcal{D}x(t)\mathcal{D}p(t)\; e^{i\int (p\cdot\dot{x} - H(p,x))/\hbar} \\ &= \int \tfrac{dp_0}{2\pi\hbar} \int dx_1 \tfrac{dp_1}{2\pi\hbar} \int dx_2 \tfrac{dp_2}{2\pi\hbar} \;\cdots\; \int dx_{N-1} \tfrac{dp_{N-1}}{2\pi\hbar} \\ &\quad \times \exp\left\{ \tfrac{i\epsilon}{\hbar} \textstyle\sum_{n=1}^{N} \left[p_n \cdot \tfrac{x_n - x_{n-1}}{\epsilon} - \tfrac{1}{2m} p_n^2 - \left(\tfrac{x_n + x_{n-1}}{2} \right) \right] \right\}, \end{aligned} \tag{A.1}$$

where no normalizing factor, as a function of the time increment ϵ, is needed. The Lagrangian $L = (p\dot{x} - H(p, x))$ may come from a Hamiltonian H in which the momenta p enter other than quadratically.

To obtain the path integral for the Blue function $B(x''t'', x't'\tau') =$ $G^*(x''t''; x' - \frac{\tau'}{2}t')G(x''t''; x' + \frac{\tau'}{2})$, we take two copies of the path integral for G, much as we did in section 2.3 for the configuration space path integral. Let the two sampled paths through phase space be specified as

$$\begin{aligned} \tilde{x}_0 = \left(x' - \tfrac{\tau'}{2}\right), &\qquad \tilde{x}_1, \ldots, \tilde{x}_{N-1}, \tilde{x}_N = \left(x'' - \tfrac{\tau''}{2}\right) \\ \tilde{p}_0, &\qquad \tilde{p}_1, \ldots, \tilde{p}_{N-1}, \tilde{p}_N \\ x_0 = \left(x' + \tfrac{\tau'}{2}\right), &\qquad x_1, \ldots, x_{N-1}, x_N = \left(x'' + \tfrac{\tau''}{2}\right) \\ p_0, &\qquad p_1, \ldots, p_{N-1}, p_N, \end{aligned}$$

with displaced spatial endpoints for G^* and G, respectively. Both paths are sampled at regular time instants $t = t_n \equiv n\epsilon$, for $n = 0, \ldots, N$. Introduce the change of variables

$$\begin{aligned} x_n &= q_n + \tau_n/2 & \tilde{x}_n &= q_n - \tau_n/2 \\ p_n &= \pi_n + \sigma_n/2 & \tilde{p}_n &= \pi_n - \sigma_n/2, \end{aligned}$$

to entangle the integrand for two paths at each time n. Then after canceling terms, the Blue kernel becomes

$$\begin{aligned} B(x''t''\tau''; x't'\tau') \;\; = \;\; & \int d\pi_N \; d\sigma_N/(4\pi^2\hbar^2) \cdot \prod_{n=1}^{N-1} dq_n \; d\tau_n \; d\pi_n \; d\sigma_n/(4\pi^2\hbar^2) \\ & \exp\left\{ \tfrac{i\epsilon}{\hbar} \textstyle\sum_{n=1}^{N} \left[\pi_n \cdot \frac{(\tau_n - \tau_{n-1})}{\epsilon} + \sigma_n \cdot \frac{(q_n - q_{n-1})}{\epsilon} \right.\right. \\ & \quad + H\left(\bar{q}_n - \bar{\tau}_n/2 + \bar{\pi}_n - \bar{\sigma}_n/2\right) \\ & \quad \left.\left. - \; H\left(\bar{q}_n + \bar{\tau}_n/2 + \bar{\pi}_n + \bar{\sigma}_n/2\right) \right] \right\}. \end{aligned} \tag{A.2}$$

For brevity, we denote the average values by $\bar{q}_n = \frac{1}{2}\left(q_n + q_{n-1}\right)$, etc. Note that at the path endpoints we have $q_0 = x'$, $\tau_0 = \tau'$, and since $x_N = \tilde{x}_N = x''$, $\tau_N = \tau''$ and $q_N = x''$. The initial momentum value p_0, and the corresponding π_0, are not used. As $N \to \infty$ and $\epsilon \to 0$, keeping $N\epsilon = T$, the Blue function can be represented formally as the continuous path integral

$$B(x''t''\tau'', x't'\tau') \; = \; \iint \mathcal{D}q(t)\mathcal{D}\tau(t)\mathcal{D}\pi(t)\mathcal{D}\sigma(t) \; e^{i\Delta S/\hbar}, \tag{A.3}$$

where the displaced action or *motion* for each possible path is now given by the line integral

$$\begin{aligned} & \Delta S[q(t), \tau(t), \pi(t), \sigma(t)] \\ & \quad = \int_{t'}^{t''} \left(\pi \cdot \dot{\tau} + \sigma \cdot \dot{q} - \left[H(q + \tfrac{\tau}{2}) - H(q - \tfrac{\tau}{2}) \right] \right) dt. \end{aligned} \tag{A.4}$$

This expression agrees with the displaced action (2.29) we got in section 2.3 from two Legendre transformations.

Appendix B: Evaluation of the Blue function path integral propagator for a free particle

For a free particle in d Cartesian dimensions,

$$B_0(x''t''\tau'';x't'\tau') = \tfrac{1}{|C(\epsilon)|^2}\iint \tfrac{dx_{N-1}d\tau_{N-1}}{|C(\epsilon)|^2}\cdots\iint \tfrac{dx_2 d\tau_2}{|C(\epsilon)|^2}\iint \tfrac{dx_1 d\tau_1}{|C(\epsilon)|^2} \exp\left\{\tfrac{i}{\hbar}\sum_{n=1}^{N} m\tfrac{(x_n-x_{n-1})\cdot(\tau_n-\tau_{n-1})}{\epsilon}\right\}, \tag{B.1}$$

where as shown in section 2.7, $|C|^{-2} = \left(\frac{m}{2\pi\hbar\epsilon}\right)^d$. We put $\alpha = \frac{m}{\hbar\epsilon}$, and begin by integrating the two terms that involve x_1 and τ_1:

$$\begin{aligned} I_1 &= \iint \tfrac{dx_1 d\tau_1}{|C(\epsilon)|^2}\exp\left\{\tfrac{im}{\hbar\epsilon}\left[(x_2-x_1)\cdot(\tau_2-\tau_1)\right.\right. \\ &\qquad \left.\left.+(x_1-x_0)\cdot(\tau_1-\tau_0)\right]\right\} \\ &= \iint dx_1 d\tau_1 \left(\tfrac{\alpha}{2\pi}\right)^d \exp\left\{i\alpha\left[2\left(x_1-\left(\tfrac{x_2+x_0}{2}\right)\right)\cdot\left(\tau_1-\left(\tfrac{\tau_2+\tau_0}{2}\right)\right)\right.\right. \\ &\qquad \left.\left.+\tfrac{1}{2}(x_2-x_0)\cdot(\tau_2-\tau_0)\right]\right\}. \end{aligned} \tag{B.2}$$

To evaluate this, consider the double integral for one dimension ($d=1$)

$$\frac{1}{2\pi}\iint e^{i(x-a)(y-b)}dx\,dy = \int e^{-ia(y-b)}\delta(y-b)\,dy = 1, \tag{B.3}$$

where we regard this as a Fourier integral. (We are accustomed to Gaussian integrals in this context. The exponent can also be expressed as a 0-trace quadratic form: $e^{ixy} = e^{\frac{i}{2}\mathbf{z}^t\sigma_1\mathbf{z}}$, for $\sigma_1 = \begin{pmatrix} 0 & 1 \\ 1 & 0 \end{pmatrix}$ and $\mathbf{z}^t = (x, y)$.) Applying (B.3) to (B.2), we get

$$I_1 = \tfrac{1}{2^d} \exp\left\{\tfrac{i\alpha}{2}(x_2 - x_0)\cdot(\tau_2 - \tau_0)\right\}. \tag{B.4}$$

We continue recursively, using the general identity for $n = 1, 2, 3, ...$

$$\begin{aligned} & (x_{n+1} - x_n)\cdot(\tau_{n+1} - \tau_n) + \tfrac{1}{n}(x_n - x_0)\cdot(\tau_n - \tau_0) \\ = \; & \tfrac{n+1}{n}\left[x_n - \left(\tfrac{nx_{n+1}+x_0}{n+1}\right)\right]\cdot\left[\tau_n - \left(\tfrac{n\tau_{n+1}+\tau_0}{n+1}\right)\right] \\ & + \tfrac{1}{n+1}(x_{n+1} - x_0)\cdot(\tau_{n+1} - \tau_0). \end{aligned} \tag{B.5}$$

Bringing in the next term involving x_2 and τ_2, we obtain

$$\begin{aligned} I_2 &= \iint dx_2 d\tau_2 \left(\tfrac{1}{2}\tfrac{\alpha}{2\pi}\right)^d \exp\{i\alpha\,[(x_3 - x_2)\cdot(\tau_3 - \tau_2) \\ &\qquad + \tfrac{1}{2}(x_2 - x_0)\cdot(\tau_2 - \tau_0)]\} \\ &= \tfrac{1}{3^d} \exp\left\{\tfrac{i\alpha}{3}(x_3 - x_0)\cdot(\tau_3 - \tau_0)\right\}. \end{aligned} \tag{B.6}$$

By induction, we continue to integrate this way until we arrive at the answer,

$$\begin{aligned} B_0(x''t''\tau''; x'\tau't') &= \left[\tfrac{m}{2\pi\hbar N\epsilon}\right]^d \exp\left\{\tfrac{im}{N\hbar\epsilon}(x_N - x_0)\cdot(\tau_N - \tau_0)\right\}. \\ &= \left[\tfrac{m}{2\pi\hbar T}\right]^d \exp\left\{\tfrac{im}{\hbar T}(x'' - x')\cdot(\tau'' - \tau')\right\}. \end{aligned} \tag{B.7}$$

This result agrees with equation (4.9), which was obtained from the free-particle Green function.

The propagator (3.53) for the current density of a free particle can be computed in almost the same way. For each path, the integral is the same as (B.1), up to the final leg of the path. But now the integrand for the final stage $N-1$ is multiplied by the d-dimensional velocity vector $\frac{1}{\epsilon}(x_N - x_{N-1})$, where $x_N = x''$ is the path endpoint. Using the identity (B.5) to take the final step, we find the last integral for the current density propagator is:

$$
\begin{aligned}
\mathbf{B}_0^{\mu}(x''t''\tau''; x'\tau't') &= I_{N-1}^{curr} \\
&= \iint dx_{N-1} d\tau_{N-1} \left(\tfrac{\alpha}{2\pi(N-1)\epsilon}\right)^d \frac{(x_N - x_{N-1})}{\epsilon} \cdot \\
&\qquad \exp\left\{ i\alpha \left[\tfrac{N}{N-1}\left(x_{N-1} - \left(\tfrac{(N-1)x_N + x_0}{N}\right)\right) \cdot \left(\tau_{N-1} - \left(\tfrac{(N-1)\tau_N + \tau_0}{N}\right)\right) \right.\right. \\
&\qquad\qquad \left.\left. + \tfrac{1}{N}(x_N - x_0) \cdot (\tau_N - \tau_0) \right] \right\} \\
&= \iint dx_{N-1} d\tau_{N-1} \left(\tfrac{\alpha}{2\pi(N-1)\epsilon}\right)^d \tfrac{1}{\epsilon}\left[\left(\tfrac{x_N - x_0}{N}\right) - \left(x_{N-1} - \left(\tfrac{(N-1)x_N + x_0}{N}\right)\right) \right] \cdot \\
&\qquad \exp\left\{ i\alpha \left[\tfrac{N}{N-1}\left(x_{N-1} - \left(\tfrac{(N-1)x_N + x_0}{N}\right)\right) \cdot \left(\tau_{N-1} - \left(\tfrac{(N-1)\tau_N + \tau_0}{N}\right)\right) \right.\right. \\
&\qquad\qquad \left.\left. + \tfrac{1}{N}(x_N - x_0) \cdot (\tau_N - \tau_0) \right] \right\} \\
&= \left(\tfrac{m}{2\pi\hbar N\epsilon}\right)^d \tfrac{(x_N - x_0)}{N\epsilon} \exp\left\{ i\alpha \left[\tfrac{1}{N}(x_N - x_0) \cdot (\tau_N - \tau_0) \right] \right\} \\
&\equiv \left(\tfrac{m}{2\pi\hbar T}\right)^d \tfrac{(x'' - x')}{T} \exp\left\{ \tfrac{im}{\hbar T}(x'' - x') \cdot (\tau'' - \tau') \right\} && \text{(B.8)} \\
&= \mathbf{v} B_0, && \text{(B.9)}
\end{aligned}
$$

for components $\mu = 1, 2, \ldots, d$. We have integrated by applying the double integrals (2.58) and (2.59) to each dimension of the vectors. Note that the vector factor $\mathbf{v} = \frac{(x''-x')}{T}$ can be interpreted as the mean velocity between the start and end points. Since $T = t'' - t'$, we can include time as the $d+1$ coordinate in $\mathbf{v}$ as the case $\mu = 0$ given by (B.7), in this formula as well. That is, $\mathbf{v}_0 = 1$. We do not modify the exponent, a spatial dot product.

Appendix C: Perturbation integral

To integrate $B_{(1)}$, we use these identities, whose proofs are left to the reader:

$$\breve{p} \cdot \breve{\tau} \;=\; \tfrac{m}{2\alpha\beta T}\left[|r-\tilde{r}|^2 - |s-\tilde{s}|^2\right]. \tag{C.1}$$

$$\begin{aligned} \tfrac{1}{\alpha\beta}|r-\tilde{r}|^2 &= \tfrac{1}{\alpha}|r-r'|^2 + \tfrac{1}{\beta}|r-r''|^2 - |r'-r''|^2 \\ \tfrac{1}{\alpha\beta}|s-\tilde{s}|^2 &= \tfrac{1}{\alpha}|s-s'|^2 + \tfrac{1}{\beta}|s-s''|^2 - |s'-s''|^2 \end{aligned} \tag{C.2}$$

$$\begin{aligned} p'' &= p_0 - \alpha\breve{p} \\ p' &= p_0 + \beta\breve{p} \end{aligned} \tag{C.3}$$

$$\tfrac{1}{\alpha\beta} \;=\; \tfrac{1}{\alpha} + \tfrac{1}{\beta} \tag{C.4}$$

Here $\breve{p} = p' - p''$ is the momentum transfer, and the momenta all have the form $p(x_b t_b x_a t_a) = m(x_b - x_a)/(t_b - t_a)$, deriving from the formula for B_0 in appendix B. In particular, we define $p_0 = m(x'' - x')/(t'' - t')$, $p' = m(x - x')/(t - t')$, $p'' = m(x'' - x)/(t'' - t)$. To separate ΔV below, we will change variables to $r = x + \frac{\tau}{2}, s = x - \frac{\tau}{2}$. For brevity we put $T = t'' - t'$ as usual, and $\alpha = (t - t')/T, \beta = (t'' - t)/T$. Also put $\tilde{r} = \alpha r'' + \beta r'$, $\tilde{\tau} = \alpha\tau'' + \beta\tau'$, $\breve{\tau} = \tau - \tilde{\tau}$.

Then

$$
\begin{aligned}
B_{(1)} &= -\tfrac{i}{\hbar}\iiint B_0(x''t''\tau''; xt\tau)\Delta V(xt\tau)B_0(xt\tau; x't'\tau')\ dxd\tau dt \\
&= -\tfrac{i}{\hbar}\int_{t'}^{t''}\left[\tfrac{m}{2\pi\hbar(t''-t)}\right]^d\left[\tfrac{m}{2\pi\hbar(t-t')}\right]^d \\
&\quad \times \iint \Delta V(x,\tau)\exp\left\{\tfrac{i}{\hbar}\left[p''\cdot(\tau''-\tau)+p'\cdot(\tau-\tau')\right]\right\}\ dxd\tau dt \\
&= -\tfrac{i}{\hbar}\int_{t'}^{t''}\left[\tfrac{m}{2\pi\hbar(t''-t)}\right]^d\left[\tfrac{m}{2\pi\hbar(t-t')}\right]^d\exp\left\{\tfrac{i}{\hbar}p_0\cdot[\tau''-\tau']\right\} \\
&\quad \times \iint \Delta V(x,\tau)\exp\left\{\tfrac{i}{\hbar}\breve{p}\cdot\breve{\tau}\right\}\ dxd\tau dt \\
&= -\tfrac{i}{\hbar}\int_{t'}^{t''}\left[\tfrac{m}{2\pi\hbar\beta T}\right]^d\left[\tfrac{m}{2\pi\hbar\alpha T}\right]^d\exp\left\{\tfrac{im}{2\hbar T}\left[|r''-r'|^2-|s''-s'|^2\right]\right\} \\
&\quad \times \iint [V(r)-V(s)]\exp\left\{\tfrac{im}{2\hbar\alpha\beta T}\left[|r-\tilde{r}|^2-|s-\tilde{s}|^2\right]\right\}\ drdsdt \\
&= -\tfrac{i}{\hbar}\int_{t'}^{t''}\left[\tfrac{i2\pi\hbar\alpha\beta T}{m}\right]^{d/2}\left[\tfrac{m}{2\pi\hbar\beta T}\right]^d\left[\tfrac{m}{2\pi\hbar\alpha T}\right]^d\exp\left\{\tfrac{im}{2\hbar T}\left[|r''-r'|^2-|s''-s'|^2\right]\right\} \\
&\quad \times \left[\int V(r)\exp\left\{\tfrac{im}{2\hbar\alpha\beta T}|r-\tilde{r}|^2\right\}dr-\int V(s)\exp\left\{-\tfrac{im}{2\hbar\alpha\beta T}|s-\tilde{s}|^2\right\}ds\right]dt \\
&= -\tfrac{i}{\hbar}\left[\tfrac{m}{2\pi\hbar}\right]^{\frac{3d}{2}}\left[\tfrac{i}{T}\right]^{\frac{d}{2}} \\
&\quad \times \left[\int V(r)\int_{t'}^{t''}\frac{1}{\sqrt{(t''-t)(t-t')}^d}\exp\left\{\tfrac{im}{2\hbar}\left[\tfrac{|r-r'|^2}{t-t'}+\tfrac{|r-r''|^2}{t''-t}\right]\right\}\ dtdr\right. \\
&\quad \left. -\int V(s)\int_{t'}^{t''}\frac{1}{\sqrt{(t''-t)(t-t')}^d}\exp\left\{-\tfrac{im}{2\hbar}\left[\tfrac{|s-s'|^2}{t-t'}+\tfrac{|s-s''|^2}{t''-t}\right]\right\}\ dtds\right] \\
&= -\tfrac{i}{\hbar T^3}\left[\tfrac{m}{2\pi\hbar}\right]^4 \\
&\quad \times \left[\int V(r)\left[\tfrac{1}{|r-r'|}+\tfrac{1}{|r-r''|}\right]\exp\left\{\tfrac{im}{2\hbar T}\left[|r-r'|+|r-r''|\right]^2\right\}\ dr\right. \\
&\quad \left. -\int V(s)\left[\tfrac{1}{|s-s'|}+\tfrac{1}{|s-s''|}\right]\exp\left\{-\tfrac{im}{2\hbar T}\left[|s-s'|+|s-s''|\right]^2\right\}\ ds\right]
\end{aligned}
\tag{C.5}
$$

To carry out the time integration in the last step, we assume V is a time-independent potential. We have specialized to $d = 3$ and employed the integral formula (A.5) in [1]. Here $r', s' = x' \pm \frac{\tau'}{2}$, and $r'', s'' = x'' \pm \frac{\tau''}{2}$.

Appendix D: Calculating with Green vs. Blue propagators

Using the bilocal picture of quantum mechanics, with Blue kernels, we have calculated closed-form expressions in three-dimensions for (4.53) and (4.54), the total probability and current densities arriving at one or both detectors. It is instructive to compare how we would calculate these new, inherently bilocal quantities in closed form using standard wave mechanics, with Green kernels. (We do not address numerical computing here.)

Consider the total probability density first. We propagate the wavefunction from the point source through each gaussian slit at time t' to each detector at time t'', using the quadratic Green kernel in formula (4.8) [1]) four times (*cf.* the bilinear Blue kernel in formula (4.9)). The sum of the four amplitudes results in the wavefunction for the twin-detector twin-slit experiment,

$$
\begin{aligned}
\overline{\psi}(x'' \pm \tfrac{\tau''}{2}, t'') \quad = \quad & \psi(x'' + \tfrac{\tau''}{2}; x' + \tfrac{\tau'}{2}) + \psi(x'' - \tfrac{\tau''}{2}; x' + \tfrac{\tau'}{2}) \\
& + \psi(x'' + \tfrac{\tau''}{2}; x' - \tfrac{\tau'}{2}) + \psi(x'' - \tfrac{\tau''}{2}; x' - \tfrac{\tau'}{2}) \qquad \text{(D.1)}
\end{aligned}
$$

Then the total probability density is

$$
\begin{aligned}
\overline{\mathsf{P}}(x'' \pm \tfrac{\tau''}{2}, t'') \quad = \quad & \Big| \psi(x'' + \tfrac{\tau''}{2}; x' + \tfrac{\tau'}{2}) + \psi(x'' - \tfrac{\tau''}{2}; x' + \tfrac{\tau'}{2}) \\
& + \psi(x'' + \tfrac{\tau''}{2}; x' - \tfrac{\tau'}{2}) + \psi(x'' - \tfrac{\tau''}{2}; x' - \tfrac{\tau'}{2}) \Big|^2 \qquad \text{(D.2)}
\end{aligned}
$$

Expanding the square, we have 16 displaced probability terms. (Compare the formula (4.40) for the one-dimensional one-gaussian-slit wavefunction to the simpler one for the probability (4.38).) These are the same terms we obtain in four evaluations of equation (4.55), each with four terms as given by equation (4.51).

The current density (single or twin) has no Green propagator. We would use the four wavefunctions again, after propagating them to time t''. The single-detector current for each term could be calculated in the usual way, first taking gradients of each term in $\overline{\psi}(x''\pm\frac{\tau''}{2},t'')$ in equation (D.1). The single-detector velocity for each term can be obtained from the gradients of the phase. The twin (bilocal) current defined by (4.54) could be calculated using the polar formula (32) in [63], not a trivial exercise in algebra. The corresponding bilocal mean velocity would then follow from (4.56).

These closed-form calculations have not been carried out with Green kernels, but they may turn out to be more complex than those done with Blue kernels in chapter 3. The two methods, Green and Blue, are equivalent. Some might prefer to minimize algebra and let the computer do all of the work numerically. Using either kind of propagator, and taking any jumping-off point to stop algebra and begin stable numerical computing, we will, of course, obtain the same results, to within small numerical errors.

The Blue propagator theory provides its own bilocal structure and insight. The Blue propagator formulas are often simpler than the Green. The Blue formulas, being bilocal, are more general than the Green, but for that reason, they also entail integrating over two spatial paths instead of one. The Blue propagators carry the current, as well as the probability. They organize the computing steps in an intuitive way, and give us fairly simple, physically meaningful, real-valued, algebraic answers for the twin gaussian slit, twin-detector experiment. The Blue kernel propagator originated as a way to propagate twin (bilocal) probabilities and currents. In turn, this theory has borne fruit such as the bicontinuity equation (4.3), and the total current density entering one or both detectors $\bar{\mathrm{j}}(x'' \pm \frac{\tau''}{2}, t'')$ of equation (4.55). These considerations suggest that Blue propagators, as well as Green, will be useful things to have at hand in our quantum-mechanical toolkit.

Bibliography

Bibliography

[1] Feynman R P and Hibbs A R 1965 *Quantum Mechanics and Path Integrals* emended by D Styer 2005 (Mineola NY: Dover Publications)

[2] Styer D F, Balkin M S, Becker K M, Burns M R, Dudley C E, Forth S T, Gaumer J S, Kramer M A, Oertel D C, Park L H, Rinkoski M T, Smith C T and Wotherspoon T D 2002 Nine formulations of quantum mechanics *Am. J. Phys.* **70** 288-297

[3] Case W B 2008 Wigner functions and Weyl transforms for pedestrians *Am. J. Phys.* **76** 937-946

[4] Weyl H 1927 Quantenmechanik und Gruppentheorie *Z. Phys.* **46** 1-46

[5] Wigner E P 1932 On the quantum correction for thermodynamic equilibrium *Phys. Rev.* **40** 749-759

[6] Gröchenig K 2001 *Foundations of Time-Frequency Analysis* (Boston: Birkhäuser)

[7] Mori H, Oppenheim I and Ross J 1965 in *Studies in Statistical Mechanics*, eds. de Boer J and Uhlenbeck, G E, Vol. 1, p. 213 (Amsterdam: North-Holland)

[8] Moyal J E 1949 Stochastic processes and statistical physics *Proc. Cambridge Phil. Soc* **45** 99

[9] Kim Y S and Wigner E P 1990 Canonical transformations in quantum mechanics *Am. J. Phys.* **58** 439-448

[10] Snygg J 1977 Wave functions rotated in phase space *Am. J. Phys.* 45, 58-60

[11] Stenholm S 1980 The Wigner function: I. The physical interpretation *Eur. J. Phys.* **1** 244-248

[12] Chaturvedi S, Ercolessi E, Marmo G, Morandi G, Mukunda N and Simon R 2006 Wigner-Weyl correspondence in quantum mechanics for continuous and discrete systems – a Dirac-inspired view *J. Phys. A: Math. Gen.* **39** 1405-1423

[13] Wigner E P 1971 Quantum-mechanical distribution functions revisited in *Perspectives in Quantum Theory: Essays in Honor of Alfred Landé*, Yourgrau and van der Merwe, eds. (Cambridge MA: MIT Press)

[14] Hillery M, OConnell R F, Scully M O and Wigner E P 1984 Distribution functions in physics: Fundamentals *Phys. Rep.* **106** 121-167

[15] Feynman R P 1942 *The Principle of Least Action in Quantum Mechanics*, PhD thesis Princeton Univ., pub. 2005 as *Feynman's Thesis: A New Approach to Quantum Theory* edited by L. Brown (Singapore: World Scientific)

[16] Shankar R 1994 *Principles of Quantum Mechanics* 2nd ed. (New York NY: Springer)

[17] Huang K 2010 *Quantum Field Theory* 2nd ed. (Weinheim: Wiley-VCH)

[18] Feynman R P 1948 Space-time approach to non-relativistic quantum mechanics *Rev. Mod. Phys.* **20** 367-387

[19] Thornton S and Marion J 2004 *Classical Dynamics of Particles and Systems* 5th ed. (Belmont CA: Thompson Brooks/Cole).

[20] Bracewell R 2000 *The Fourier Transform and Its Applications* 3rd ed. pp. 74-104 (New York: McGraw-Hill).

[21] Walnut D 2002 *Introduction to Wavelet Analysis* (Boston: Birkhäuser)

[22] Almeida L B 1994 The fractional Fourier transform and time-frequency representations *IEEE Trans. Signal Processing* **42** 3084-3091

[23] Ryder L 1996 *Quantum Field Theory* 2nd ed. (Cambridge Univ. Press)

[24] Manoukian E 2006 *Quantum Theory: a Wide Spectrum* (Dordrecht: Springer)

[25] Withers L P Jr, Blue functions: probability and current density propagators in non-relativistic quantum mechanics *J. Phys. A* 44 (2011), no. 41, 415301, 26 pp.; MR2842544, doi:10.1088/1751-8113/44/41/415301, online at stacks.iop.org/JPhysA/44/415301 .

[26] Keldysh L V 1964 *Zh. Eksp. Teor. Fiz.* 20 1018 [1965 Diagram technique for nonequilibrium processes *Sov. Phys. JETP* **20** 235]

[27] Altshuler B L, Aronov A G, and Khmelnitskii D E 1982 Effects of electron-electron collisions with small energy transfers on quantum localisation *J. Phys. C* 15 7367

[28] Weiss U 2012 *Quantum Dissipative Systems* 4th edn. (Singapore: World Scientific)

[29] Kleinert H 2009 *Path Integrals in Quantum Mechanics, Statistics, Polymer Physics, and Financial Markets* 5th edn. (Singapore: World Scientific)

[30] Goldstein H, Poole C, and Safko J 2002 *Classical Mechanics* 3rd edn. (San Francisco: Addison-Wesley)

[31] Yukawa H 1950 Quantum theory of nonlocal fields. 1. Free fields *Phys.Rev.* 77 219-226 DOI: 10.1103/PhysRev.77.219

[32] Bohm D, Billion P, Takabayasi T, Vigier J P 1960 Relativistic rotators and bilocal theory *Progress of Theoretical Physics* 23 (3) 496-511

[33] Madelung E 1927 Quantum Theory in Hydrodynamical Form *Z. Phys.* 40 322

[34] Aharonov Y and Rohrlich D 2005 *Quantum Paradoxes: Quantum Theory for the Perplexed* (Weinheim: Wiley-VCH)

[35] Ramsey N F 1950 A molecular beam resonance method with separated oscillating fields *Phys.Rev.* 78 696-699

[36] Feynman R P, Leighton R B, Sands M 1963 *The Feynman Lectures on Physics* Vol. III Reading MA: Addison-Wesley

[37] Billingsley P 1995 *Probability and Measure*, 3rd ed. (New York: John Wiley and Sons)

[38] Dirac P 1942 Bakerian Lecture. The Physical Interpretation of Quantum Mechanics. Proceedings of the Royal Society of London, A, vol. 180 (980; March 18 1942), 1-40. (http://rspa. royalsocietypublishing.org/content/180/980/1.full.pdf+html

[39] Feynman R 1991 Negative Probability 235-248 in *Quantum Implications: Essays in Honour of David Bohm* eds. Hiley B, Bohm D, Peat D (London,New York: Routledge)

[40] Scully M O, Walther H, Schleich W 1994 Feynman's approach to negative probability in quantum mechanics *Phys. Rev. A* 49 15621566

[41] Sinha U, Couteau C, Jennewein T, Laflamme R, Weihs G 2010 Ruling Out Multi-Order Interference in Quantum Mechanics, *Science* **329** 418, doi: 10.1126/science.1190545

[42] Bliokh K, Bekshaev A Y, Kofman A G, and Nori F 2013 Photon trajectories, anomalous velocities and weak measurements: a classical interpretation *New J. of Physics* 15 (7) 073022

[43] Griffiths D J 2005, *Introduction to Quantum Mechanics* 2nd ed. (Upper Saddle River NJ: Pearson-Prentice-Hall).

[44] Liboff R L 2003 *Introductory Quantum Mechanics* 4th edn. (San Francisco CA: Pearson-Addison-Wesley)

[45] Loudon R 2000 *The Quantum Theory of Light,* 3rd edn. (New York NY: Oxford Univ. Press)

[46] Schattschneider P, Schachinger T, Stöger-Pollach M, Löffler S, Steiger-Thirsfeld A, Bliokh K Y, and Nori F 2014 Imaging the dynamics of free-electron Landau states *Nature Communications* 5:4586 DOI: 10.1038/ncomms5586

[47] Kocsis S, Braverman B, Ravets S, Stevens M, Mirin R P, Shalm L K, Steinberg A M 2011 Observing the average trajectories of single photons in a two-slit interferometer *Science* **332** 1170 doi: 10.1126/science.1202218

[48] Garrison J C, Chiao R Y 2008 *Quantum Optics*, (Oxford: Oxford Univ. Press)

[49] Fowles G R 1989 *Introduction to Modern Optics,* 2nd edn. (Mineola NY: Dover Publications)

[50] Mandel L, Wolf E 1995 *Optical Coherence and Quantum Optics* (Cambridge: Cambridge Univ. Press)

[51] Scully M O, Zubairy S 1997 *Quantum Optics* (Oxford: Oxford Univ. Press)

[52] Bach R, Pope D, Liou S H, Batelaan H 2013 Controlled double-slit electron diffraction, *New J. Physics* 15(3) 033018. http://iopscience.iop.org/1367-2630/15/3/033018/pdf/

[53] Byrne J 2011 *Neutrons, Nuclei & Matter* (Mineola NY: Dover Publications)

[54] Bell J S 1980 de Broglie-Bohm, delayed-choice, double-slit experiment, and density matrix *Int'l. J. Quantum Chemistry* Supplement: *Proc. Int'l. Symp. on Atomic, Molecular, and Solid-State Theory, Collision Phenomena, Quantum Statistics, and Computational Methods* 18 S14 155159 doi: 10.1002/qua.560180819

[55] Jacques V *et al* 2007 Experimental realization of Wheeler's delayed-choice gedanken experiment, doi:10.1126/science.1136303 *Science* **315** 966

[56] Peruzzo A *et al.* 2012 A quantum delayed-choice experiment, *Science* **338** 634 doi:10.1126/science.1226719

[57] Kaiser F *et al.* 2012 Entanglement-enabled delayed-choice experiment *Science* **338** 637 doi:10.1126/science.1226719

[58] Aharonov Y and Rohrlich D 2005 *Quantum Paradoxes: Quantum Theory for the Perplexed* (Weinheim: Wiley-VCH)

[59] Wiseman H M 2003 Directly observing momentum transfer in twin-slit which-way experiments, *Physics Letters A* 311 285291

[60] Wiseman H M 2007 Grounding Bohmian mechanics in weak values and bayesianism, *New Journal of Physics* 9 165. doi:10.1088/1367-2630/9/6/165

[61] Matzkin A 2012 Observing trajectories with weak measurements in quantum systems in the semiclassical regime *Phys. Rev. Lett.* **109** 150407

[62] Davidović M, Sanz A S, Božić M, Arsenović D, and Dimić D 2013 Trajectory-based interpretation of Young's experiment, the Arago-Fresnel laws and the Poisson-Arago spot for photons and massive particles *Physica Scripta* T153 014015.

[63] Withers L P Jr, Narducci F A 2015 A bilocal picture of quantum mechanics, *J. Phys. A*, accepted for publication.

[64] Philippidis C, Dewdney C, Hiley B J 1979 Quantum interference and the quantum potential, *Il Nuovo Cimento B* Series 11 **52** 1 15-28

[65] Vigier J-P, Dewdney C, Holland P R, Kyprianidis A 1991 Causal particle trajectories and the interpretation of quantum mechanics 169-204 in *Quantum Implications: Essays in Honour of David Bohm* (eds. Hiley B, Bohm D, Peat D) (London New York: Routledge)

[66] Zee A 2010 *Quantum Field Theory in a Nutshell* 2nd ed. (Princeton Univ. Press)

[67] Altland A, Simon B 2010 *Condensed Matter Field Theory,* 2nd edn. (Cambridge UK: Cambridge Univ. Press)

[68] Ou Z Y, Zou X Y, Wang L J, Mandel L 1990 Observation of nonlocal interference in separated photon channels *Phys. Rev. Lett.* 65 3

[69] Withers L P Jr, Narducci F A 2015 Bilocal current densities and mean trajectories in a Young interferometer with two Gaussian slits and two detectors *J. Math. Physics*, submitted.

[70] Moler K, Weiss D S, Kasevich M, and Chu S 1992 Theoretical analysis of velocity-selective Raman transitions *Phys. Rev. A* 45 1

[71] Steck D 2014 *Quantum and Atom Optics*, http://atomoptics-nas.uoregon.edu/ dsteck/teaching/quantum-optics

[72] Kasevich M A 1992 *Atom Interferometry in an Atomic Fountain* PhD dissertation, Stanford University

[73] Braje D A, DeSavage S A, Adler C L, Davis J P & Narducci F A, 2014 A frequency selective atom interferometer magnetometer, *Journal of Modern Optics* DOI: 10.1080/09500340.2013.850776

Curriculum Vitae

Lang Withers Jr. was born in Columbus, Nebraska in 1951, only the first of four children of Langhorne Putney and Betty Peitzmeier Withers. After moving around the U.S. and Germany with his family in the U.S. Army, in 1968 he went to Caltech, whose school logo was (until lost in 1984) Jesus' stirring statement, "*the truth shall make you free*," beneath a shielded torch emblem. While a student (of sorts) there, in 1970 he became convinced of the historical validity of the Christian faith and converted from atheism. This did him a world of good. He received an M.A. in mathematics from the University of Colorado at Boulder in May 1975, forty years ago. During 1978-1980 he studied statistics at George Washington University. During 1983-1985 he studied mathematics at the University of Maryland at College Park.

In 1980 he married his beautiful bride, Christine Hayes. They have raised three wonderful daughters, Carolyn Cokes, Rebecca Myles, and Hannah Withers (their pride and joy). After his daughters grew up, he began his studies in physics (his favorite subject all along) at George Mason University in 2003. He has also served for four decades in the U.S. defense industry, focusing on signal and image processing algorithms. He imagines that he missed his calling as a professor, and hopes to make good on it in the sequel.